Reliability assessment of corroded reinforced concrete structures

The effect of using random fields and nonlinear finite element analysis

Master of Science, Thesis report

Quanxin Jiang

August 2018

Thesis project during the Master of Science in Structural Engineering

Faculty of Civil Engineering & Geosciences
Structural Mechanics

Delft University of Technology, the Netherlands

Author: Quanxin Jiang
Student number: 4607422
E-mail: quanxinjiang@gmail.com

Thesis committee:
Prof. Dr. M.A.N. Hendriks (Chair)
Prof. Dr. M.A. Hicks
Prof. Dr. J.G. Rots
Dr. A. Rózsás (Main supervisor)
Dr. A.T Slobbe
Dr. Y. Yang

List of symbols

Roman uppercase letters

A_c	Area of the concrete
$A_{res(mod)}$	Modified total residual cross section of rebars
A_{uni}	Cross section reduction of a rebar due to uniform corrosion
A_{pit}	Cross section reduction of a rebar due to pitting corrosion
A_s	Area of the reinforcement
A_{st}	Area of the top reinforcement
A_{sm}	Area of the bottom reinforcement at midspan
A_{ss}	Area of the bottom reinforcement at sidespan
C_{cr}	Critical threshold chloride concentration
D_0	Original diameter of the bar
E	Model error
E_s	Young's modulus of steel
$F(.)$	Cumulative probability
$G(.)$	Exact limit state function
$G^*(.)$	Response surface function
$H(.)$	Random field
L_u	Length of an element in discretization
L_0	Reference length of reinforcement
R_{fb}	Ratio of bond strength at a certain corrosion level to the original bond strength for the uncorroded specimen.
P^*	Design point
P_{av}	Penetration calculated based on general corrosion
P_f	Probability of failure
P_{tr}	Ratio of transverse reinforcement area at anchorage length versus the area of the main bars
$P_f{}^+$	Upper characteristic value of failure probability
$P_f{}^-$	Lower characteristic value of failure probability
Q	Action load
R	Pitting factor
$R(.)$	Value of resistance based on random variable
X	Corrosion level defined as the loss of weight of reinforcing bar due to corrosion expressed as a percentage of the original bar weight
X	Vector of random variables
X_{-Q}	Vector of random variables other than Q

Roman lowercase letters

a	Constant parameter
b	Constant parameter
b_0	Width of pit
f_b	Strength of the bond between reinforcement and concrete
f_{cc}	Compressive strength of concrete

f_s	Strength of reinforcement
f_su	Tensile strength of reinforcement
f_sy	Yield strength of reinforcement
f_t	Tensile strength of concrete
$g(.)$	Performance function
i_corr	Corrosion current density
l_cor	Correlation length
l_p	Distance between pits in two adjacent rebars
l_r	Distance between tensile rebars
p	Maximum pit depth
t	Time since corrosion initiation
x	Corrosion level measured by corrosion penetration depth

Greek lowercase letters

α	Gumbel parameter
α_x	Sensitivity factor of variable x
β	Reliability index
β_int	Interference factor of the pits
γ	Ration between the width of pit and the depth of pit
δ	Penetration index
ε_cu	Ultimate strain of concrete
ε_su	Ultimate strain of reinforcement
μ	Gumbel parameter
ρ_{ij}	Correlation coefficient
σ	Standard deviation

Notations

$._0$	The properties of the uncorroded reinforcements
$\bar{.}$	Mean value

List of Abbreviations

ADIS	Adaptive Directional Importance Sampling
AK-MCS	Adaptive Kriging Monte Carlo Simulation
AS	Analytical Solution
COV	Coefficient of variation
CSS	Charged System Search method
FEA	Finite Element Analysis
fib	International Federation for Structural Concrete
FORM	First Order Reliability Method
JCSS	Joint Committee on Structural Safety
IS	Importance Sampling
ISO	International Organization for Standardization
HORM	Higher order approximation methods
MCS	Mote-Carlo Simulation
MP	midpoint method
N/A	Not applicable
NLFEA	nonlinear finite element analysis
PVD	the principle of virtual displacements
RC	Reinforced concrete
SLS	Serviceability Limit State
SORM	the second order reliability method
SS	Subset Simulation
TM	Third-Moment method
ULS	Ultimate Limit State

Abstract

One of the most severe deteriorations in reinforced concrete structures is associated with reinforcement corrosion, where the corrosion distribution shows considerable spatial variability. In the existing investigations of spatial variability of corrosion on the reliability of reinforced concrete structures, symbolic expressions are used for the structural performance. However, structural behaviors like stress redistribution and plasticity spread are not captured. In this research, a computational framework is designed to couple the probabilistic analysis with the nonlinear finite element analysis. Random fields is used with the computational framework to represent the spatial variability of corrosion.

A 60 m girder of a reinforced concrete bridge is taken as the case study to explore the effect of spatial variability of corrosion on reliability of static indeterminate reinforced concrete structures. The reliability analysis is target on ultimate capacity of the beam to carry the traffic load. The girder is modeled as a 3 span continuous beam. The modelling of corrosion damages on reinforcement (area of cross section and physical properties) is based on assumption of pure pitting corrosion. In the axial direction of the beam, spatial variability is modeled with random field. In order to study the effect of different level of spatial variability, the correlation length of the random field is set from infinite large to 125 mm. Between adjacent bars, extreme cases of fully spatial correlated and totally spatial independent are studied.

The case study shows:
i) when corrosion develops, pitting corrosion can severely reduce resistance of the structure and localized damage may lead to a brittle structural response.
ii) spatial variability of pitting corrosion in the axial direction of the beam leads to higher failure probability of the structure.
iii) spatial variability of pitting corrosion between adjacent bars leads to lower failure probability of the structure.
iv) the effect of spatial variability of corrosion on reliability of static indeterminate reinforced concrete structure is a collective effect of probabilistic and physical characteristic.

In order to facilitate the reliability assessment of corroded reinforced concrete structures, additional efforts are also contributed to: quantification of uncertainty for the bond model of corroded reinforcement; comparison of various reliability methods with the probabilistic nonlinear finite element analysis framework.

The thesis fills the knowledge gap of probabilistic nonlinear finite element analysis of reinforced concrete structures with spatial varied corrosion and quantifies the effects of spatial variability of corrosion on the reliability of a static indeterminate reinforced concrete structure. The analysis framework designed in this thesis is also applicable for other reliability assessment of corroded reinforced concrete structures.

Preface

In this report the results of the my master's project is presented. The master's project is carried out for the Structural Reliability group of TNO and is part of the master's program in Structural Engineering at Delft University of Technology.

In August 2017, the research objective regarding to reliability assessment of reinforced concrete structures was raised by the Structural Reliability group in TNO. One of the research question is how the spatial randomness of corrosion influence the reliability of structures. The project officially started in November 2017. In 10 months, a thoroughly study is performed to response to the raised research question.

In this thesis, details of the master's project are well reported, from the theory to the application. A computational framework is designed to couple the probabilistic analysis with the nonlinear finite element analysis. Random fields is used with the computational framework to represent the spatial variability of corrosion on a reinforced concrete girder. The girder is taken as the case study to explore the effect of spatial variability of corrosion on reliability of static indeterminate reinforced concrete structures. Additional efforts are also contributed to facilitate the reliability assessment of corroded reinforced concrete structures: quantification of uncertainty for the bond model of corroded reinforcement; comparison of various reliability methods in the analysis framework.

I would like to thank my Thesis Committee members for their tremendous support during this project. I am glad to have Professor Max Hendriks being the chair of my committee and helping me from the beginning to the end of the graduation. I would to thank Professor Michael Hicks for his suggestions on reliability analysis and application of random fields. The guidance of Professor Jan Rots and Dr. Yuguang Yang on finite element modelling of concrete structures is essential for the project. The daily supervise of Dr. Arthur Slobbe helps significantly on the computational modelling and on the writing of the thesis. I would like to address special thanks to Dr. Arpad Rózsás, for his guidance on probabilistic theory and programming, and for his encouragement on my research interest. I am also very grateful for the opportunity to work at TNO and cooperate with all the talented people. The staff in Structural Reliability give me generous help and precious advices.

Finally, I would like to thank my family for their mental support and my friends for their accompanies. With my family and friends, I find my courage to overcome all the difficulties and become a better person.

Quanxin Jiang
Delft, August, 2018

Content

1   Introduction

1.1   Background

Modern societies increasingly depend on complex infrastructures. Buildings and civil infrastructure comprise about 80% of the national wealth of industrialized nations (Sarja, 2005). Hence, their prudent management is of outmost importance, since failures and outages can have immense economical and societal consequences. Most of the structures - comprising the building and infrastructure stocks - are built multiple decades ago (typically in the 1950s and 1960s), and their intended service life is close to the end. As a result of this, the number of aging and deteriorating structures is rapidly increasing and putting larger and larger burden on asset managers. One example is in the United States where 25.8% of the 596808 existing bridges were structurally deficient or functionally obsolete as of the end of 2006 (Frangopol, 2009).

One of the most severe type of deteriorations in concrete structures is associated with reinforcement corrosion. The study of Koch et al. (2001) shows that the estimated total annual direct cost of corrosion in the United States is a staggering $276 billion—approximately 3.1% of the nation's Gross Domestic Product. Steel is transformed into iron oxides through the corrosion process. Effective area of the steel is reduced and the ductility of reinforcement bars are changed. Moreover, the concrete cover cracks due to splitting stresses generated by the volume expansion of iron oxides. The volume expansion also affects the bond between reinforcements and concrete. Because of all the effects (cross-sectional area loss of reinforcing bars, spalling of concrete, loss of ductility of reinforcing bar and degradation of bond), reinforcement corrosion can influence structural performance regarding both ultimate strength and serviceability.

The assessment in respect to residual safety level of existing concrete structures subject to corrosion is currently an important research topic. The assessment of corroded structures requires combined models of the corrosion process and mechanical behavior. Furthermore, it should account for the uncertainties in the models and input data. One way to assess deteriorating structures is to calculate their failure probability based on residual safety level that can be verified on both ultimate limit state and serviceability limit state, and to compare that with a socially acceptable target value. This approach is referred as Probabilistic Method in Eurocode 1990:2002 and Reliability Based Assessment in ISO 2394:2015. Reliability-based methods can be used to derive semi-probabilistic methods, such as Partial Factor Method, which do not require fully probabilistic calculation. However, semi-probabilistic methods are not available for the assessment of corroded structures. This thesis is addressing research questions related to the reliability analysis of corroded structures and can be considered as a step towards establishing reliability-based calculations of corroded structures, and contributing to the derivation of semi-probabilistic methods.

The   assessment of corroded reinforced concrete (RC) structures assumed the material properties and geometrical parameters either as deterministic values or as random values

uniformly distributed in space. Stewart (2004) found that probabilities of failure considering spatial variability of pitting corrosion were up to three times higher than probabilities of failure obtained from a non-spatial analysis in structural reliability analysis for RC members in flexure. Therefore, it is necessary to consider spatial randomness of corrosion effects in reliability assessment of corroded RC structures.

Despite of the fact that a lot of researches have investigated failure probability calculation or spatial variability of corrosion on RC structures, the analyses to combine them are still at a level far from maturity. In Chapter 2, there is a concise literature review that concludes two major limitations as the knowledge gap of existing studies. One of the limitations is that, most of researchers use symbolic expressions to calculate structural strength and load effects. The strategies used by them are not applicable in case more realistic physical representations are preferred. Another limitation is that there are no well-founded probabilistic models of influencing parameters in the modelling of corroded reinforced structures, which leads to the lack of reliable inputs for the reliability analysis.

1.2   Problem statement

The main objective of this research is to perform reliability analysis for reinforced concrete structures considering spatial variability of corrosion in order to answer the research question:

What are the effects of the spatial variability of corrosion on the reliability of reinforced concrete structures?

The research question is proposed in response of the knowledge gap in existing study: that the reliability assessment of corroded RC structures taking account spatial variability is available only for simple structures with simple physical models where analytical solutions are available. By combining full probabilistic analysis and nonlinear finite element modelling together, structures with more complexity can be assessed. With using of random fields, the spatial variability of corrosion can be represented and the influence of the type and the level of such spatial variability can be explored. Thus the research can provide insights for reliability analysis of corroded RC structures from a practical view.

With the main objective, there are many other questions addressed without available answers. The next section *Scope and limitations* introduced some of the questions that are out of the research scope. However, due to the fact that the model uncertainty is a relatively important input in the reliability analysis, a sub-research objective is devoted to quantifying model uncertainty for corroded RC structures and explore its influence on reliability. The uncertainty quantification is only focus on the bond model due to two reasons: compared with other properties, the bond strength is difficult to be directly measured from a real structure; and compared to empirical models of other properties, the proposed model of bond degradation for corroded reinforcement contains relatively large uncertainty.

1.3   Scope and limitations

The scope of the research is restricted to reliability analysis based on ultimate limit state. Serviceable limit state is not concerned in this thesis. The spatial variability of corrosion is considered in two cases: along the reinforcement and between adjacent reinforcements. Along

the reinforcement, one dimensional homogeneous random fields are used to model the spatial variability. However, the consideration of correlation between reinforcing bars are only treated with two extreme case: full correlation between reinforcing bars and full independency between reinforcing bars. The one dimensional homogeneous random fields along the reinforcements are coupled with the correlation between reinforcing bars.

The thesis contains a case study of a corroded concrete bridge investigated by Jacinto et al. (2015). The analysis is about one of the girder of the bridge, as preliminary analysis proved that the outer girder is the critical member. The girder is treated as one dimensional beam because the relative small height/span ratio. Pitting corrosion is regarded only occurring at the bottom reinforcements, according to the investigation reported by Jacinto. Although the corrosion can be a combination of general corrosion and pitting corrosion, this thesis does not explore the further effects. Other simplifications with respect to the probabilistic and physical modelling are mentioned and explained in the Chapter 4 to Chapter 6.

Due to the prematurity of related researches, many other questions are addressed but are treated with assumptions or references: i, the current research is based on a case study of concrete bridge where the determination of probability distributions is already available in reference and the data extracted from reference is assumed to be trustworthy and representative; ii, the effects of corrosion included in this research are limited to reduction of reinforcement bar area, change of reinforcement strength and ductility, and loss of bond between reinforcement and concrete; iii, current research only focus on the propagation stage of corrosion where the model to present time-dependent characteristics is directly taken from a reference.

Although the research is mainly analysis at member level, the findings should also be valid for analysis of structural system because the influence of stress/strength redistribution and multi-failure mechanism has be captured. The scope of this thesis is indicated with
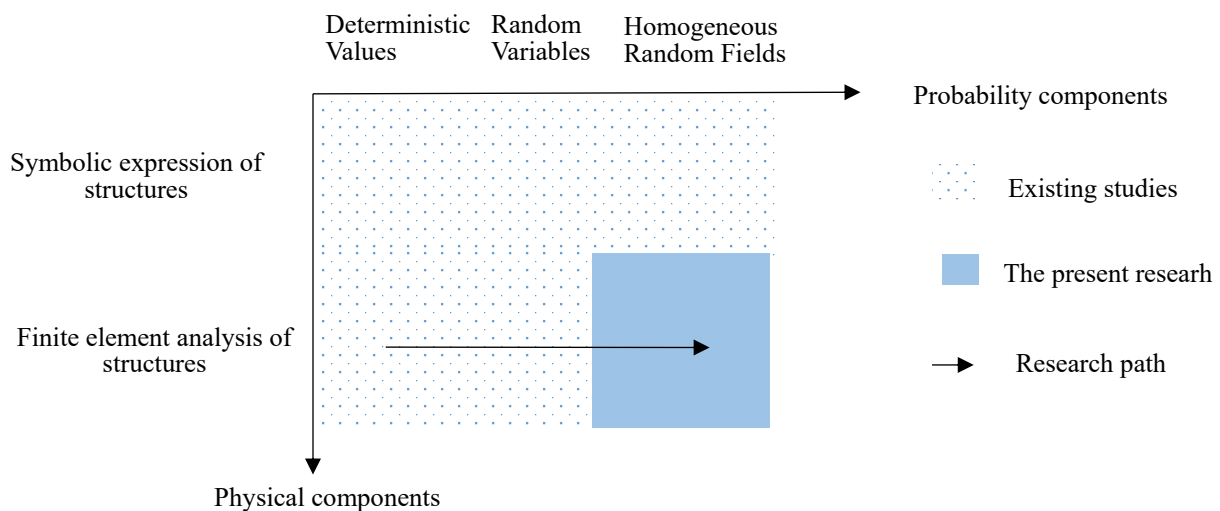Fig 1.1.

Fig 1.1 Research scope

1.4 Approach

The thesis takes a concrete bridge studied by Jacinto et al. (2015) as the case study to answer the research question. The case is analysed step by step, moving from finite element analysis to reliability analysis with spatial uniform variables to reliability analysis with random field.

Being able to perform reliability analyses of the chosen case, three components should be available:

-Numerical modelling of the corrosion effects to predict the load bearing capacity of complex, realistic structures;

-Algorithm to couple the probabilistic analysis with nonlinear finite element analysis.

-Probabilistic models account for uncertainties of structural properties, including the spatial variability;
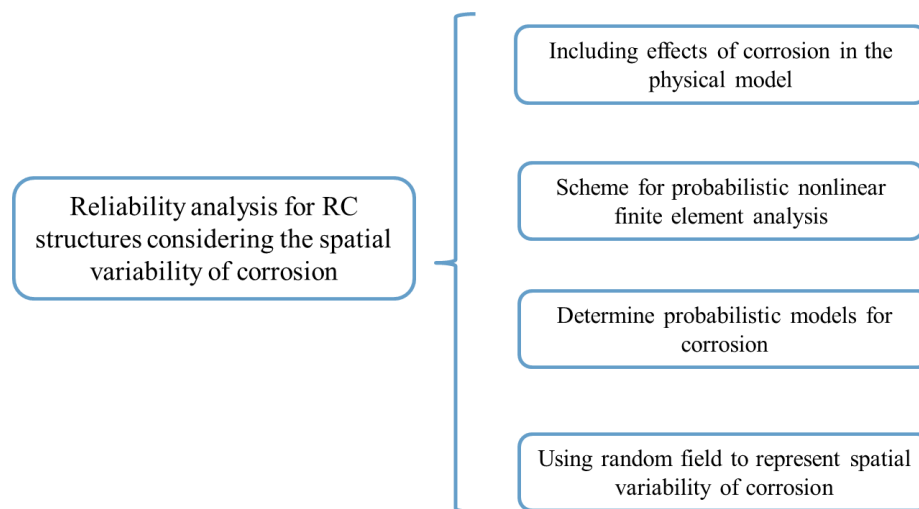
Fig 1.2 Components of the research

Thus, three steps are taken to develop the method used in the reliability assessment of corroded reinforced concrete structures. First, the numerical model of the physical problem; second, realizing a computational method for probabilistic nonlinear finite element analysis; third, including the probabilistic models into the reliability analyses.

In the reliability analysis considering spatial variability of corrosion, different levels of spatial variability along reinforcements are considered by a parameter study. The influence of spatial variability between reinforcing bars are also considered. Based on the results of case study, the effect of using random field to represent spatial variability on corroded concrete structures is estimated.

An analysis framework is designed and implemented in MATLAB to couple the probabilistic methods with finite element analysis. Fig 1.3 shows the workflow of the analysis framework. There are four steps in the framework: the definition of the inputs, the pre-processing to define the probabilistic model and the finite element model, the reliability analysis, and the post processing of the calculated results. External program OpenSees is applied to perform the

nonlinear finite element analysis. The reliability analysis is performed with MATLAB based tool boxes. In the following paragraphs, details of the framework will be introduced.
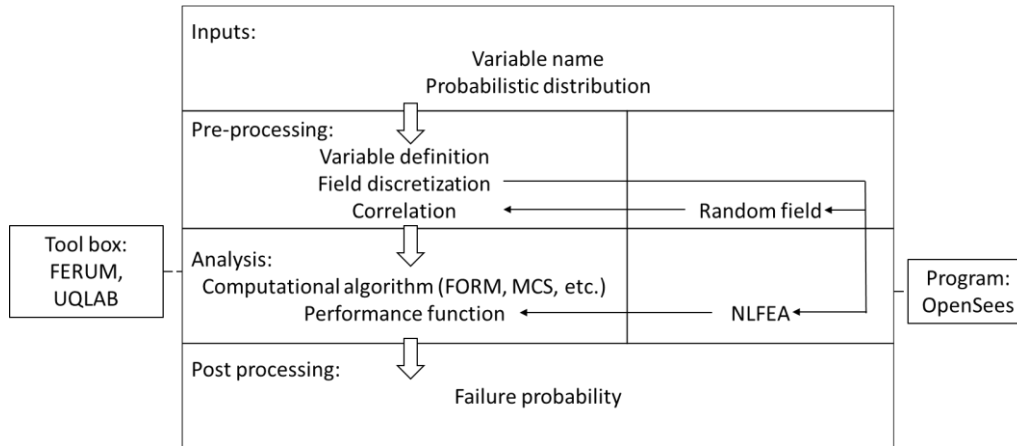

Fig 1.3 Work flow of the computation scheme

The framework starts with the definition of the inputs. These inputs include: name of variables, probabilistic distribution of variables (i.e. distribution type, mean value and standard deviation), information of finite element mesh, and correlation length. Furthermore, the input contains settings, such as the chosen reliability method, convergence criteria, etc. If spatial variability is included, a random field will be generated. In this study, the random field has the same discretization as the finite element mesh. The generation of the correlation matrix is based on the discretization and a selected auto-correlation function and correlation length. The type of the auto-correlation function and the correlation length should also be defined as inputs before the performance of reliability analysis. After the definition of the probabilistic distributions and the generation of the correlation matrix, the reliability analysis can be performed the same way as without a random field.

In the reliability analysis part, the analysis can be conducted using different toolboxes (e.g. FERUM, UQLab), the available methods and settings are conditioned on the selected toolbox. During the reliability analysis, irrespectively of the chosen computational algorithm, the evaluation of the performance function is needed. The performance function is defined as $g(X_{-Q}) = R(X_{-Q}) - Q$, where Q is the variable of action, X_{-Q} is a vector of random variables other than Q, and $R(X_{-Q})$ is the value returned by after evaluating the mechanical model.

For the calculation of the resistance, a finite element model is generated based on a realization from **X** and a nonlinear finite element analysis is performed. The finite element analysis returns the maximum load that the structure can carry, which is the resistance $R(X_{-Q})$. For each exact evaluation of limit state function, the finite element analysis is called once. The finite element model is automatically generated from the realization of one set of variables that is sent by the reliability analysis. The MATLAB code is programmed to create and modify command files that can be used to generate models and analyses in the finite element program. Depending on the physical problem, some physical properties are set as variables that get value from the realization sent by the reliability analysis, while other properties and solution procedure settings

are fixed. The output of each finite element analysis is the load applied on the structure of each load step. The maximum applied load is selected as the capacity of the structure and the value of this capacity is returned to the performance function evaluation.

The details of the calculation steps are depended on the specific computational algorithm. There are five algorithms used in this thesis: FORM, Subset Simulation, ADIS, AK-MCS and Importance Sampling. Brief introductions of the calculation steps are presented in the Annex. Based on the evaluation of the performance function, the reliability analysis calculates the failure probability and other optional outputs. The optional outputs can be: sensitivity factors and design point (FORM), or confidence intervals and coefficient variation of the failure probability (simulation methods). All the reliability analyses in this thesis are evaluated with three criterions. The convergence criterion is used to evaluate the accuracy; the physical meaning criterion is used to evaluate the reasonability; and the number of exact evaluation of performance function is used to evaluate efficiency.

1.5 Thesis structure

The thesis contains eight chapters which can be regarded as four parts. The first part is the introduction of the thesis that includes the research objectives, research approaches, and the structure of the thesis. A literature review is conducted to show the limitation of existing researches and the value of the present thesis. The second part explained the technique background that involves modelling of structural effects of corrosion, reliability methods and random field, probabilistic models of corroded reinforced concrete structures. The third part studies the effect of spatial variability of pitting corrosion based on a case study. In the case study, the approaches and methods described in Part I and II are used on a continuous beam of a RC bridge. Part IV contributes to a study of the model uncertainty of the bond model, in order to compliment the limitation of ignoring model uncertainties in the case study. The final part is the conclusions of the thesis and also recommendations on further research. Such conclusions and recommendations are in term of both general reliability assessment of corroded reinforced concrete structures and the effect of spatial variability of corrosion on the studied case.

Table 1.1. Thesis structure

Part I: Introduction	Introduction
	Literature review
Part II: Methods	Methods
Part III: Case study	Nonlinear finite element analysis of the RC continuous girder
	Reliability analysis of the RC continuous girder
	Corrosion distribution on adjacent rebars
Part IV: Model uncertainties	Uncertainty of the bond model
Part V: Conclusion	Conclusion and recommendation

2 Literature review

2.1 Probabilistic modelling of corrosion

In a reliability based assessment, variabilities and uncertainties are typically represented by probabilistic models: random variables and stochastic processes. There are two ways to determine the probabilistic models: to analyze data from direct measurement and to take the existing models based on trustable database. In many cases, direct measurements are not available or require too much extra cost, that general applicable probabilistic models are taken from guidelines or widely accepted literature. For example, CEB/fib (2016) and JCSS (2000) provide well established probabilistic models of concrete and reinforcement properties for non-deteriorated structures. However, for deteriorated structures, the probabilistic models are often missing.

Corrosion of reinforcement will influence the strength and ductility of reinforcement, as well as the bond strength. The empirical models to describe such influences contains certain degree of uncertainties or variabilities, which do not exist in the probabilistic models for sound structures. There are studies aiming to propose modelling uncertainty for corroded reinforced concrete structures (Allaix et. al, 2015). The modelling uncertainty of resistance is expressed as the probabilistic distribution of the ratio between actual resistance (experimental value) with numerical resistance (with certain combination of model parameters). This approach provides inspiration for involving extra uncertainties or variabilities of corroded structures with utilization of the probabilistic models for undeteriorated structures. However, the disadvantage is, the approach integral uncertainties and variabilities of a wide range sources into one parameter, which could be an over simplification.

In terms of spatial variability of corrosion, the probabilistic model represent corrosion distribution is studied by Stewart and Al-Harthy (2008), Melchers (2005) for pitting corrosion. However, the spatial correlation in the probabilistic model is not explicitly quantified. Although Engelund and Sorensen (1998) and Teixeira & Soares (2008) concerned spatial correlation for chloride-ingress and corrosion effects, they separately applied different correlation length which are based on assumption rather than experimental evidence.

2.2 Reliability assessment of corroded reinforced concrete structures without spatial randomness

Since last century, several scholars started to study the reliability assessment of corroded reinforced concrete structures. Sheikh et al. (1990) employed pitting corrosion statistical models to characterize the cumulative number of leaks in pipeline and the time-to-perforation. D. V Val et al. (1998) studied the effect of reinforcement corrosion on the reliability of highway bridges taking account reduction of steel area and loss of bond. Akgül and Frangopol (2004) studied time-dependent interaction between load rating and reliability of deteriorating bridges considering reduction of steel area due to corrosion. While the early investigations focus on the undesirable consequences of corrosion, later studies also proposed approaches to optimize design against corrosion effects. Chiu et al. (2014) proposed a novel computational procedure

for calculating the risk of corrosion of reinforcing steel bars induced by the environmental hazards. The risk curve is provided to identify the minimal thicknesses of concrete cover.

Methods are also proposed to improve the efficiency of calculation, especially to get rid of the time-consuming Monte Carlo Simulation. Zhang et al. (2015) developed a third-moment (TM) method to evaluate the time-dependent probability of chloride-induced corrosion of reinforced concrete structures in marine environments. It is shown that the third-moment method is simpler and more efficient than traditional approaches such as Monte Carlo in analyzing the corrosion-induced probability. Nogueira and Leonel (2013) used FORM with direct coupling approach to determine corrosion occurrence probability in order to evaluate the concrete structures strength. The FORM analysis was compared with Monte-Carlo simulation method. It was verified that the direct coupling procedure gives accurate results and stable convergence rate with low number of mechanical analyses. Shayanfar et al. (2015) used meta-heuristic approach of charged system search (CSS) to calculate corrosion occurrence probability due to chloride ions penetration. The model efficiency is verified by comparing the available examples in technical literature and results of Monte Carlo analysis.

The common limitation of these researches is that the spatial randomness is never included. The same limitation also exists in the studies of corrosion initiation progress, where the corrosion initiation progress is assumed uniformly distributed over the structures (Han et al. 2013, Ryan and O'Connor (2013)).

2.3 Involvement of spatial randomness on reliability assessment of corroded reinforced concrete structures

The great importance of spatial randomness of material properties and environmental conditions are gradually involved since more realistic probabilistic models have been developed by research community (Lay and Schießl (2003), fib 2006). Frier and Sørensen (2007) conducted a research to estimate the effect of randomness of main parameters on corrosion initiation. Meanwhile, scholars like Li (2004) and Lim et al. (2016) contributed to measurement and representation of spatial variability of corrosion.

With the available knowledge as foundation, reliability assessment of corroded concrete structures with spatial randomness have been widely investigated. Stewart and Suo (2009) assessed reliability of a simply supported beam with pitting corrosion at both ultimate limit state and serviceability limit state using one dimensional random fields. Kenshel and O'Connor (2009) did a similar reliability assessment and compare the influence of general corrosion and pitting corrosion. Papakonstantinou and Shinozuka (2013) presented a comprehensive model to simulate the concrete cracking induced by corrosion in concrete structures that appropriate for implementation on large-scale structures. Table 2.1 shows an overview of the related researches, where noticeable distinctions present among the involvement of corrosion effects and interpretation of spatial randomness. For instance, Marsh and Frangopol (2008) used Lognormal fields for the distribution of corrosion while Hajializadeh et al. (2015) used Normal fields and D. V Val (2007) used Gumbel fields. It is remarkable that the reliability assessment is not necessarily based on failure probability. B. Sudret (2008) used a probabilistic distribution of the Damage Length instead of failure probability to express the reliability of structures.

Although there are plenty of studies that involve spatial randomness into the assessment of time-developed corrosion effects, most of them perform reliability assessment based on a symbolic expression for the failure of cross sections or simple structural members. Except Allaix et al. (2011) combined Monte Carlo Simulation with Finite Element Analysis for corrosion progress, but evaluation of structural capacity is not included. The main reason of such limitation relates to the impletion of traditional compute methods such as the Monte Carlo simulation which is extremely unpractical to be combined with numerical structural computation.

2.4 Concluding remarks

The review of literature drives to the conclusion that has already been mentioned in Chapter 1, that the analysis to combine failure probability calculation and spatial variability of corrosion effects on reinforced concrete structures has two major limitations:

One of the limitations is that, most of researchers use symbolic expression to calculate structural strength and load effects, which is only applicable for simple structures. There are some studies that combined structural reliability with finite element analysis to calculate structural resistance but never included corrosion. One example is the research of Cheng (2014), that FORM analysis is performed with the models including spatial variability of Young's modulus and sectional moment.

Another limitation is that the probabilistic models in term of corrosion are not well established. The structural influence of corrosion is not expressed in a statistical term where the uncertainties are quantified. Also the statistic model of corrosion distribution is proposed without the concern of spatial correlation and even the experimental quantification of the spatial correlation is not available.

Table 2.1 Overview of related studies

Reference	Structure	Corrosion effects				Spatial variability	Methods	Load effects	Time dependence
		Concrete crack	Bar area	Steel property	Bond loss				
Stewart & Suo, 2009	Simply supported beam	√	√	√		1D Gumbel field	MCS with AS	√	√
Stewart & Mullard, 2007	Cover of a deck	√				2D Normal field	MCS with AS	No	√
Marsh & Frangopol 2008	Critical section of a slab		√			2D Lognormal field	MCS with AS	√	√
Hajializadeh et al. 2016	Simply supported beam		√	√		2D Normal field	MCS with AS	√	√
Kenshel & O'Connor 2009	Simply supported beam	√	√			1D Normal field	MCS with AS	√	√
Sudret, 2007	Bar area		√			1D Lognormal field	FORM and MSC with AS	No	√
Allaix et al. 2011	Cross-section	√	√	√		2D Normal field	MCS with FEA for corrosion progress	No	√
Papakonstantinou & Shinozuka, 2013	Surface of a slab	√				2D Normal and lognormal field	MCS with AS	No	√
Li, 2004	Surface of a beam	√				1D Normal field	MCS with AS	No	√
Val, 2007	Simply supported beam					1D Gumbel field	MCS with AS	√	√
Cheng, 2014	Fixed end beam	ULS and SLS considering Young's modulus, sectional moments of inertia				1D Lognormal field	FORM with FEA	√	No
Lim et al., 2016	Simply supported beam	√	√	√	√	2D Gumbel field	Single FEA of experimental sample	√	No
Akgül & Frangopol, 2004	Critical section of girders	√	√			No	MCS with AS	√	√
Val at al. 1998	2D Slab		√		√	No	FORM with FEA	√	√
Sheikh et al. 1990	Pipe	Pipe leaking occurance				No	MCS with AS	No	√
Frier & Sørensen, 2007	Surface of piers	Corrosion initiation				2D Lognormal field	MCS with FEA for corrosion progress	No	√
Shayanfar et al. 2015	No detail	Corrosion initiation				No	MCS and CSS with AS	No	√
Nogueira & Leonel, 2013	No detail	Corrosion initiation				No	MCS and FORM with AS	No	√
Zhang et al. 2015	No detail	√				No	MCS and TM with AS	No	√
Chiu et al. 2015	No detail	√				No	MCS with AS	No	√
Ryan & O'Connor, 2013	No detail	Corrosion initiation				No	MCS with AS	No	√
Han et al. 2013	Surface of harbor facilities	Corrosion initiation				No	FORM with AS	No	√

Note:

MCS=Mote-Carlo Simulation;   AS=Analytical Solution;   CSS= Charged System Search method;   TM= Third-Moment method

FORM=First Order Reliability Method;   FEA=Finite Element Analysis;   ULS=Ultimate Limit State;   SLS=Serviceability Limit State

3 Methods

3.1 Modelling of corrosion of reinforcement in concrete

Reinforcement corrosion is one of the most common deterioration mechanism in concrete structures. Mechanical behaviors of reinforced concrete structures including the strength, stiffness and force redistribution are affected by reinforcement corrosion. Reinforcement corrosion also can cause severe surface cracking that expose the structure to detrimental environment and aggravate the deterioration progress.

3.1.1 Deterioration process

3.1.1.1 Corrosion initiation

In reinforced concrete, the reinforcements are protected from corrosion by the concrete, not only because of the physical resistance, but also a protective passive layer forms on the surface of steel due to the high PH within the concrete. However, two factors may break this passive layer and initiate corrosion: chloride ions that come mostly from deicing salts or seawater, and carbon dioxide from the atmosphere.

Chloride ions penetration is a complex process. Different transport mechanisms are involved, such as ionic diffusion, permeation, migration and convection. Simpler models based on Fick's second law of diffusion are often used in practice. By solving equation of Fick's second law of diffusion for the constant surface chloride conditions, chloride ion penetration equation is written in terms of depth (c) over time (t) as $C(c,t)$.

Carbon dioxide (CO_2) from the atmospheric can have chemical reactions with the alkaline components of the cement paste and the carbonation of concrete will introduce corrosion. There are two conditions that allow the reactions occur: a certain amount of water and significantly decrease of the PH in concrete. The critical carbonation depth is used to judge the initiation of steel corrosion in fully carbonated concrete. Carbonation depth is the average distance from the surface of concrete to where carbon dioxide reacts with the alkalinity in the cement. In the mid-1970s Martin et al. (1975) and Schiessl (1976) presented a modified model based on Fick's first law taking into account the influence of the moisture content of the concrete on the diffusion coefficient of CO_2 and the back diffusion of $Ca(OH)_2$. They ended up with the conclusion that there was a final carbonation depth given in the equation by Kropp and Hilsdorf (1995).

3.1.1.2 Corrosion propagation

Corrosion rate is an important parameter used to quantitatively predict the corrosion deterioration of reinforced concrete structures. The corrosion rate is usually described in terms of the corrosion current density, i_{corr} ($\mu A/cm^2$).

An empirical model has been developed by Liu (1998). 2927 measurements were recorded during a 5-year outdoor exposure of the large reinforced concrete slab specimens. According to the test results, the corrosion current density i_{corr} depended on the chloride concentration, temperature, ohmic resistance of the concrete cover and time. Based on the data of Liu, Vu and

Stewart (2000) developed a simplified model with assumption that oxygen availability on the steel surface is the governing corrosion factor. This model is expressed as:

$$i_{corr}(t_p) = i_{corr}(1) \cdot 0.85 t^{-0.29} \tag{3-1}$$

where t is time since corrosion initiation and $i_{corr}(1)$ is the corrosion rate at the start of corrosion.

The model proposed by Vu and Stewart only depends on concrete characteristics (water/cement ratio and concrete cover) and time, which is more suitable for the case study in this thesis. However, the model may not be applicable to cases where concrete resistivity is the dominant factor.

3.1.2 Effects of corrosion

3.1.2.1 Bar-section reduction and change of steel properties

In report of CEB/fib (2000), corrosion of reinforcement is classified into general corrosion and local corrosion. General corrosion is caused by chloride contamination or carbonation. Its main consequence is the volume expansion of iron oxides, which lead to concrete cracking and spalling before large reduction of steel cross section. On the contrary, local corrosion is caused by chloride contamination and has a consequence of extreme loss of bar section as well as loss of strength and ductility of reinforcement.

Reduction of the reinforcement bar area leads to decrease of shear and moment capacities as well as decrease of stiffness of the structure. Both general and local corrosion reduce the reinforcement bar area. However, the models of decreased bar area caused by general corrosion and local corrosion are different. Fig 3.1 shows simplified models to take account (a) general corrosion (b) local corrosion and (c) a mix of them. All of the models use the corrosion penetration index $\delta = p / D_0$ to measure the reduction of the cross-section, where p stands for the corrosion penetration depth and D_0 is the original diameter of the bar. For general corrosion, $p=2x$ and $A_s(\delta) = [1 - \delta_s(\delta)]A_{s0}$, where $\delta_s = \delta(2-\delta)$ For local corrosion, D. V. Val and Melchersz (1997) proposed the model to predict the loss of cross-sectional area of a reinforcing bar assuming that p=xmax.

$$\delta_s = \begin{cases} \dfrac{1}{2\pi}(\theta_1 - 2\gamma|1-2\delta^2|) + \dfrac{2\delta^2}{\pi}(\theta_2 - \gamma) & , 0 \le \delta \le 1/\sqrt{2} \\[3mm] 1 - \dfrac{1}{2\pi}(\theta_1 - 2\gamma|1-2\delta^2|) + \dfrac{2\delta^2}{\pi}(\theta_2 - \gamma) & , 1/\sqrt{2} \le \delta \le 1 \end{cases} \tag{3-2}$$

Where $\gamma = b_0/D_0 = 2\delta\sqrt{1-\delta^2}$, $\theta_1 = 2\arcsin\gamma$, $\theta_2 = 2\arcsin(\gamma/2\delta)$.
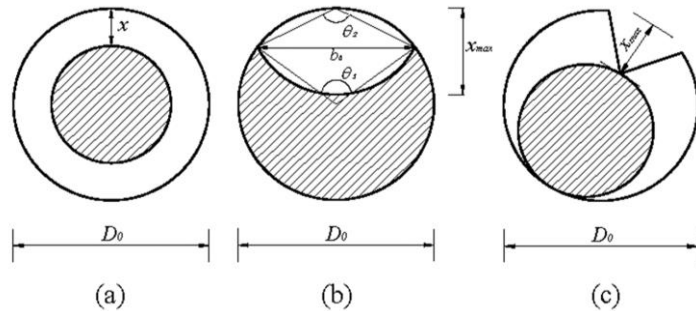

Fig 3.1 Models of reduction of reinforcement bar area (Biondini & Vergan, 2012)

In the case of local corrosion, the ultimate strain of reinforcement is severely reduced and ductility is lost. Du et al. (2005) proposed a linear expression $\varepsilon_{su} = (1 - a \cdot X)\varepsilon_{su0}$ to assess the reduction of ductility, and suggested that with only 10 % of local corrosion the ductility of bars embedded in the concrete can be reduced to below the minimum requirement specified in design codes for use in high ductility situation. Furthermore, Almusallam (2001) found that reinforcements show brittle behaviour when corrosion loss exceeds 12.6% and others found complete loss of ductility when corrosion loss = 20%. A change in rebar ductility directly influences the stiffness of the structure, which leads to force redistribution and limits the load-carrying capacity of a statically indeterminate structure. Based on the results of experimental tests reported in Apostolopoulos & Papadakis (2008), the steel ultimate strain can be related to the damage index δ as follows (Vergani, 2010):

$$
\varepsilon_{su} = \begin{cases} \varepsilon_{su0} & ,0 \le \delta_s < 0.016 \\ 0.1521\delta_s^{-0.4583}\varepsilon_{su0} & ,0.016 < \delta_s \le 1 \end{cases} \tag{3-3}
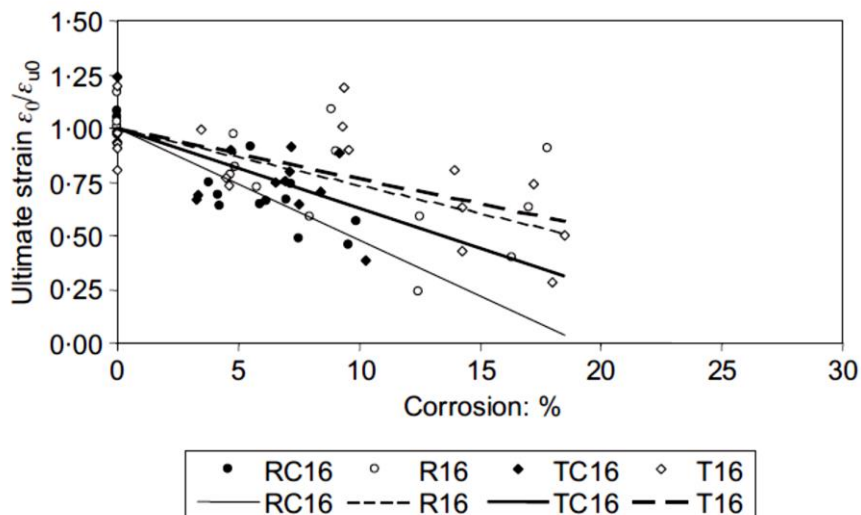$$

Fig 3.2 Reduction of reinforcement ultimate strain with corrosion loss (Du et al. 2005)
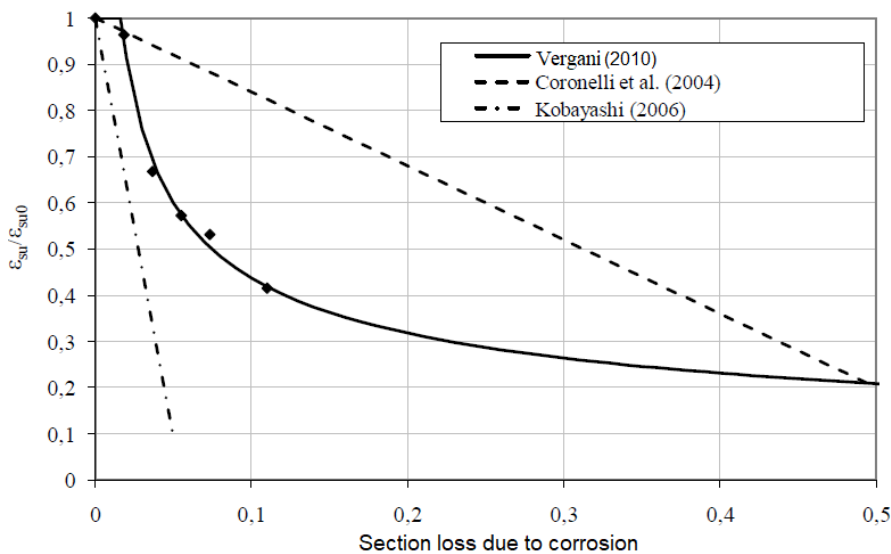

Fig 3.3 Reduction of reinforcement ultimate strain with corrosion loss (Vergani. 2010)

Yield strength and tensile strength of reinforcement are also reduced by local corrosion. Du et al. (2005) concluded the following equation that yield strength and tensile strength reduces linearly with corrosion loss: $f_s = (1 - b \cdot X) f_{s0}$, where X is the weight loss of reinforcement. They also provided b regressed from test results of different types of reinforcement, for both yield strength reduction and tensile strength reduction.
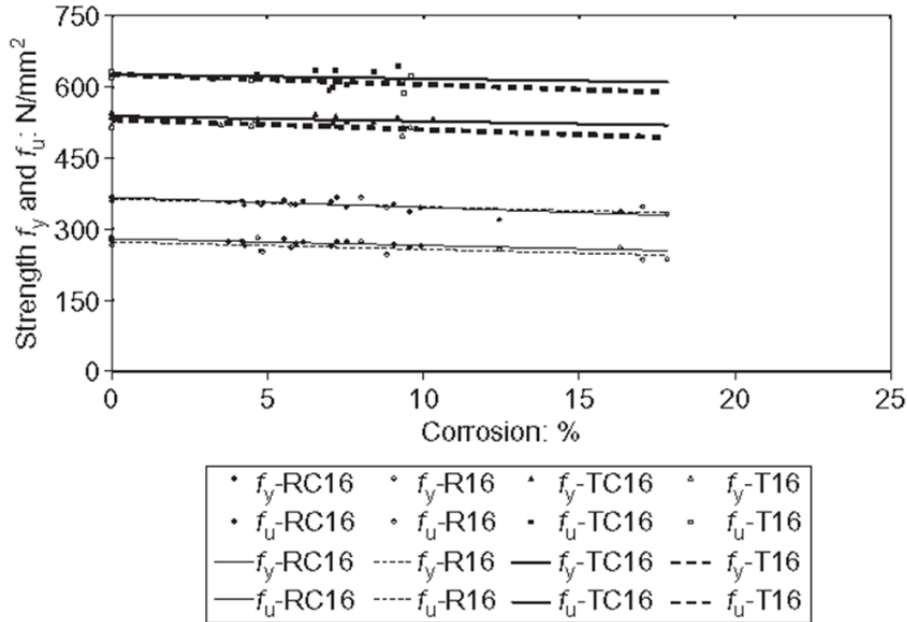

Fig 3.4 Reduction of reinforcement yield stress with corrosion loss (Du et al. 2005)

3.1.2.2   Loss of bond

The loss of the bond between reinforcement and concrete is a consequence caused by the volume expansion of the oxidation of metallic iron produced by reinforcement corrosion. Additional radial pressure at the steel-concrete interface and hoop tensile stresses in the surrounding concrete are generated by the volume expansion. Once the maximum hoop tensile stress exceeds the tensile strength of the concrete, the concrete will start to crack and the bond between reinforcement and concrete is weaken.

According to CEB-fib (2000), bond strength changes qualitatively as indicated in Fig 3.5. At the precracking stage for limited corrosion levels, the bond strength slightly increases due to the extra confinement introduced by the radical pressure develops at the concrete–steel interface. After the occurrence of corrosion-induced cracking, the splitting of the concrete cover leads to decrease of the bond strength. CEB-fib (2000) mentioned a linear reduction empirical model to take account the loss of bond for concrete with stirrup:

$$f_b = 4.75 - 6.64x \ for \ P_{tr} > 0.25 \tag{3-4}$$

$$f_b = 10.04 + (-6.62 + 1.98\frac{P_{tr}}{0.25}) \cdot (1.14 + x) \ \ for \ P_{tr} < 0.25 \tag{3-5}$$

Where P_{tr} is the ratiro of transverse reinforcement area at anchorage length versus the area of the main bars and x is the corrosion level measured by corrosion penetration depth.
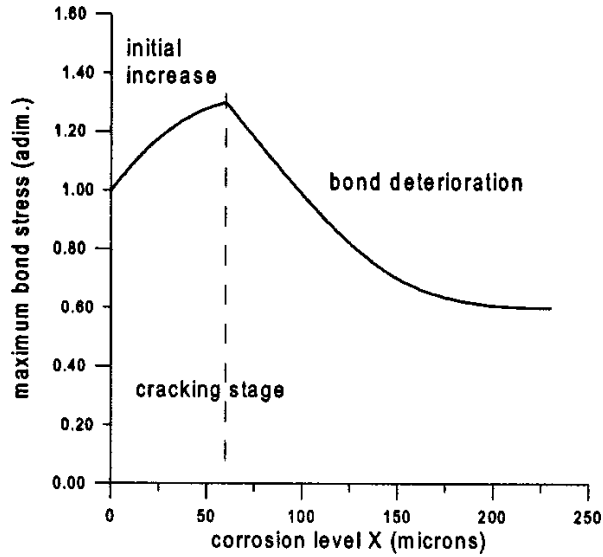
Fig 3.5 Relation between bond strength and corrosion level (fib, 2000)

Bhargava et al. (2008) reviewed a large set of experimental data from flexural testing and pullout testing. In spite of their large scattering, an empirical model to numerically evaluate the progressive bond degradation between the concrete and the reinforcing steel for the concrete specimens without stirrups is proposed.

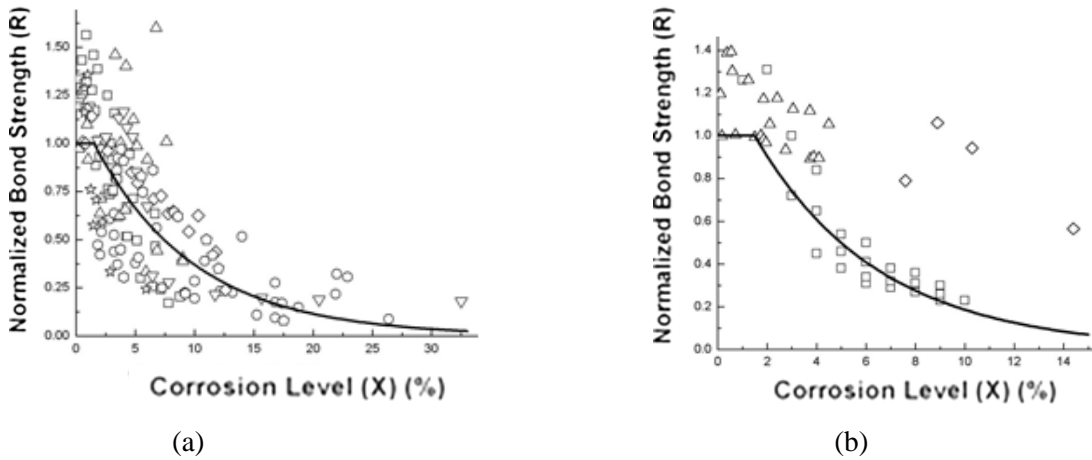| (a) | (b) |

Fig 3.6 Normalized bond strength as function of corrosion level for experimental data of (a) flexural testing and (b) pullout testing (Bhargava et al. 2008)

Based on flexural testing experimental data :
$$R_{\mathrm{fb}} = 1.0 \; for \; X < 1.5\%; \; R_{\mathrm{fb}} = 1.346e^{-0.198X} \; for \; X > 1.5\% \tag{3-6}$$
Based on pullout testing experimental data:
$$R_{\mathrm{fb}} = 1.0 \; for \; X < 1.5\%; \; R_{\mathrm{fb}} = 1.192e^{-0.117X} \; for \; X > 1.5\% \tag{3-7}$$
Where corrosion level X is defined as the loss of weight of reinforcing bar due to corrosion expressed as a percentage of the original bar weight and R_{fb} is defined as the ratio of bond strength at X to the original bond strength for the uncorroded specimen.

Compared to the linear reduction model of fib, the model has three advantages:

a) The model is presented in the normalized form to take care of the varied primitive bond strength due to differences in strength of concrete, type of reinforcements and confinement conditions.

b) The model is in exponential format, which is capable to capture the nonlinearity when corrosion level changes from low to high.

c) The model separately takes account for flexural testing and pull-out testing, which prevents obstructions caused by large variety between test methods.

Therefore the exponential model is used in this thesis.

3.1.2.3   Concrete cracking and spalling

Despite of the loss of bond, another consequence of the volume expansion is concrete spalling after severe concrete cracking occurs. Cover spalling results in reduction of the concrete cross section, which leads to a decrease of the internal lever arm and a decrease of the bending moment capacity. Severe loss of cover may result in full exposure of tension reinforcements that could change the structural behavior from flexural to tied arch with secondary effects (Zandi, 2015).

There are two approaches to model the local deterioration of concrete: one is with a degradation law of the effective area of concrete and the other one is to reduce the concrete strength. The degradation law of effective area of concrete can be expressed as $A_c = [1 - \delta_c (\delta)] A_{c0}$ (F. Biondini, 2004). However, the relationship between damage function δ_c and corrosion penetration index δ is not straightforward to establish. The reduction of concrete compression strength is a more direct approach. Coronelli and Gambarova (2004) provided detailed explanation for the expression $f_c = [1 - \delta_c (\delta)] f_{c0}$. The reduction of concrete strength is generally applied to the entire concrete cover. For the case that the corroded reinforcing bars are limited in the tensile zones and zero tensile strength is assumed for concrete, there is no necessity to model the local deterioration for concrete.

3.2   Random field and reliability methods

3.2.1   Random field: modelling of spatial variability

During the manufacturing, erection, and utilization of structural elements, random variability in spatial distribution is shown in many structural parameters, such as material properties, geometric parameters and loads show. Random fields are usually used to represent the uncertain quantities in consideration of the spatial variability. A random field $H(x, \vartheta)$ can be defined as a curve in $L^2(\Theta, F, P)$, where $L^2(\Theta, F, P)$ refers to vectoral space of real random variables with finite second moment ($E[X^2] < \infty$). $H(x, \vartheta)$ is a collection of random variables indexed by a continuous parameter x (B Sudret & Der Kiureghian, 2000).

In terms of the physical problem in this thesis, x can be regarded as the location in the space. If the random field $H(x, \vartheta)$ is considered at a fixed location, x, it is a random variable and is called a sample. For a fixed outcome, ϑ, of all the possible outcomes in the sample space, $H(x, \vartheta)$ is a deterministic function of x and is called a realization of the field. A random field can also be denoted with $H(x)$ in short. If the quantity $H(x)$ attached to location x is a random variable then the random field is called univariate. If the quantity $H(x)$ attached to location x is a random

vector, the random field is called multivariate. The random field can be defined in one dimension or in multiple dimensions according to the dimension of x.
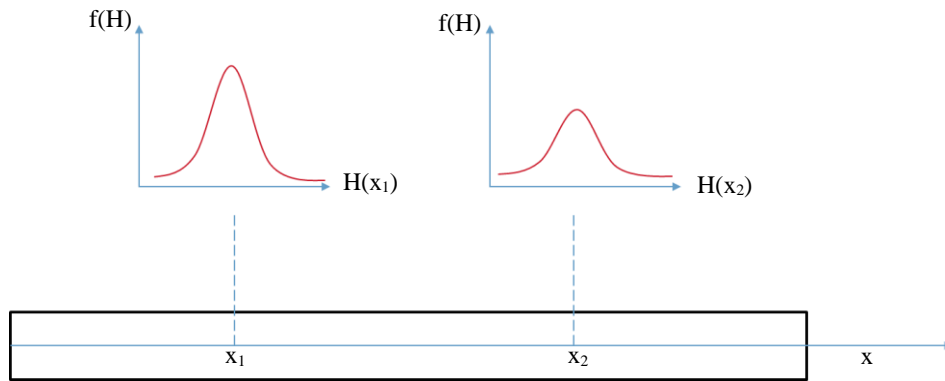

Fig 3.7   Illustration of a one dimensional random field

The random fields used in this thesis are characterized by the probability distribution function and correlation function between points (x). Moreover, the random field is homogeneous as the probability distribution is constant and the correlation function is only depend on the difference of x_i-x_j only. The probability distribution function is parameterized by distribution type and stochastic moments. For random fields, the moments can become functions over space as well. The correlation function between points is described by correlation length or scale of fluctuation. Correlation length or scale of fluctuation l_{cor} is a measure of the distance within which points are significantly correlated (Vanmarcke 1984). Take the exponential auto-correlation function for a one dimensional problem as an example, the correlation coefficient between location i and j is:

$$\rho_{ij} = \exp\left[\frac{-|x_i - x_j|}{l_{cor}}\right] \qquad (3\text{-}8)$$

Where ρ_{ij} is the correlation coefficient, x_i and x_j are the locations in the one dimensional space, and l_{cor} is correlation length.
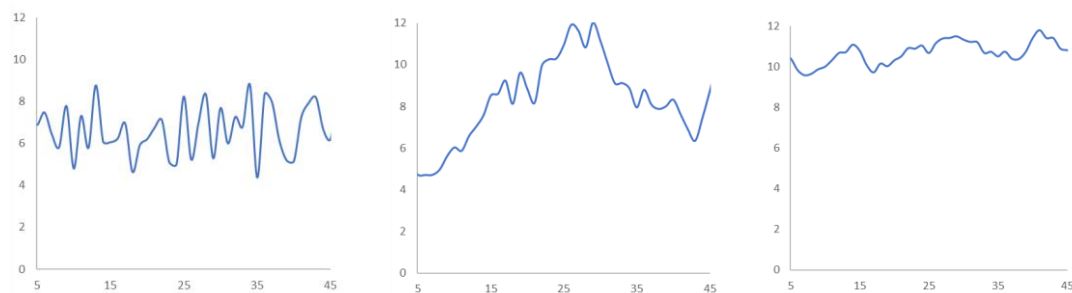
Fig 3.8 Realization of a one dimensional random field with different correlation length
(from left to right, the correlation length increases)

Points separated by a larger distance than l_{cor} will show little correlation, and practically no correlation will be observed when points are separated by a significant larger distance than l_{cor}.

3.2.2   Discretization of random field
If the random fields are to be treated numerically, an approximation of continuous random fields

by means of a finite set of random variables is required, which is called. random field discretization. The discretization reduces the random fields to a set of random variables which are contained in the vector **X**. The distance between two adjacent random variables in a discretization is limited by an upper bound and a lower bound. First, an upper bound of the distance is given based on the correlation length. In order to capture the essential features of the random field, the distance between two adjacent random variables has to be short enough. The element size should be smaller than half of the correlation length for a satisfactory representation of the random field. However, an excessively fine mesh yields highly correlated random variables and may result in a nearly singular correlation matrix. A nearly singular correlation matrix may cause numerical difficulties when a transformation to the standard normal space is required (Matthies et al., 1997).

The discretization methods can be divided into three groups: point discretization, average discretization and series expansion methods. Only point discretization and especially midpoint method is detailed explained here, as it is the chosen method used in this thesis.

Point discretization refers to that the random variables are selected values of $H(\boldsymbol{x}, \boldsymbol{\vartheta})$ at some given points $\boldsymbol{x}_i$. There are three advantages of the point discretization methods:
    i. the covariance matrix is easy to compute;
    ii. the covariance matrix is positive defined;
    iii. there is no restriction to Gaussian random fields.

The midpoint method (MP) introduced by Der Kiureghian and Ke (1988), approximates the random field in each element by a single random variable defined as the value of the field at the centroid $\boldsymbol{x}_c$ of this element. The approximated field is then entirely defined by the random vector. Its mean and covariance matrix are obtained from the mean, variance and autocorrelation coefficient functions of $H(\boldsymbol{x}, \boldsymbol{\vartheta})$ evaluated at the element centroids. Each realization of $H(\boldsymbol{x}, \boldsymbol{\vartheta})$ is piecewise constant, the discontinuities being localized at the element boundaries. (Sudret and Der Kiureghian, 2000)

There are three disadvantages of midpoint method:
    i. the MP method tends to over-represent the variability of the random field;
    ii. the point discretization methods are only useful for medium to long correlation distances due to the requirement of the small mesh size;
    iii. the shape and size of all these elements should be the same.

3.2.3   Theories and methods of the reliability analysis

Reliability methods aim at evaluating the failure probability of a system where randomness is taken into account in the modelling. Classically, the system is decomposed into components and the system failure is defined by the joint failure of components in terms of various scenario. The determination of the failure probability of each component is of paramount importance.

3.2.3.1   Limit states of concrete structures

The concept of limit state is used to define failure in the context of structural reliability analyses. A limit state is a boundary between desired and undesired performance of structures. The desired performance and undesired performance can be expressed by a performance function g

(X), which is defined as follows:

$g(X) > 0$ defines the safe state.

$g(X) < 0$ defines the failure state.

$g(X) = 0$ defines the limit state.

The failure state does not necessarily mean the breakdown of the structure, but the fact that certain requirements of serviceability or safety limit states have been reached or exceeded.

Limit states can be of different categories. The principal categories are ultimate limit states and serviceability limit states. The ultimate limit state represents a situation where the structure starts to lose its integrity. From the ultimate limit state, the structure passes into an irreversible state that may have a catastrophic nature. A serviceability limit-state corresponds to the limit between an acceptable and a not acceptable state under normal use. The serviceability limit-state is with respect to reversible damage of the structure that the structure can back to the safe set by unloading.

For serviceability limit-state of corroded reinforced concrete structures, controlling of the maximum width of surface cracking is one of the requirements. Another commonly consideration for serviceability is the maximum deflection. As for ultimate limit states, the losing of integrity can be interpreted in several ways. The most evident representation is the resistance to applied load. However, sometimes it is difficult to directly calculate the resistance in terms of the load. Then the resistance in terms of critical load effects should be chosen as the criteria. For example, tensile strength of concrete or bond-slip strength between reinforcement and concrete.

3.2.3.2 Compute methods

Reliability methods can be classified into four groups according to Probabilistic Model Code proposed by the Joint Committee on Structural Safety:

Level IV risk-based methods: Risk is used as a measure of the consequences of failure. Different designs are compared on an economic basis taking into account uncertainty, costs and benefits.

Level III fully probabilistic methods: The uncertain quantities are modelled by their joint distribution functions. The probability of failure is calculated exactly.

Level II probabilistic methods with approximations: The stochastic variables are implicitly assumed to be normally distributed, which are modelled by the mean values, the standard deviations and the correlation coefficients.

Level I semi-probabilistic methods: The uncertain parameters are modelled by one characteristic value for load and resistance with safety factors.

In structural design and assessment, level I semi-probabilistic methods are already widely used. The simplifications regarding the probabilistic component in the modelling makes this method suitable for relatively fast design calculations. Level IV risk-based method is aimed at decision making on an economic basis, which is not the objective of this research. Therefore, representative computation methods on level III and level II are introduced here.

For fully probabilistic analysis, the calculation of the probability of failure P_f through numerical

integration is computationally not feasible for more than five variables. In those cases, a commonly used solution to calculate P_f is by generating random samples, such as using the Monte-Carlo simulation (MCS) method. Variables can be drawn from a known joint probability distribution function. For each variable x_i (i = 1, …, m), one simulates N realizations x_{i1}, …, x_{iN}. For each set j (j = 1, …, N), one calculates $g(x_{1j}, ..., x_{mj})$. In case $g(.) < 0$, a counter N_f is increased by one. After N simulations one calculates: $P_f = N_f / N$. In case $N \to \infty$, one obtains the failure probability P_f. The number of simulations N is determined by the desired relative accuracy of P_f. Different "variance reducing" techniques have been developed to improve the efficiency of simulation. Importance sampling technique is one of the most widely used one. However, Importance Sampling requires pre-knowledge of the most likely failure point, which are not always available. Subset Simulation overcomes this disadvantage of Importance Sampling. Thus Subset Simulation is used in this thesis.

Subset Simulation is a technique introduced by Au and Beck (2001) that improve the efficiency of simulation by solving a series of simpler reliability problems with intermediate failure thresholds. Consider a sequence of failure domains $D_1 \supset D_2 \supset ... \supset D_m = D_f$ that $D_f = \bigcap_{k=1}^{m} D_k$. The probability mass of each intermediate failure region can be combined by means of conditional probability. With an appropriate choice of the intermediate thresholds for each failure domain, P_f can be evaluated as a series of structural reliability problems with relatively high probabilities of failure that are then solved with MCS. The convergence of each intermediate estimation is therefore much faster than the direct search for P_f.
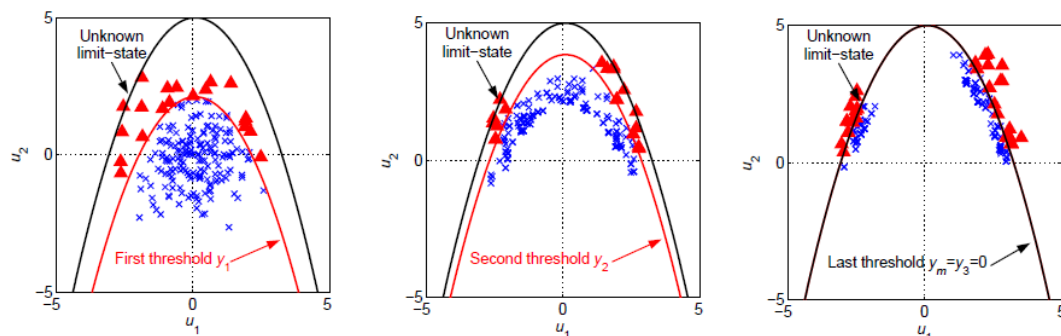

Fig 3.9 Illustration of Subset simulation (Bourinet, 2010)

In level II methods the variables need to be transferred into normal distributions where mean of the base variables and their covariance matrix are taken into account to determine the failure probability. The joint probability density function is simplified and the limit state function is approximated at the design point. The first order reliability method (FORM) and the second order reliability method (SORM) are two common used solutions to approximate the nonlinear limit state function. The two methods have similar steps. The first step is mapping the problem in the standard normal space by using an iso-probabilistic transformation. The second step is to evaluate reliability index and find the design point. The last step is to obtain an approximation of the probability of failure from the reliability index.

The concepts of reliability index and design point often come with probabilistic analysis with approximations. The most complete form of these concept is credited to Hasofer and Lind, who gave it a precise definition. Hasofer and Lind proposed not considering a physical variable

space, but performing a transformation of variables to a new space of statistically independent Gaussian variables, with zero mean and unit standard deviations. In the standard Gaussian space of variables u_i, P*is the point closest to the origin in the limit-state surface and is defined as the design point or the point with most probable failure. The reliability index β is defined as the distance between the origin O and the point P*. Reliability index β is considered positive if the origin point belongs to the safety domain; if the origin point belongs to the failure domain, β is defined as negative.

Apart from the index, important information is given by the direction cosines $α_i$. $α_i$ is the cosine value of the vector P*O oriented from P*toward O. The value $α_i$ represents the influence of the random variable u_i in the limit state and an approximation of the influence of the physical variable x_i which is associated with it. The direction cosines $α_i$ is also called sensitivity factor in a sensitivity analysis. One important application of the sensitivity factor is found by Mahadevan and Haldar (1991). From their numerical investigation, only variable x_i with $|α_i| >$ 0.3 deserves to be modelled with random fields for a better accuracy of the results.
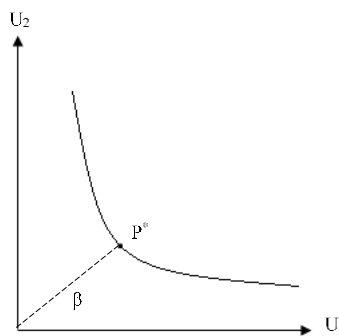

Fig 3.10 Definition of reliability index and design point

The difference between FORM and SORM is that FORM replace the limit state surface by a linear surface while SORM replace the limit state surface by a quadratic surface. FORM is used as the level II method in thesis. Although FORM is proven to be very effective, that require much less evaluation of the limit state function to yield a convergent result than Subset Simulation, it can be inaccurate for nonlinear limit state function with high failure probability and can be difficult to solve for multi-design point problem.

During the probabilistic finite element analysis, a number of evaluations of limit state function is carried out. For probabilistic finite element analysis, the exact limit state function evaluations are evaluations of limit state function, $G(X)$, where the structural response, $R(X)$, is computed by finite element analyses. The exact limit state function evaluation is computationally expensive and drastically reduces the efficiency of the probabilistic finite element analysis.

The response surface function, G^*, is constructed and updated by fitting a symbolic expression to the exact limit state evaluations. In other word, the response surface function provides an approximation of the structural response. Approximate limit state function evaluations refer to the evaluation of limit state function where the response surface function is applied to compute

the structural response. The approximate limit state function evaluation is computationally cheap and significantly increases the efficiency of the probabilistic finite element analysis.

There are two types of response surface used in this thesis: polynomial response surface and kriging response surface. For the polynomial response surface, a polynomial expression (up to three order) is regressed from a collection of the exact limit state evaluations. The exact limit state evaluations lay around the approximated polynomial fitting but not necessarily lay on it. For the Kriging response surface, it is a stochastic interpolation algorithm which assumes that the model output is a realization of a Gaussian process. Given a set of exact limit state evaluations, a Kriging predictor returns the mean and the variance of a Gaussian process that interpolates them. One great advantage of Kriging model is that not only one best expression is given, but a confident interval is also indicated.

3.3 Probabilistic models for corroded reinforced concrete structures

3.3.1 Probabilistic models for properties of the non-deteriorated structures

For a particular failure mode under consideration, uncertainty modelling must take in account of those variables whose variability is judged to be important in the corresponding performance function. Calculation models shall describe the structure and its behavior according to the limit state under consideration, including relevant actions and environmental influences. Models should generally be regarded as simplifications that involve the decisive factors while neglect the less important ones.

Most engineering structures are affected by the following four types of uncertainty:
- intrinsic physical or mechanical uncertainty
- measurement uncertainty arisen from random and systematic errors in the measurement of the physical quantities
- statistical uncertainty due to reliance on limited information and finite samples
- model uncertainty related to the predictive accuracy of calculation models used.

Probabilistic models of non-deteriorated structures exist in literatures with two format: statistical analysis of measurement of test based on specific cases, or standardizations in guidelines or codes based on a wide range of data resources. Some influential standardizations of probabilistic models are Probabilistic Model Code (JCSS, 2000), Bases for design of structures - Assessment of existing structures (ISO, 2010), General Principles on Reliability for Structures (ISO, 2015), and Partial Factor Methods for Existing Concrete Structures (fib, 2016). The standardizations often classify the probabilistic models for:
- action models
- structural models which give action effects (internal forces, moments etc.)
- resistance models which give resistances corresponding to the action effects
- material models and geometry models .

Table 3.1 Summary of probabilistic models provided by JCSS and fib.

Variable	JCSS	fib
Concrete compressive strength	Basic property f_{c0} follows lognormal distribution. Mean and	Lognormal distribution. COV is 0.15

	COV* depend on the concrete class	
Other concrete characteristics	Related to f_{c0} with additional parameters	N/A*
Steel tensile strength	Normal distribution with Std. 40MPa	N/A
Steel yield strength	Normal distribution with Std 30MPa	Lognormal distribution. COV is 0.05
Steel ultimate strain	Normal distribution with COV 0.09	N/A
Model uncertainty of concrete	Lognormal distribution with mean of 1.2 and COV of 0.15 (static , bending moment capacity)	Lognormal distribution. If concrete governs then COV is 0.14. If reinforcement governs then COV is 0.06
Permanente load	Normal distribution, COV depends on the source of the load	Normal distribution with COV 0.1
Traffic load	N/A	Annual maximum value is Gumbel distribution of COV 0.75. Time invariant component is lognormal distribution with COV 0.1

*Note: COV=Coefficient of variation   N/A=Not available

In addition to the standardization, there are individual researchers provided statistical analysis of experimental data or numerical simulations based on some specific cases. Their works commensurate the lacking models in standardization and gives a view from practical use. For example: Unanwa and Mahan (2014) performed statistical analysis of compressive strength of concrete for highway bridges; Engen et al. (2017) quantified the modelling uncertainty of non-linear finite element analyses of large concrete structures.

3.3.2   Model uncertainties for the corroded reinforced concrete structures

The corrosion effects on ultimate limit state is introduced in Chapter 4. Accordingly, the models considering such effects also contain uncertainties, which are rarely studied before. Generally speaking, the models used to describe relation between corrosion level with material properties leads to higher level of model uncertainty. fib (2016) gives suggestions on model uncertainty variables of corroded structures. Allaix et. al (2015) conducted statistical analysis of model uncertainty for the loadbearing capacity of corroded simply supported RC beams. These works provide valuable information for reliability assessment of corroded reinforced concrete structures. However, the model uncertainty terms integral the uncertainties of different models together, and also account for the variabilities in corrosion. Such integral brings convenience for calculation, but can be an over simplified or over general approach for specific cases.

An alternative way is to quantify the model uncertainty of each model describe the corrosion effect. Such quantification can be derived from existing experimental data. Sajedi and Huang (2015) proposed a probabilistic prediction model for average bond strength considering corrosion effect. This probabilistic prediction model is inspired for uncertainty quantification for models of corroded reinforced concrete structures. There are two disadvantages of this model: first, the model is in a complex form that contains seven variables; second, the model is

expressed in terms of concrete compressive strength that will repeatedly account uncertainty of concrete properties. In the present thesis, the uncertainty of bond model is quantified in a different method, which can be also used to quantify uncertainties for other models of corrosion effect. Meanwhile, the coupled probabilistic finite element analysis scheme is used to propagation the uncertainty of bond model into reliability analysis of a simply supported RC beam. The computation is also served as an example of the utilization of the computation scheme.

3.3.3 Spatial variability of corrosion

Pitting corrosion is described with pitting factor $R = p/P_{av}$, where p is the maximum pit depth and P_{av} is the penetration calculated based on general corrosion ($P_{av} = 0.0116 i_{corr} t$). A popular approach to modeling the spatial variety of pitting corrosion is based on statistical characterization of maximum pit depth using extreme value theory, in particular, the Gumbel distribution. The pitting factor R for each discretized element is treated as a random variable modeled by the Gumbel distribution where the Gumbel parameter are modified from suggested value by Stewart (2009).

The cumulative distribution function and equation to modify the Gumbel parameter are:

$$F(x) = \exp\left\{-\exp\left[-(x-\mu)\alpha\right]\right\} \tag{3-9}$$

$$\mu = \mu_0 + \frac{1}{\alpha_0}\ln(L_u / L_0) \tag{3-10}$$

$$\alpha = \alpha_0 \tag{3-11}$$

Where μ_0 and α_0 are Gumbel parameter measured from specimens with length of L_0, μ and α are Gumbel parameter for an element in discretization with length of L_u.

Equation (5-1) is based on the following assumption that when a larger element of length L_u is divided into L_u / L_0 smaller elements of length L_0:

i. Variables for each smaller elements are independent from each other;

ii. The capacity of the larger element is determined by the smaller element with largest pitting depth.

Then, for the small element:

$$P_f = P_0(\exists R > x_1) = 1 - \exp\left\{-\exp\left[-(x_1 - \mu_0)\alpha\right]\right\} \tag{3-12}$$

For the large element:

$$\begin{aligned} P_f &= P_u(\exists R > x_1) \\ &= 1 - (1 - P_0)^{L_u/L_0} \\ &= 1 - \left\{\exp\left[-\exp(-(x-\mu_0)\alpha)\right]\right\}^{L_u/L_0} \\ &= 1 - \left\{\exp\left[-\exp(-(x-\mu_0 - \frac{1}{\alpha}\ln(L_u/L_0))\alpha)\right]\right\} \end{aligned} \tag{3-13}$$

Which leads to equation (3-9)-(3-11).

If condition (i) is not satisfied: for smaller elements are fully correlated, $P_f = P_u(\exists R > x_1) = P_0$; for unknown correlation, $P_0 < P_f < 1 - (1 - P_0)^{L_u/L_0}$ which leads to $\mu_0 < \mu < \mu_0 + [\ln(L_u/L_0)]/\alpha_0$. If condition (ii) is not satisfied, Gumbel distribution is not suitable to model the pitting depth. For a finite element model, if the mesh is optimized to a convergent one, then the element length equal to the mesh size can be regarded to satisfy condition (ii).

There is no general conclusion of the spatial correlation of pitting corrosion. While some scholars (Stewart, Val, Kioumarsi) assume no spatial correlation of pitting corrosion, Kenshel and O'Connor (2009) adopted auto correlation function with correlation length 2000 mm. Therefore, the effect of the spatial correlation of pitting corrosion in reliability assessment of corroded RC structures will be studied for the case study.

4 Nonlinear finite element analysis of a RC continuous girder

A reinforced concrete continuous girder is adopted as the case study to illustrate the influence of spatial variability of corrosion on structural reliability. In this chapter, the case will be concisely introduced. The finite element modelling of the continuous girder will be described. Modelling of corrosion effects in the finite element model will be explained. Nonlinear finite element analyses of the continuous girder will be performed for the case with and without corrosion. A comparison will be presented to show the difference in structural response of uniform distributed corrosion and localized distributed corrosion.

4.1   Description of the case study

The case study is based on a real, corroded, reinforced concrete bridge. The bridge was built in the seventies, located in Portugal, and was in a very advanced state of degradation. Finally, the bridge was demolished. The bridge is composed of a deck of four longitudinal beams joined by a slab. The deck is supported by two abutments and two piers founded in the bed of the river Lis. All structural elements are reinforced, non-prestressed concrete. The bridge is located near to the mouth of the river, where a marine environment is formed due to the saline water of the Atlantic Ocean. As a consequence, the bottom side of beams are heavily corroded due to the high level chloride contamination level, especially for the beam near sea side.

The total length of the deck is 60 m, distributed in three spans: 18.6 m, 22.8 m and 18.6 m. Dimensions of the structure and cross-sections are shown in Fig 4.1 and Fig 4.2. The four longitudinal beams have identical geometry. The cross section changes linearly from rectangular shape into T shape from support to span. The beam height is 1.25 m. The width of the flange is 1.1 m along the entire beam. The width of the web is 0.5 m at the center of side span and at the middle span. The reinforcement arrangement of reinforcement also differs in the side span, at supports and in the middle span.

In this study, only the ultimate limit state of the bridge is considered, that is flexural failure. Furthermore, solely the governing load combination is analyzed: combination of permanent loads and traffic load. The permanent load on the beam includes self-weight of the beam and extra dead load equal to 20 % of the self-weight. After Jacinto et al.(2015) the traffic load is assumed to be a tridem truck (3 axes). To reduce the computational burden the transverse load distribution of the bridge is treated in a simplified manner. This way the loads are reduced to a single beam that is analyzed separately. All subsequent analyses concern a single, isolated beam. On the single beam, the live load can be presented as three identical point load. Each point load is 150 kN and the distance between point loads are 1.5 m.
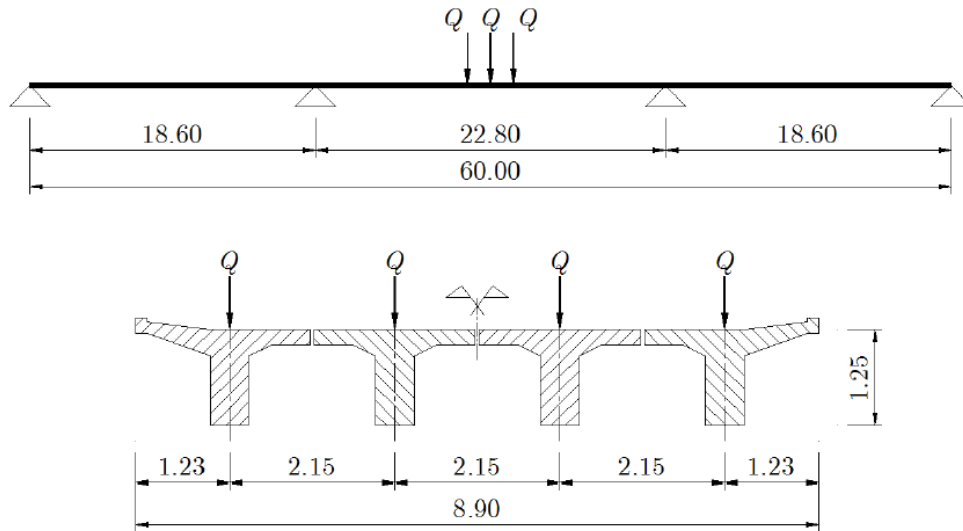
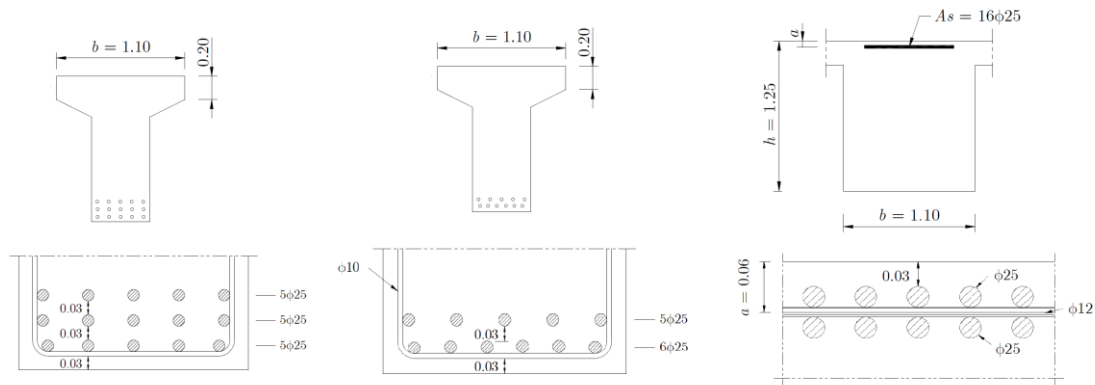Fig 4.1 Geometry, with dimensions in meter (Jacinto et al., 2015)

Fig 4.2 Cross-section of side span (left), mid span (middle) and supports (right), with the dimensions in meters and the bar diameters in millimeter (Jacinto 2011)

4.2 Finite element modelling

4.2.1 Physical model of sound structure

In this work, only one of the continuous beam is considered. Although the shape of the cross section varies along the length of the beam, it can be modeled as rectangular shape with constant area (width 1100 mm, height 1250 mm) along the entire length, if ultimate limit state is the criteria to assess the structure. The rectangular cross section approximation is appropriate since : (i) at ultimate stage the compression zone of concrete is inside the flange, and (ii) the concrete outside the flange zone does not contribute to the flexural resistance, and (iii) the critical cross section is in the midspan. The following section describes the applied finite element model that is based on the above assumptions and then verifies these three assumption through the results of finite element analysis.

A schematic representation of the model used in later analyses is shown in Fig 4.3 and important information as material properties, element type and load conditions are provided in Table 4.1, Table 4.2 and Table 4.3, respectively. Considering the real situation, the traffic load is live load

that can occur at any location along the beam. However, the ultimate capacity of the structure depends on the most unfavorable position of the traffic load. Under uniform distributed damages, the most critical sections of the structure are at the supports and in the midspan. As on-site observation indicates only bottom reinforcements suffered from corrosion, it can be regarded that the midspan is the critical section after corrosion. Thus, the traffic load is placed at the most unfavorable position for midspan cross-section, namely at the midspan.
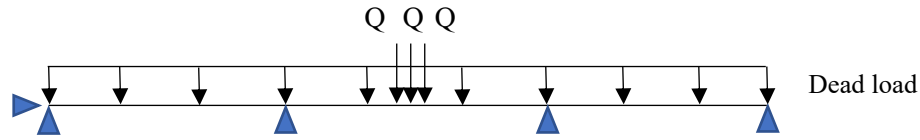

Fig 4.3 Schematic representation of the boundary condition and load condition

Table 4.1   Applied material models and properties

Material	Parameters	Constitutive model
Concrete	f_{cc}=-51.2 MPa, f_t=0 ε_1=0.002 ε_u=0.0035	
Steel	f_{sy}=440 MPa, f_{su}=550 MPa Es=200 GPa ε_{su}=0.08	

* Uniaxial constitutive models

The behavior of the concrete under tension is fully neglected. The behavior of the concrete under compression is modelled with an uniaxial parabolic-rectangular stress-strain curve. This parabolic-rectangular curve is described in Eurocode 2 for the design of concrete sections. Although the parabola-rectangular diagram is not an advisable model for nonlinear structural analysis of concrete due to the lack of a softening branch, it can be used for simplification of the concrete behavior with checking of the largest strain in concrete.

Uniaxial elasto-plastic material model with hardening is used for reinforcement. Failure of reinforcement is defined as rupture at ultimate strain. In the reliability analysis of the case study, with the inclusion of corrosion effect and the uncertainty of yield strength and ultimate strength, rarely the ultimate strength of corroded reinforcement is smaller than the yield stress of the corroded reinforcement. Such a conflict is a purely numerical phenomenon and does not have any physical meaning. In order to avoid physically impossible inputs and in turn an error in the finite element analysis, the ultimate strength is enforced to not smaller than the yield stress. In

symbolic expression: if $f_{sy} > f_{su}$ then $f_{su} = f_{sy}$.

Perfect bond is assumed, although corrosion may weaken the bond and increase slip between concrete and reinforcement. Due to proper anchorage, enough strength can always be developed in reinforcement even with weak bond. The ultimate strength of the continuous beam will not be influenced by the weak bond as long as the anchorage is adequate. As the limit state of the structure is targeted on the ultimate strength, the perfect bond assumption will not influence the calculated failure probability.

Table 4.2 Applied element types

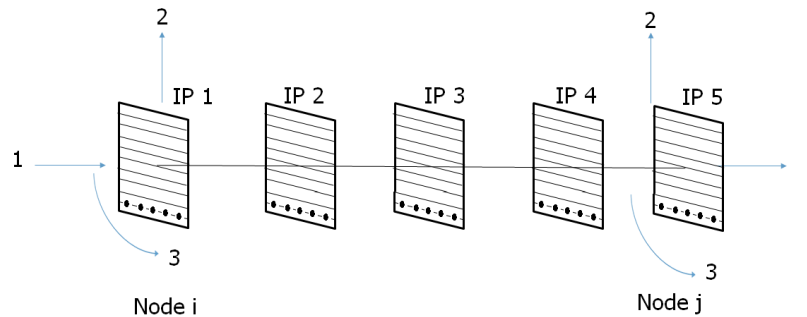| Element	Number	Length	Component	IPs along length	Section
Displacement-Based Beam-Column Element	200	300 mm	Concrete fiber and steel fiber	5	Width 1100 mm Height 1250 mm

Fig 4.4 Elements used in numerical simulations.

The discretized element is defined as displacement beam element with fiber section, that is discretized along their length (integration points) and across their cross-sections (fibers) to explicitly model the spread of plasticity. Displacement based element is different to concentrated plasticity models where elastic element is with rotational springs at the ends. Displacement based element permit spread of plasticity along the element and allows yielding to occur at any location along the element. To approximate nonlinear element response, constant axial deformation and linear curvature distribution are enforced along the element length. The beam element is discretized along their length by five integration points and across their depth by ten concrete fibers. Since the beam is subjected to unidirectional bending, only a single fiber is considered in transverse direction. Each individual reinforcing bar is represented by a steel fiber.

The permanent load is applied as uniformly distributed line load while the traffic load is modeled as three equal point loads. OpenSees take care of the equal loads, though the traffic load is in displacement control. The load step and convergence criteria are listed in Table 4.3. Regular Newton-Raphson algorithm is used for the nonlinear analysis. First the permanent load is applied to the structure with its full intensity, then the traffic load is gradually added until

failure (increase of displacements without further load increment).

Table 4.3 Load conditions

Load	Dead load	Traffic load
Descriptions	30 kN/m	3 point loads
Control method	Load control	Displacement control
Load step	1.5 kN/m per step, 20 steps	0.2 mm per step
Convergence	Displacement norm 10^{-3}	Energy norm 10^{-4}

4.2.2 Modeling of corrosion effects

In the case study, corrosion is assumed only occurs for (all) bottom reinforcements and is classified as pitting corrosion. The pitting factor $R= p/P_{av}$ is used to define the extent of pitting corrosion, where p is the maximum pit depth and P_{av} is the penetration calculated based on general corrosion ($P_{av} = 0.0116 i_{corr}t$). The maximum pit depth along a reinforcing bar affects the load capacity. For a given value of pitting factor R, the pitting depth after corrosion ignition time t is: $p(t) = 0.0116\, i_{corr}\, R\, t$. Where i_{corr} is the corrosion rate in $\mu A/cm^2$, and t is the time in years since corrosion has initiated. In this study i_{corr} is set to 2 $\mu A/cm^2$ corresponding to a stage with rapid propagating corrosion.

The corrosion effects included in this study are the reduction of rebar area (A_s), rebar yield strength (f_{sy}), rebar ultimate strength (f_{su}), and rebar ultimate strain (ε_{su}). The bond strength could also be affected by corrosion. However in the studied bridge, the reinforcements are properly anchored, and hence for this ultimate limit state verification no differences in structural behavior are expected between the case considering bond without and with corrosion. All corrosion effects are quantified by equations in terms of penetration index $\delta= p/D_0$. As mentioned in Chapter 3, the remaining area of reinforcement is expressed as: $A_s(\delta)=[1-\delta_s(\delta)]A_{s0}$, and

$$\delta_s = \begin{cases} \dfrac{1}{2\pi}(\theta_1 - 2\gamma\,|1-2\delta^2|) + \dfrac{2\delta^2}{\pi}(\theta_2 - \gamma) & ,0 \leq \delta \leq 1/\sqrt{2} \\[4mm] 1 - \dfrac{1}{2\pi}(\theta_1 - 2\gamma\,|1-2\delta^2|) + \dfrac{2\delta^2}{\pi}(\theta_2 - \gamma) & ,1/\sqrt{2} \leq \delta \leq 1 \end{cases} \tag{4-1}$$

Where $\gamma = b_0/D_0 = 2\delta\sqrt{1-\delta^2}$, $\theta_1 = 2\arcsin\gamma$, $\theta_2 = 2\arcsin(\gamma/2\delta)$.

Yield strength and tensile strength of reinforcement follows the expression: $f_s = (1-b\cdot\delta_s)f_{s0}$. The value of b is adopted from Du et al. (2005), using $b = 0.0016$ when calculating the yield strength and $b = 0.0026$ for the tensile strength. For ultimate strain of the reinforcement, the relation proposed by Vergani (2010) is adopted in thesis:

$$\varepsilon_{su} = \begin{cases} \varepsilon_{su0} & ,0 \leq \delta_s < 0.016 \\[2mm] 0.1521\delta_s^{-0.4583}\varepsilon_{su0} & ,0.016 < \delta_s \leq 1 \end{cases} \tag{4-2}$$

Fig 4.5 shows the normalized residual properties of the reinforcement with different level of average loss of cross section, assuming a corrosion initiation time of 50 years, which is approximated the existing life of the bridge, Fig 4.6 shows the relation between average loss of

cross-section with the pitting factor, with the corrosion ignition time t ranging from 20 years to 50 years. If t increases, corrosion will be more severe for the same pitting factor and reduction of the rebar cross-section will be more apparent.
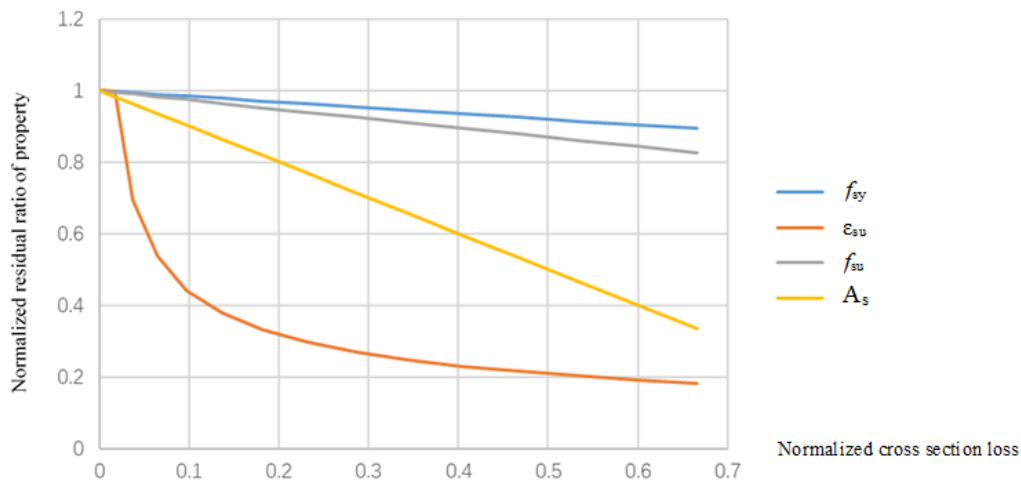

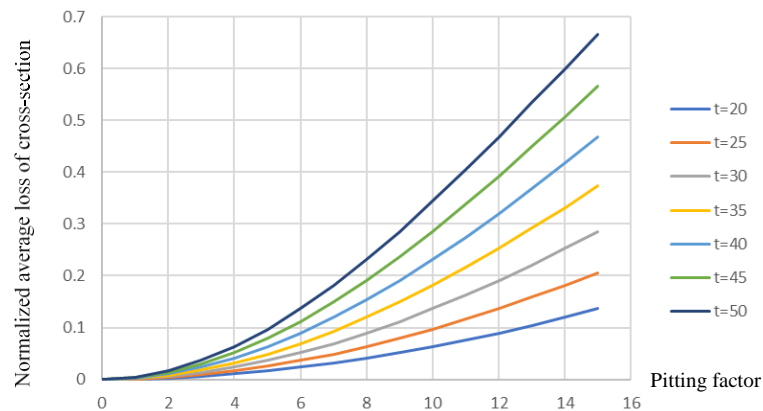Fig 4.5 Normalized residual of properties with cross section loss (t=50 years, i_{corr}=2 μA/cm^2)

Fig 4.6 Normalized loss of rebar area   (R=10, i_{corr} = 2 μA/cm^2)

4.3   Results nonlinear finite element analysis

4.3.1   Sound structure

Fig 4.7 shows the deflection and moment distribution of the structure at ultimate stage (failure) with combination of dead load and traffic load. The failure at ultimate stage is the rupture of the bottom reinforcement at midspan. Despite of the larger moment at support, the support has higher capacity compared to the midspan and it is in hardening stage when the midspan fails. Fig 4.8 shows the strain distribution in the cross section at midspan and at support. The strain distribution at midspan also confirms that the compression zone of concrete lays inside the flange. Thus, the modelling assumptions are satisfied. The strain distribution also shows that the concrete compressive strain is lower than the ultimate strain, which confirms the parabolic-rectangular diagram is proper to be used. Fig 4.9 shows the curve of value of one point load and deflection at midspan. Stage A corresponds to the yielding at midspan, stage B corresponds to the yielding at support and stage C corresponds to the rupture of reinforcement at midspan.

Fig 4.10 shows a comparison of the simplified model used in this thesis (OpenSees model) and a more complex model built in Diana. The Diana model reflects the change of cross section dimension along the beam and use a more advanced concrete model. The compressive strength of concrete is modeled with parabolic compression diagram where compressive strength is 51.2 MPa and fracture energy is 37.1 N/mm. The tensile strength of concrete is modeled by Hordijk softening, where the tensile strength is 3.69 MPa and fracture energy is 0.148 N/mm. The steel model is the same as the OpenSees model. The dead load is line load applied by force control and the point load is applied by arc-length control. In the comparison, it can be noticed that the load-deflection curves are very close and the capacity of the Dinana model is slightly higher (0.4 %) than the OpenSees model due to the tensile strength of the concrete.
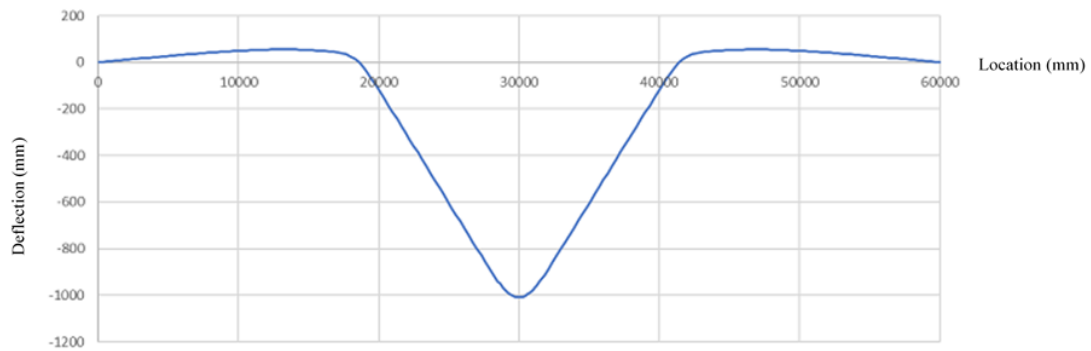
(i)
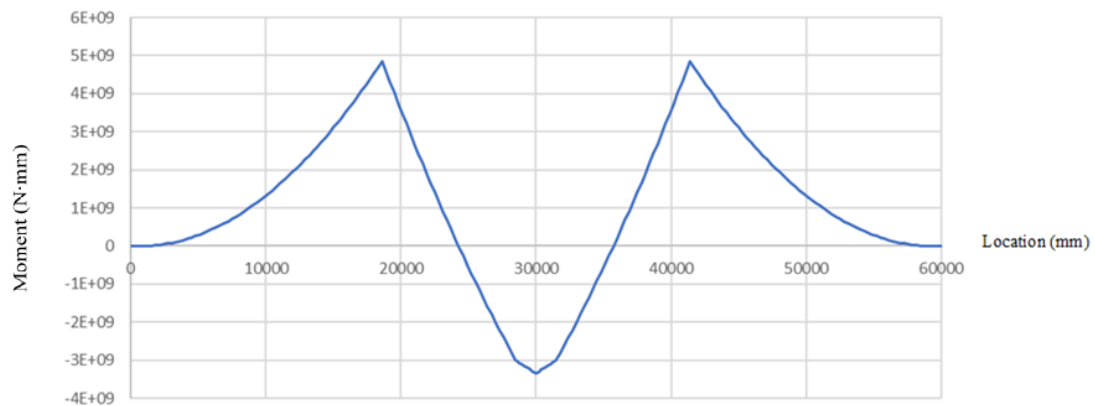
(ii)

Fig 4.7 (i) Deflection and (ii) moment distribution at ultimate stage

$\varepsilon_{top}= -0.0018$

$\varepsilon_{top}= 0.0712$

$\varepsilon_{s}= 0.0686$

$\varepsilon_{s}= 0.0790$
$\varepsilon_{bottom}= 0.0836$

$\varepsilon_{bottom}= -0.0032$
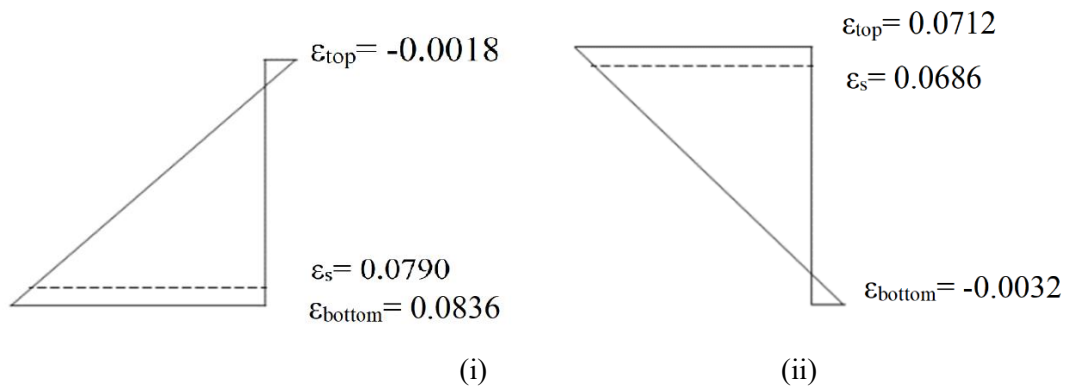
(i)   (ii)

Fig 4.8 Strain distribution at (i) midspan and (ii) support (ultimate stage)
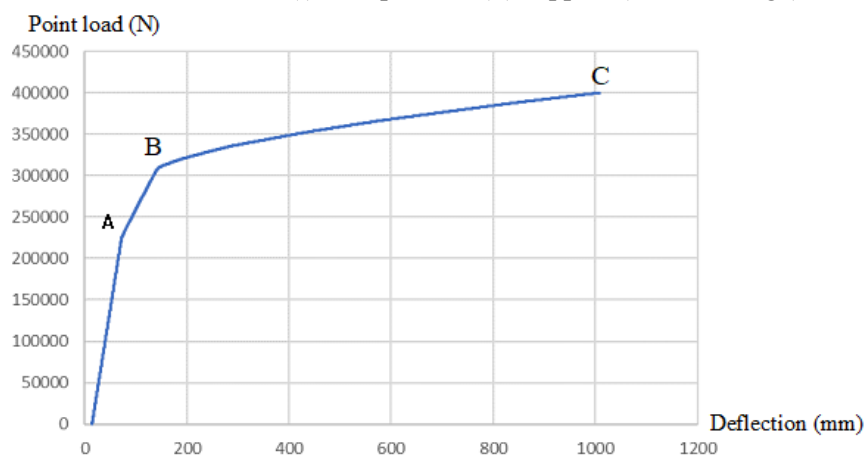

Fig 4.9 Load-deflection curve (value of one point load vs. deflection at midspan)
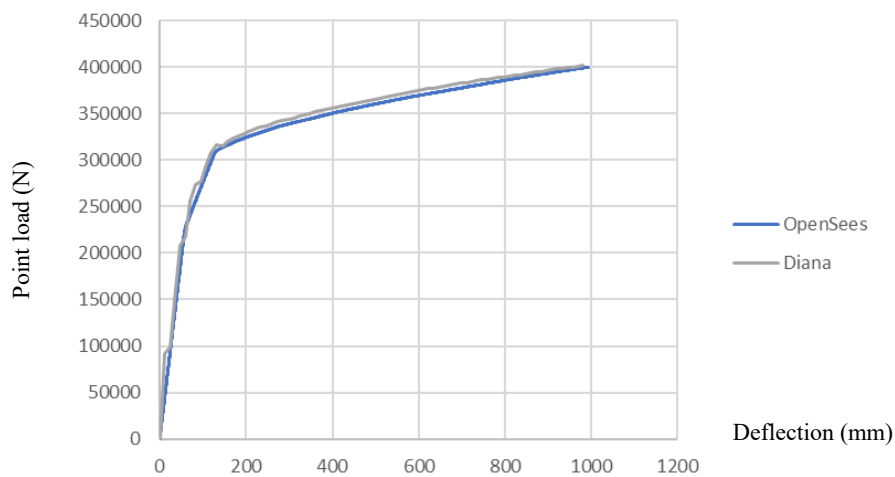
Fig 4.10 Comparison of the finite element analysis in OpenSees and in Diana

4.3.2 Corroded structure

In the analyses ignoring the spatial variability of corrosion, the pitting factor is assumed as uniform distributed along the entire beam (the pitting factor of each element has the same value). This pattern of corrosion is referred as uniform damage in the following text. It should be noticed that the uniform damage is also pitting corrosion rather than general corrosion. The uniform pattern indicates that the pits at different location has same depth. Fig 4.11 shows the different between an uniform damage and a spatial various damage. Under the assumption of uniform damage, Fig 4.12 shows the normalized residual capacity of the structure with different

value of pitting factors (t=50 year). The corrosion damages are also "isolated" from each other to show how the corrosion influenced the capacity. The isolated influence means only one of the corrosion damage is considered. Such isolated influence will not occur in reality. According to Fig 4.12, corrosion influence the capacity mainly through the reduction of reinforcing bar area.
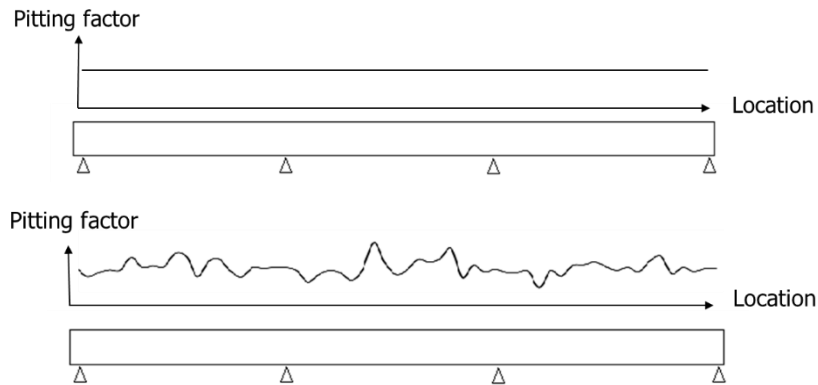
Fig 4.11 Comparison of uniform damage and spatial various damage
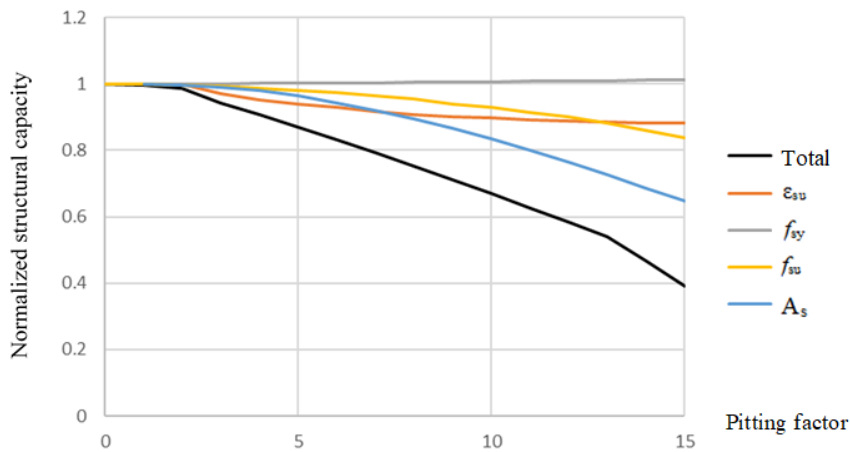
Fig 4.12 Normalized structural capacity with pitting factor

The above discussion is based on the uniformly distributed pitting corrosion. However, in reality, the pitting corrosion is not uniformly distributed and spatial variability is observed. One of the consequence of spatial varying pitting corrosion is the occurrence of localized damage. Fig 4.13 shows an example of localized damage, where pitting corrosion is with pitting factor 9 at the midspan and with pitting factor 7 at other locations. Fig 4.14, Fig 4.15 and Fig 4.16 present the different structural responses of the localized damage and the uniform damage corresponding to Fig 4.13.
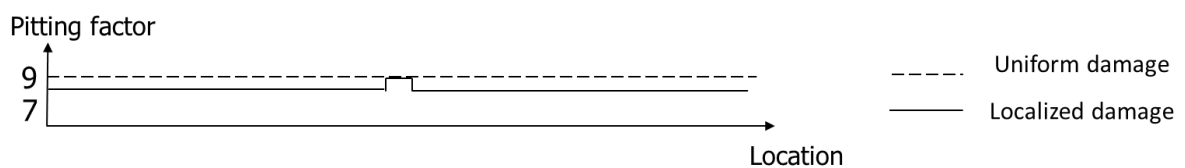
Fig 4.13 Localized damage compared with uniform damage
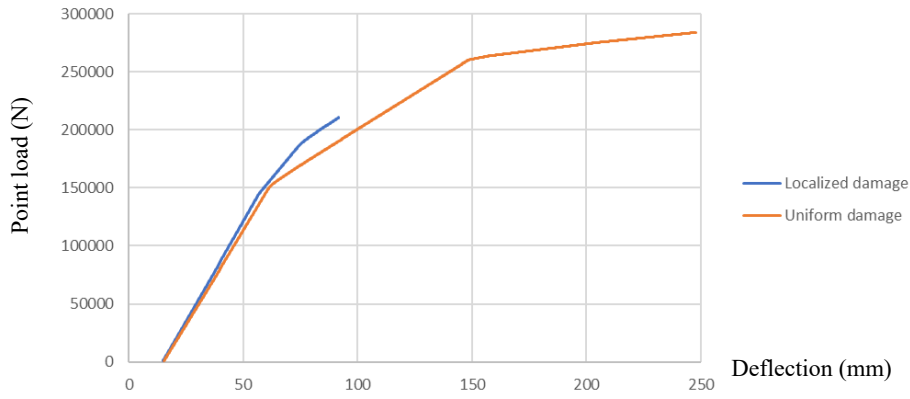
Fig 4.14 Load-deflection curve (value of one point load vs. deflection at midspan)
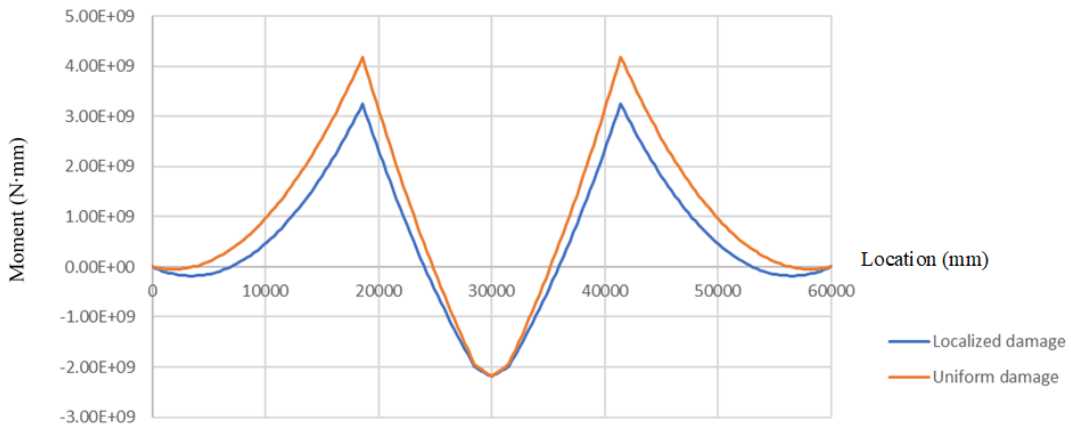
Fig 4.15 Moment distribution at ultimate stage
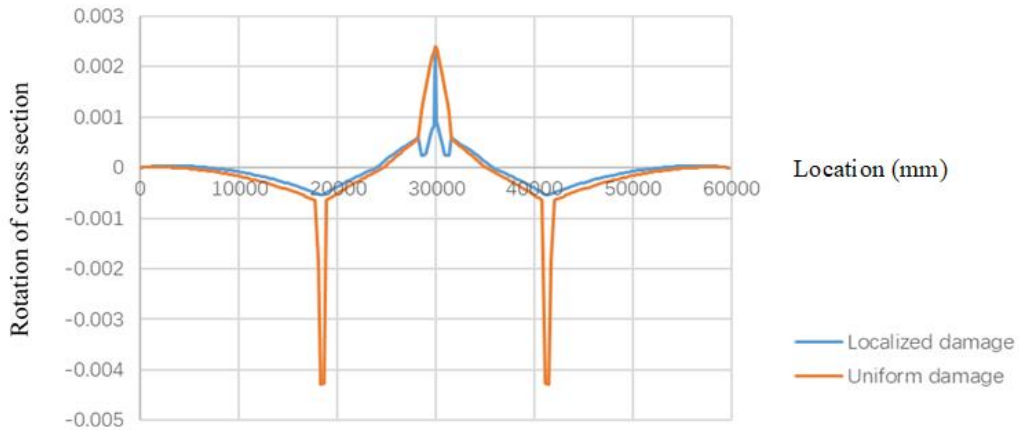
Fig 4.16 Rotation of cross section at ultimate stage

For uniform damage, the structure is able to develop certain ductility after the midspan starts to yield. On the contrary, with localized damage, the structure loses ductility very soon after the midspan starts to yield. Therefore, the uniformly damaged structure shows more ductile structural response and has higher capacity. The moment distribution and rotation of cross section reveal the cause.

For uniform damage, a ductile area is formed at the midspan after the yielding of bottom reinforcement. The ductile area covers several elements and allows relatively large deformation to developed. Due to uniform damage, no sudden change exists between neighboring elements and the stress distribution of the reinforcements follows same trend of the moment distribution. The strains of the reinforcements in the neighboring elements between load points gradually increase and reach the peak at midspan. The large deformation in the sagging part leads to a large deformation of the element at the supports. As result, the strain and stress of the reinforcement at hogging part increase. When the reinforcement at hogging part is in elastic stage while reinforcement at sagging part start to yield, the stress of reinforcement at hogging part develops more fast than the stress of reinforcement at sagging part. As result, the ratio between moment carried at supports and moment carried at the midspan keep increasing, which is also called moment redistribution. When the hogging parts are also yield, the structure forms plastic hinges at the midspan and at the supports, the load carried by the structure can slowly increase as the reinforcement can harden and the structure fails when the plastic hinge at the midspan fails due to reinforcement rupture.

For localized damage, the ductile area is not developed among elements and only the element with the largest damage developed considerable deformation. There is a sudden change between the element with the largest damage and the other neighboring elements. The stress distribution of the reinforcements do not follow the same trend of the moment distribution. Instead, the stress and strain increases rapidly in the element with the largest damage. While the reinforcements yield at the localized damage, the reinforcements at neighboring locations are in elastic stage. As result, the plastic hinge is only formed in one element and the deformation at hogging part is not as large as with the uniform damage. Although there are moment redistribution during the period where sagging part start to yield and hogging part is in elastic deformation, this period ends fast as the plastic hinge at midspan soon fails because of reinforcement rupture. When the structure fails, the reinforcements at hogging part are still in elastic stage. The structure fails before forming a plastic mechanism,

5 Reliability analysis of a RC continuous girder

In order to study the effect of spatial variability of corrosion on structural reliability, a series of reliability analyses are performed for the RC continuous girder. First, exploratory analyses are conducted to determine the influential variables and the range of the beam that should be modelled with random field. Then, part of the beam is modelled with a random field and the level of spatial variability is represented by correlation length. The presented analyses study the influence of different correlation length and reveals that spatial variability of corrosion has a significant influence on the failure probability.

Potential factors that could influence the reliability analysis are tested. The range covered by random field is enough and the approach to correlate area covered by random field and remaining area of the structure is adequate. Discretization of the structure will have complex influence on reliability analysis. However, for the case study, the discretization do not lead to considerable effects.

5.1 Exploratory reliability analysis

In order to identify (i) the important random variables, and (ii) the critical area that need to apply random field of corrosion damage, exploratory reliability analyses are performed with and without a random field. The random field will be applied to the entire beam. Each element will be attached with a variable stands for the maximum pitting factor within the element. In order to limit the dimension of the reliability problem (amount of variables) in a reasonable/practical range, relatively coarse mesh is used in the exploratory analyses. In total, 60 beam elements are used and the element size is listed in Table 5.1. Compared with the finite element analysis with 200 beam elements, the coarse mesh has an relative error of 7% of the ultimate capacity.

Table 5.1 Discretization

Element	Span	Number	Length
Displacement-Based Beam-Column Element	Left span	20	930 mm
	Mid span	20	1100 mm, 1500 mm
	Right span	20	930 mm

FORM is used to calculate the failure probability and the sensitivity factors of the random variables. The sensitivity factors are used to compare the relative importance of variables, to identify the most essential ones and to reduce the dimensionality of the reliability problem. The convergence criteria of the FORM analysis is 0.05 for both the search of limit state and search of design point. The performance function is defined as $G(X_{-Q}, Q) = R(X_{-Q}) - Q$, where X_{-Q} is a set of variables including material properties, geometrical properties and corrosion, $R(X_{-Q})$ is the structural capacity calculated by the finite element analysis based on the value of X_{-Q}, Q is the traffic load (value of one point load).

5.1.1 Reliability analysis without spatial variability

Table 5.2 shows the random variables and their probabilistic models used in the case without spatial variability. The following parameters are considered as random variables: the concrete compressive strength, the yield strength and the tensile strength of reinforcement, the ultimate strain of reinforcement, the area of top and bottom reinforcement, the pitting factor and the traffic load. The coefficient of variation of traffic load is taken from CEB/fib (2016). The coefficients of variation of other variables are taken from JCSS (2000). The mean values of the material and geometric properties are taken from Jacinto 2011. Gumbel parameters of the pitting factor R is modified from the suggested value for a bar with diameter 27 mm and length 100 mm, where $\mu_0 = 6.55$ and $\alpha_0 = 1.07$. The modification of the Gumbel parameters follows equation (3-10). The L_u is set to be the average element length. After modifying the Gumbel parameter, the mean value of variable R is 9.24 and the coefficient of variance is 0.13.

Table 5.2 Input parameters for reliability analysis

Variables	Symbol	Distribution	Mean	Coefficient of variation
Concrete compressive strength	f_{cc}	Lognormal	51.2 MPa	0.07
Reinforcement yield strength	f_{sy}	Lognormal	440 MPa	0.065
Reinforcement ultimate strength	f_{su}	Lognormal	550 MPa	0.07
Reinforcement ultimate strain	ε_{su}	Lognormal	0.08	0.09
Top rebar area (total)	A_{st}	Lognormal	7856 mm^2	0.02
Bottom rebar area (total) in midspan	A_{sm}	Lognormal	5400 mm^2	0.02
Bottom rebar area (total) in side span	A_{ss}	Lognormal	7364 mm^2	0.02
Pitting factor	R	Gumbel	9.24	0.13
Traffic load (one point)	Q	Gumbel	150 kN	0.1

Pitting corrosion is assumed to occur in bottom reinforcement along the entire length. Corrosion effects on the material properties, as discussed in Chapter 4 are considered and a constant corrosion rate of 2 μA/cm^2 is assumed. Three corrosion ignition times are considered: 0, 20 and 50 years. With the constant corrosion rate assumption, the development of time since corrosion initiation represents different levels of corrosion.

Table 5.3 Comparison of results

Symbol	t=0		t=20		t=50	
	α	Design point	α	Design point	α	Design point
f_{cc}	-0.0010	51.05 MPa	-0.0014	51.05 MPa	-0.0120	50.94 MPa
f_{sy}	-0.1431	415.9 MPa	-0.1798	412.3 MPa	-0.0010	439.0 MPa
f_{su}	-0.3323	481.2 MPa	-0.3317	485.3 MPa	-0.0419	543.6 MPa

ε_{su}	-0.0095	0.0792	-0.0077	0.07935	-0.1042	0.0775
A_{st}	-0.0745	7790 mm^2	-0.0763	7793 mm^2	-0.0252	7845 mm^2
A_{sm}	-0.0533	5364 mm^2	-0.0529	5368 mm^2	-0.0102	5395 mm^2
A_{ss}	-0.0014	7361 mm^2	-0.0014	7361 mm^2	-0.0041	7361 mm^2
R	0	8.992	0.1169	10.00	0.9773	16.05
Q	0.9277	340368	0.9139	313773	0.1772	155794
β	5.7414		5.3608		2.9259	
P_f	4.6946·10^{-9}		4.1439·10^{-8}		1.7173·10^{-3}	
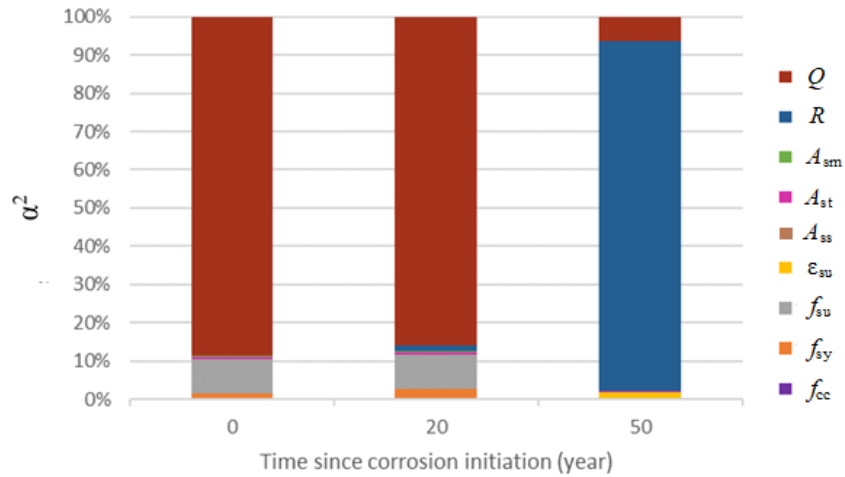
Fig 5.1 Change of sensitivity factors

Table 5.3 and Fig 5.1 show the comparison among the results for 0, 20 and 50 years since corrosion initiation. In the table, α is the sensitivity factor, β is the reliability index and P_f is the failure probability. As time develops the probability of failure increases and importance of pitting factor in reliability analysis (indicated by the value of α) grows. It corresponds to the finding that corrosion become severe (with a constant pitting factor) and structural resistance decreases as time develops.

5.1.2 Reliability analysis with spatial variability

Midpoint discretization is used for the random field. The discretization of random field is the same as discretization of finite element model. For each element in the finite element model, a variable is attached to represent the maximum pitting depth within the element. Because of relative large size of discretization, correlation is assumed to be zero between elements. Gumbel distribution of R remains the same as in the reliability analysis without spatial variability. An example of the realization of random field is shown in Fig 5.2.

Fig 5.2 Example of realization of the random field

Based on the analysis without spatial variability, the variables f_c, A_{st}, A_{sm}, and A_{ss} are identified not important for both $t=0$, $t=20$ and $t=50$, as the sensitivity 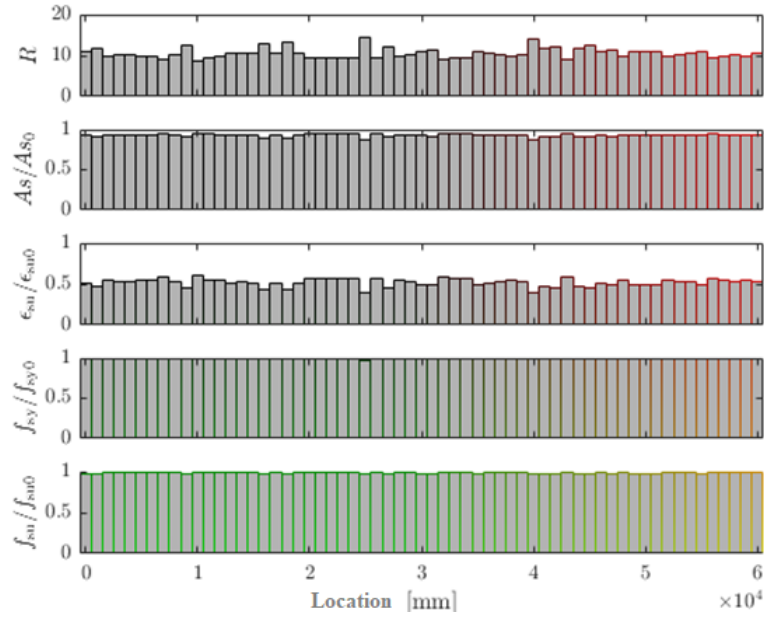factor of such variables are less than 0.1. In order to reduce the number of variables, the concrete compressive strength , and the uncorroded reinforcement area are treated as deterministic. FORM analysis is also performed to identify the most important region of the structure. The convergence criteria of the FORM analysis is 0.05 for both the search of limit state and search of design point.

Table 5.4 Input parameters for reliability analysis

Random variable	Distribution	Mean	COV
Pitting factor (R_i)	Gumbel	9.24	0.13
Steel yield strength (f_{sy})	Lognormal	440 MPa	0.065
Steel tensile strength (f_{su})	Lognormal	550 MPa	0.07
Steel ultimate strain (ε_{su})	Lognormal	0.08	0.09
Live load for each point (Q)	Gumbel	150 kN	0.1
Deterministic term		Value	
Concrete compressive strength (f_{cc})		-51.2 MPa	
Top rebar area (total) (A_{st})		7856 mm²	
Bottom rebar area (total) in midspan(A_{sm})		5400 mm²	
Bottom rebar area (total) in sidespan(A_{ss})		7364 mm²	
Self-weight (P)		30 kN/m	

Table 5.5 shows a comparison between the results of analyses with a corrosion ignition time of 20 years and 50 years, without spatial variability and with spatial variability. In the table, α is the sensitivity factor, β is the reliability index and P_f is the failure probability. While the analyses with and without spatial variability have no apparent difference for $t=20$ years, using random fields increases probability of failure more than 10 times for $t=50$ years. This finding is expected

based on reliability analysis without using random fields. For $t=20$ years, the traffic load Q is the dominant variable and using random field for nondominant variable R should not lead to much difference. For $t=50$ years, pitting factor R is the dominant variable and is on 'action side' (increase value of R will reduce resistance and increase probability of failure). Using random field increase the variability of R and leads to higher probability of failure.

Table 5.5 Comparison of results

| Variabel | $t=20$ | | $t=50$ | |
| | No RF | RF | No RF | RF |
	α	α	α	α
f_{sy}	-0.1798	-0.1387	-0.0010	-0.0079
f_{su}	-0.3317	-0.3262	-0.0419	-0.2261
ε_{su}	-0.0077	0.0204	-0.1042	0.0079
R_{mid} (R at midspan)	0.1169	0.1572	0.9773	0.8713
Q	0.9139	0.9215	0.1772	0.3366
β	5.3608	5.4759	2.9259	2.2368
P_f	$4.1439 \cdot 10^{-8}$	$2.1759 \cdot 10^{-8}$	$1.7173 \cdot 10^{-3}$	$1.2648 \cdot 10^{-2}$

Another finding is that the structural behavior may change in the reliability analysis for $t=50$ years. Fig 5.3 shows the load-deflection curves of the finite element analysis called by reliability analysis. For $t=50$, some curves reflect less ductile structural behavior, where the midspan fails due to rupture of bottom reinforcement while elements at supports are at elastic stage. For $t=20$ years, all curves shows ductile structural behavior where midspan fails due to rupture of bottom reinforcement while elements at supports are at hardening stage. The less ductile structural behavior is caused by severe localized corrosion of $t=50$ years and contributes to the increase of probability of failure.
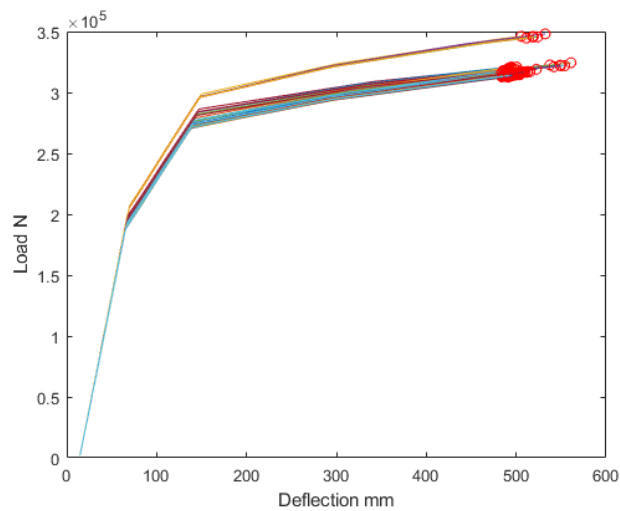
(i) $t=20$ years
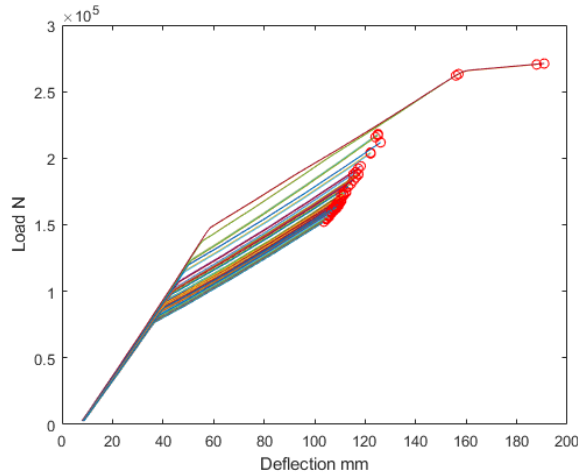
(ii) t=50 years

Fig 5.3 Load-deflection curves in reliability analysis

For both the case t=20 years and t=50 years, only the pitting factor of element at midspan has a sensitivity factor larger than 0.1. The sensitivity factors of the pitting factor of other elements are minimal. It reveals that the area near midspan is the essential/most sensitive part of the structure. For the following analyses, the pitting corrosion in the zone around the midspan should be modelled with a random field, while the pitting corrosion at the other zones of the beam can be represented by a single random variable.

5.1.3   Discussion of the exploratory study

The exploratory FORM reliability calculations reveal that, the pitting corrosion near the midspan is most essential for the failure probability of the structure. The moment distribution also indicates that the capacity of elements near the midspan determines the capacity of the structure. Based on the calculated sensitivity factors, the pitting factor of the element near the midspan is the important variable that need to be modeled by random field.

The reliability analyses also show, that of the case t=50 variables of the concrete compressive strength, the area of uncorroded reinforcements and the dead load, are relatively less important and can be modeled with deterministic values. The structural reliability is relatively sensitive to the reinforcement properties and the traffic load. Thus the reinforcement properties and the traffic load should be modeled with probabilistic distributions.

5.2   Parameter study of spatial variability

5.2.1   Introduction

The uncertainty of the pitting corrosion along the continuous beam is considered in two different ways. In the zone around the midspan and the traffic load, the pitting corrosion factor R is represented as a random field (indicated by zone 1 in Fig 5.4). This zone has a length of 3 m, corresponding to the dimension of the traffic load vehicle. In the left and right part of the beam, indicated by zone 2 in Fig 5.4, R is represented by a single random variable.

As before, the random field discretization is coupled to the finite element discretization. The element size in zone 1 is set to 125 mm, which leads to 24 elements in this zone. The element size in zone 2 is set to 300 mm, resulting in 214 elements.
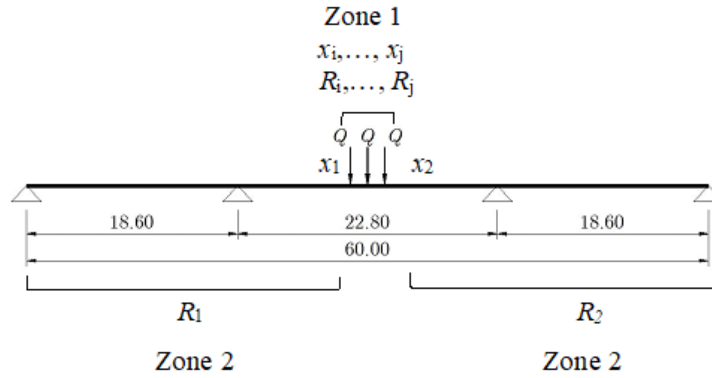
Fig 5.4 Zone 1 and 2 along the continuous beam.

When averaged element size is 300 mm, the relative change of computation result is 0.6 % if the amount of element doubles. The Gumbel parameters are also modified according to the element length. The mean value of pitting factor for element with 125 mm length is 7.30, while the mean value of pitting factor for element with 300 mm length is 8.12. The standard deviation for all the element is 1.20.

Table 5.6 Element type

Element	Number	Length	Component	Section
Beam element	214 (24 in region 1)	300 mm for zone 2, 125 mm for zone 1	Concrete fiber and steel fiber	Width 1100 mm Height 1250 mm

Midpoint discretization is used for the random field, see chapter 3. An exponential correlation function according to equation (3-8) used to describe the correlation between the elements in zone 1. Since the quantified spatial correlation of pitting corrosion is unknown for the presented concrete bridge and no general applicable information is available, correlation length of 125 mm, 250 mm, 500 mm, 1000 mm and 2000 mm are used to study the effect of different levels of spatial variety. Larger correlation length results in higher level of correlation between elements and lower level of spatial variety of the pitting corrosion.

The uncertainty of the pitting factor in zone 2 is represented by a single random variable for the left part (R_1) and the right part (R_2). The distribution of pitting factor along the beam is assumed to be uniform. The random variables R_1 and R_2 are correlated with the pitting factors in zone 1, via $|x_i - x_1|$ and $|x_j - x_2|$, where x_i and x_j are the location of midpoint of the edge elements in zone 1, x_1 and x_2 are the representative location in zone 2. There are two bounds of the value of x_1 and x_2. One is the midpoint of the closest element to region 1 and the other one is the midpoint of the farthest element to zone 1. The two bounds of the value of x_1 and x_2 are sequentially used in the following analyses to evaluate the influence of this choice.

In addition, the maximum pit depth is equal to $p(t) = 0.0116\, i_{corr}\, R\, t$, where $i_{corr} = 2$ μA/cm² corresponds to a high corrosion rate and t=50 years corresponds to the age of the bridge. The corrosion effects included in this study are the reduction of rebar area (A_s), rebar yield strength

(f_{sy}), rebar ultimate strength (f_{su}), and rebar ultimate strain (ε_{su}). The corrosion damage is only applied to the bottom reinforcement.

5.2.2   Inputs of reliability analysis

Reliability analyses are conducted with the probabilistic models as listed in

Table 5.7. Compared with the exploratory analyses in section 7.1, the only changed value is the mean value of pitting factor. Four reliability methods are used: Subset Simulation (SS), First Order Reliability Method (FORM), Adaptive Directional Importance Sampling (ADIS) and Adaptive Kriging Monte Carlo Simulation (AK-MCS) are used. For Subset Simulation and First Order Reliability Method, only exact limit state evaluations are used. For Adaptive Directional Importance Sampling and Adaptive Kriging Monte Carlo Simulation, methods include the generation of a response surface on the basis of exact performance function evaluations, which is used to calculate the failure probability. Table 5.8 summarized all relevant settings of the different reliability methods. The limit state function is defined as $G(X_{-Q}, Q) = R(X_{-Q}) - Q$, where X_{-Q} is a set of variables including material properties, geometrical properties and corrosion, $R(X_{-Q})$ is the structural capacity calculated by the finite element analysis based on the value of X_{-Q}, Q is the traffic load (value of one point load).

Table 5.7 Input parameters for reliability analysis

Random variable	Distribution	Mean	COV
Pitting factor (R_i)	Gumbel	7.30 for 125mm element	0.164
Pitting factor (R_1, R_2)	Gumbel	8.12 for 300 mm element	0.148
Steel yield strength (f_{sy})	Lognormal	440 MPa	0.065
Steel tensile strength (f_{su})	Lognormal	550 MPa	0.07
Steel ultimate strain (ε_{su})	Lognormal	0.08	0.09
Live load for each point (Q)	Gumbel	150 kN	0.1
Deterministic term	Value		
Concrete compressive strength (f_c)	-51.2 MPa		
Top rebar area (total) (A_{st})	7856 mm^2		
Bottom rebar area (total) in midspan(A_{sm})	5400 mm^2		
Bottom rebar area (total) in sidespan(A_{ss})	7364 mm^2		
Self-weight (P)	30 kN/m		

Table 5.8 Settings for reliability methods

Method	Convergence criteria	Other settings
Subset Simulation	COV (P_f) < 0.1	Each subset contains 1000 samples Predefined intermediate failure probability is 0.1
FORM	Error of 0.05 for both finding of limit state and finding of design point	N/A
AK-MCS	$(P_f^+ - P_f^-) / P_f$ <0.05	20 experimental design samples with maximum 500 added samples
ADIS	COV (P_f) < 0.1	The maximum order of polynomial in ADIS is third

5.3 Results and discussion

5.3.1 Performance of different reliability methods

Table 5.9 and Fig 5.6 present a comparison between the failure probabilities obtained from the FORM and Subset Simulation. The FORM results show smaller failure probabilities than Subset Simulation. Subset Simulation is a more general method that requires no precondition. The results indicate that FORM underestimates the failure probability. A possible reason is that the limit state function is nonlinear and the failure probability is relatively high. This hypothesis is confirmed by Fig 5.7 which shows the performance function in the R_{mid}-G plane near the design point. R_{mid} is the pitting factor of the element at midspan. The high nonlinearity cannot be well approximated by the linear function, or even polynomial, which leads to the underestimate of the failure probability of FORM. Furthermore, this may also explain the reason why the response surface based methods fail.

Table 5.9 Reliability analysis results

| Correlation length (mm) | FORM P_f | Subset Simulation P_f | | | AK-MCS |
		Lower bound	Mean	Higher bound	
125	$2.26 \cdot 10^{-2}$	$4.04 \cdot 10^{-2}$	$5.20 \cdot 10^{-2}$	$6.36 \cdot 10^{-2}$	/
500	$1.75 \cdot 10^{-2}$	$2.08 \cdot 10^{-2}$	$2.89 \cdot 10^{-2}$	$3.70 \cdot 10^{-2}$	$2.55 \cdot 10^{-2}$
2000	$0.98 \cdot 10^{-2}$	$1.24 \cdot 10^{-2}$	$1.79 \cdot 10^{-2}$	$2.34 \cdot 10^{-2}$	/

Among the four methods used for reliability analysis, FORM and Subset Simulation give convergent result for all correlation length. However, the AK-MCS results in a non-convergent meta model (the criteria $(P_f^+ - P_f^-)/P_f$ <0.05 is not satisfied) and ADIS leads to a total failure to generate a proper meta model (third order polynomial). Fig 5.5 shows the failure probability calculated by AK-MCS up to 500 added exact samples. Although the convergence criteria is not met, the failure probability calculated by AK-MCS is close to the result of Subset Simulation.
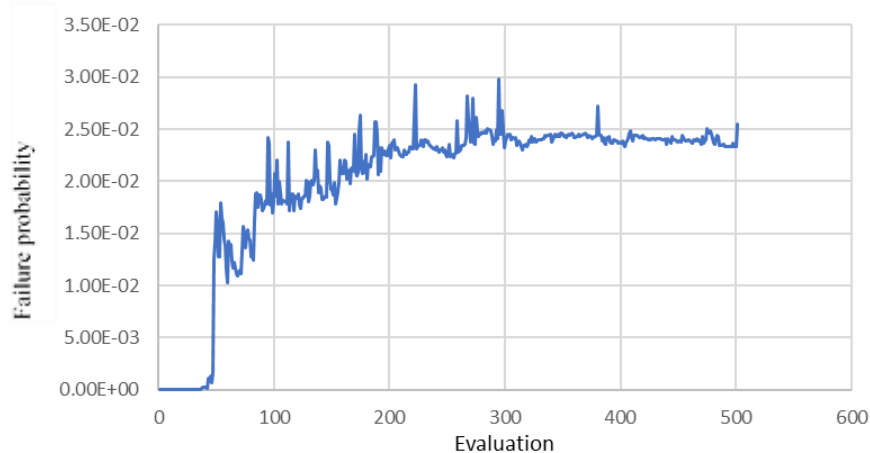
Fig 5.5 Failure probability calculated by AK-MCS
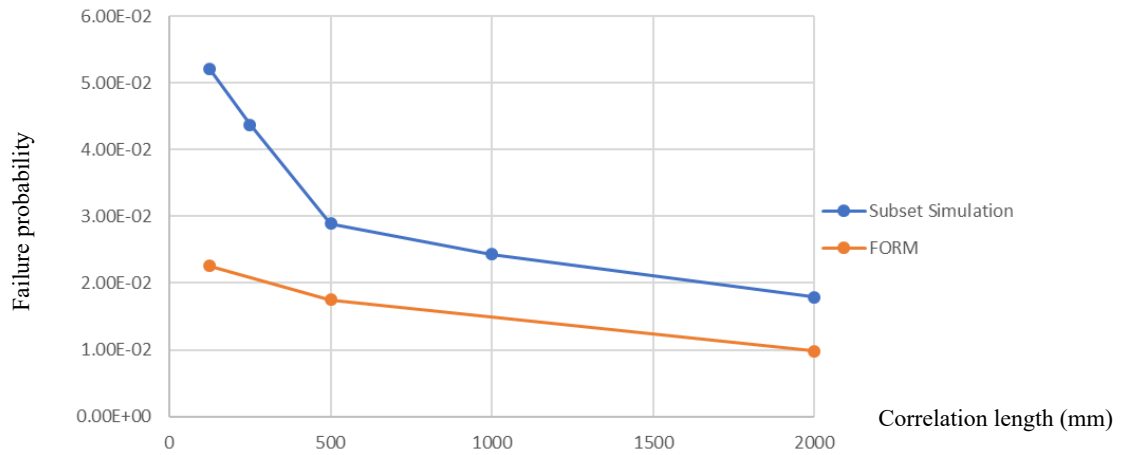
Fig 5.6 Failure probability with different correlation length.
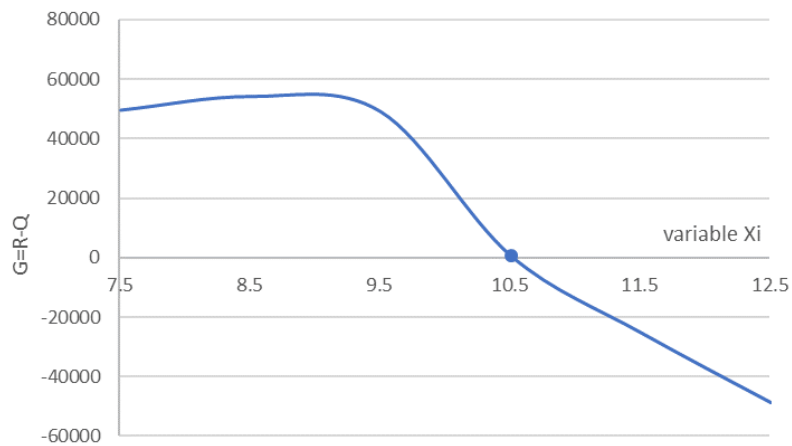
Fig 5.7 Performance function in R_{mid}-G plane near the design point

5.3.2　Influence of correlation length

Correlation lengths of 125 mm, 250 mm, 500 mm, 1000 mm and 2000 mm are used for reliability analysis. The results of Subset Simulation are listed in Table 5.10 and plotted in Fig 5.8 Failure probability with correlation lengthThe settings of the reliability method are the same as above mentioned setting for Subset Simulation.

Table 5.10 Reliability analysis results

Correlation length (mm)	Subset Simulation P_f		
	Lower bound	Mean	Higher bound
125	$4.04 \cdot 10^{-2}$	$5.20 \cdot 10^{-2}$	$6.36 \cdot 10^{-2}$
250	$3.33 \cdot 10^{-2}$	$4.37 \cdot 10^{-2}$	$5.41 \cdot 10^{-2}$
500	$2.08 \cdot 10^{-2}$	$2.89 \cdot 10^{-2}$	$3.70 \cdot 10^{-2}$
1000	$1.74 \cdot 10^{-2}$	$2.43 \cdot 10^{-2}$	$3.12 \cdot 10^{-2}$
2000	$1.24 \cdot 10^{-2}$	$1.79 \cdot 10^{-2}$	$2.34 \cdot 10^{-2}$

Fig 5.8 Failure probability with correlation length

Fig 5.8 shows that when the correlation length increases, the failure probability decreases. This trend matches with our expectation, both from a probabilistic viewpoint and a mechanical viewpoint:

(1) From the probabilistic viewpoint, an increased correlation length corresponds to a higher level of spatial correlation and thus a lower level of spatial variability of the corrosion damage. A low level of spa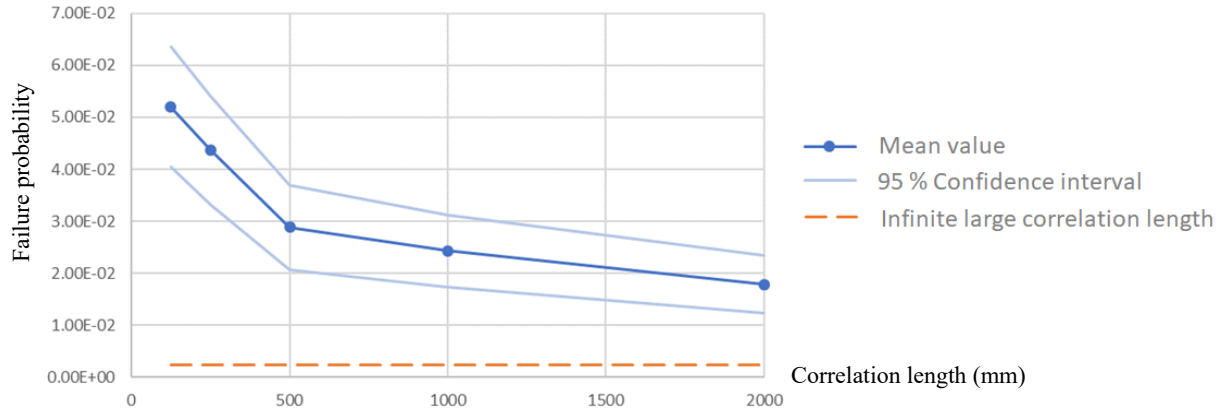tial variability of the corrosion damage leads to a low probability to have an extremely weak element among all the elements. This can be illustrated by consideration of the following two extreme cases. If 100 variables R_i ($0 \leq i \leq 100$) have the same probabilistic distribution, of which $P(R_i > R_0) = P_0$, then for fully correlated variables (i.e. low level of spatial variability) $P(\exists R_i > R_0) = P_0$ and for fully independent variables (i.e. uncorrelated and thus a high level of spatial variability) $P(\exists R_i > R_0) = 1 - (1 - P_0)^{100} \gg P_0$. On the continuous beam, the random field covers the area with the largest moment. Hence, the probability to have an extremely weak among all the elements is negatively related to the structural capacity and thus positively related to the failure probability of the structure (although, these relations are not linear).

(2) From the mechanics viewpoint, an high level of spatial correlation and low level of spatial variability mean that the damage is more uniformly distributed rather than localized distributed. In another word, for a realization of the distribution of pitting factor, the pitting factor changes smoothly in space rather than rapidly. In the exploratory study, the finite element analysis reveals that the localized damage results in a lack of development of ductile area in plastic hinge and insufficient moment redistribution between hogging and sagging. As a result, the localized damage leads to loss of ductility of structure and a low structural capacity.

Beyond the case study, the above two interpretations still have advisable meaning for general cases. First, if the structure or part of the structure can be approximated as a series system composed of several equal elements, the failure of the system depends on the failure of one of the elements in that system. In such a situation, spatial variability of damage increases the probability to have at least one heavily damaged element and thus increases the failure probability of the series system. Second, for a statistic-undetermined structure with ductility or plasticity assumed, localized damage could be more unfavorable than uniform damage. Spatial

47

variability of damage leads to a more unfavorable structural response and increases the failure probability. High level of spatial variability of corrosion increases the failure probability of the structure. Therefore, it is advised to further explore the spatial variability of corrosion and gather information to facilitate more accurate reliability analysis.

5.3.3 Influence of discretization

In the case study, the discretization of random field is the same as of the finite element model. The discretization can influence the reliability analysis on three aspects:

(1) The Gumbel distribution of the pitting factor is modified by the discretization in order to reflect the size effect. In the analyses, the parameters of the Gumbel distribution are determined by the element size according to equation (3-10). The equation is based on assumption of spatial independency of variables, as discussed in Chapter 3. If spatial correlation is included, the Gumbel distribution modified according to (3-10) is not equivalent to the Gumbel distribution of the new discretization. The model error will become more apparent when the spatial correlation becomes stronger (correlation length is large).

(2) If spatial variability of corrosion is considered, the discretization of the finite element model will influence the modelling of the localized damage. With a fine discretization, the damage can be modelled with an extremely small size. If the spatial correlation is relatively small (spatial variability is relatively large), the effect of localized damage can be reflected with fine discretization. However, with a coarse discretization (where the element size is larger than half of the correlation length), the localized damage cannot be proper modelled. Even with high spatial variability, the influence of localization is limited reflected. This phenomena only influences analyses where correlation length is small.

(3) For variables with spatial correlation, which are represented by an auto-correlation function, there is a lower bound and an upper bound for the element size, expressed by correlation length. A too large element size will result in inaccuracy of modelling the field. For exponential auto-correlation function, B Sudret and Der Kiureghian (2000) gives an estimation of the error of generated random field for different ration of element size with correlation length. The error $E(\Omega_e)$ represents:

$$E(\Omega_e) = \sup_{x \in \Omega_e} \frac{Var\left[H(x) - \widehat{H}(x)\right]}{Var\left[H(x)\right]}$$

Naturally, smaller element results in more accurate random field. However, a too small element size may lead to numerical difficulties in the calculation of the correlation matrix. If the element size is changed, the random field may not be properly generated and influence the reliability analysis. The influence on reliability analysis is difficult to quantify, as there is no 'accurate' result to compare with.
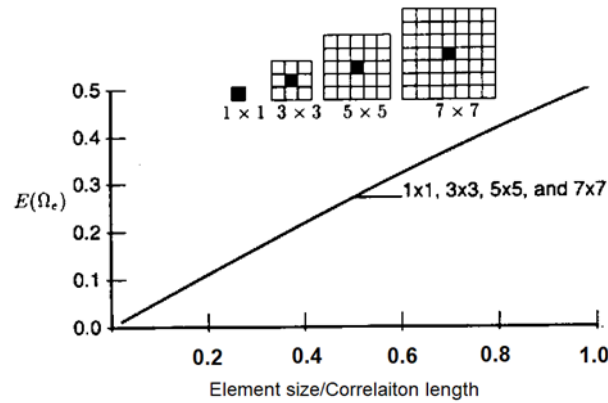
Fig 5.9 Error of random field (B Sudret and Der Kiureghian (2000))

The three aspects interact and the their separate influences cannot be easily distinguished. In order to estimate the total influence, a new calculation is made in which the discretization of the random field adopts element sizes of 300 mm. The same reliability analysis is carried out with the series of correlation length. Fig 5.10 shows the failure probabilities of the two sets of analyses. In addition to the mean value of the failure probability, the 95% confidence interval is also presented.
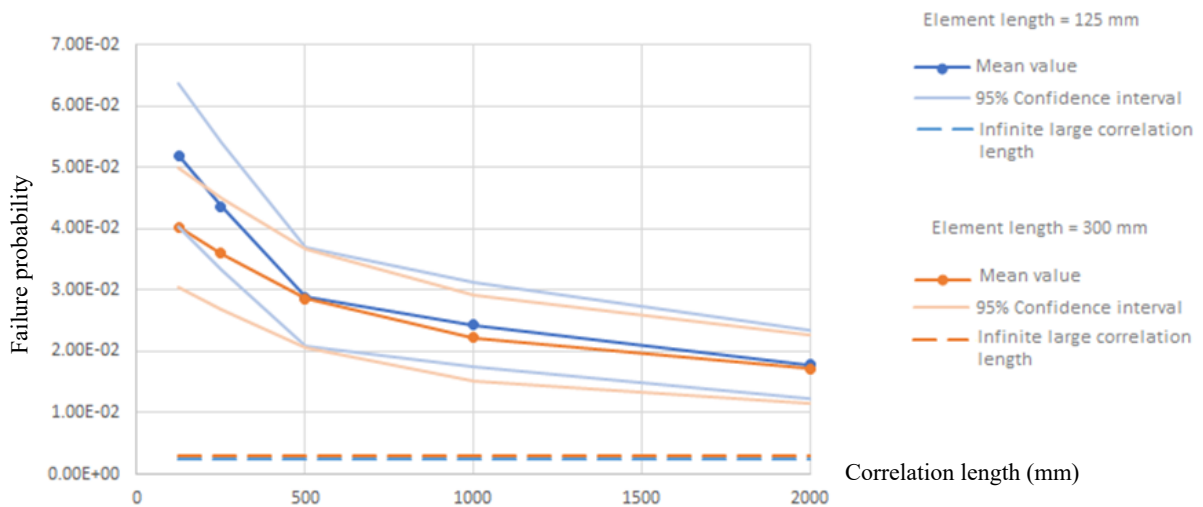
Fig 5.10 Failure probabilities by varying correlation lengths

Table 5.11 Comparison of reliability analysis with different discretization

Correlation length (mm)	P_f of 125mm element			P_f of 300 mm element		
	Lower bound	Mean	Higher bound	Lower bound	Mean	Higher bound
125	$4.04 \cdot 10^{-2}$	$5.20 \cdot 10^{-2}$	$6.36 \cdot 10^{-2}$	$3.05 \cdot 10^{-2}$	$4.03 \cdot 10^{-2}$	$5.01 \cdot 10^{-2}$
250	$3.33 \cdot 10^{-2}$	$4.37 \cdot 10^{-2}$	$5.41 \cdot 10^{-2}$	$2.69 \cdot 10^{-2}$	$3.60 \cdot 10^{-2}$	$4.51 \cdot 10^{-2}$
500	$2.08 \cdot 10^{-2}$	$2.89 \cdot 10^{-2}$	$3.70 \cdot 10^{-2}$	$2.06 \cdot 10^{-2}$	$2.86 \cdot 10^{-2}$	$3.66 \cdot 10^{-2}$
1000	$1.74 \cdot 10^{-2}$	$2.43 \cdot 10^{-2}$	$3.12 \cdot 10^{-2}$	$1.52 \cdot 10^{-2}$	$2.22 \cdot 10^{-2}$	$2.92 \cdot 10^{-2}$

| 2000 | $1.24 \cdot 10^{-2}$ | $1.79 \cdot 10^{-2}$ | $2.34 \cdot 10^{-2}$ | $1.17 \cdot 10^{-2}$ | $1.72 \cdot 10^{-2}$ | $2.27 \cdot 10^{-2}$ |
| $+\infty$ | | $2.40 \cdot 10^{-3}$ | | | $2.91 \cdot 10^{-3}$ | |

The trend in Fig 5.10 indicates that for correlation lengths of 125 mm and 200 mm, the analyses with 300 mm element sizes result in lower failure probabilities compared to those with 125 mm element sizes. For correlation lengths of 500 mm, 1000 mm, and 2000 mm, no apparent influence of the discretization is observed. For infinite large correlation length, the analysis with 300 mm element size leads to a slightly higher failure probability. This trend cannot be mathematically proven or explicitly explained by one of the aspects mentioned above. However, the trend can be interpreted by combining the three aspects.

In the above analyses, the Gumbel parameters are modified according to the element size, based on assumption of spatial independency among variables (i.e. the correlation length should be relatively small compared to the element size). The modification rule prescribe that for a larger element size, the mean value of Gumbel distribution will also be larger. In the case study, the variable is the pitting factor. Thus, larger element size leads to larger mean value of pitting factor and larger damage due to corrosion. Ideally, if the spatial independency assumption is satisfied, the modified Gumbel parameters will lead to equivalent probability distribution of pitting factor for a different discretization. The failure probability should not change. If there is spatial correlation, the modified Gumbel parameter (based on spatial independency) will lead to an overestimation of the mean value for a larger element size. Thus, the failure probability increases with a larger element size when the correlation length is infinite.

According to aspect (2), the larger element sets a limitation for modelling localized damage. With small spatial correlation between variables (small correlation length), there is a chance for the occurrence of a large change of the pitting factor within a small spatial distance, which is referred as localized damage in this thesis. The influence of the localized damage depends on the size of element. If the element is fine enough, the localized damage can be captured and reduce the capacity of the structure. If element is coarse, any localized damage that is smaller than the element size cannot be modelled. Thus, the larger element size results in less influence of the localized damage and decrease the failure probability when correlation length is small.

In conclusion, the influence of element size on the reliability analysis is a collective effect. With a large correlation length, the discretization with larger element sizes will increase the failure probability because of the existence of spatial correlation against the precondition of modifying the size-dependent Gumbel parameters. With a small correlation length, the discretization with larger element sizes will decrease the failure probability because of limiting the modelling of localized damage. With a medium correlation length, these two effect compensate each other to some extent and leads to insensitivity to element size. The influence of discretization of random field and of finite element model on reliability analysis could depend on cases. Such aspect requires further study.

5.3.4   Discussion on the length covered by random field

There are two other factors that should be considered for the random field. One is the length of the area covered by the random field. In order to reduce the dimension of the problem (amount

of variables), only the most essential area is covered by random field. For the above analyses, the random field covers 3000 mm of the beam. The influence of this length on the failure probability is studied by adopting a random field that covers 9000 mm of the beam. Table 7.6 compares the failure probability calculated by Subset Simulation with random field covering 3000 mm length and with random field covering 9000 mm length. The difference is less than 10 %, which is smaller than the coefficient of variance of failure probability. Such differences can be regarded as minimal.

Table 5.12 Comparison of failure probabilities by varying lengths of the random field and correlation lengths.

Correlation length	3000 mm	9000 mm
125 mm	$5.20 \cdot 10^{-2}$	$5.15 \cdot 10^{-2}$
2000 mm	$1.79 \cdot 10^{-2}$	$1.65 \cdot 10^{-2}$

The other factor that is checked is how the part covered by random field is correlated to the part represented by variable. The random variables R_1 and R_2 are correlated with the pitting factors R_i and R_j, via $|x_i - x_1|$ and $|x_j - x_2|$ where x_i and x_j are the location of midpoint of the edge elements in zone 1, x_1 and x_2 are the representative location in zone 2. There are two bounds of the value of x_1 and x_2. In above reliability analyses, x_1 and x_2 is the location of the midpoint of the closest element to zone 1. The other bound of the value of x_1 and x_2 is the midpoint of the farthest element to zone 1. Table 7.7 compares the failure probability with two approach to correlate the two regions. The difference of the failure probability is also minimal
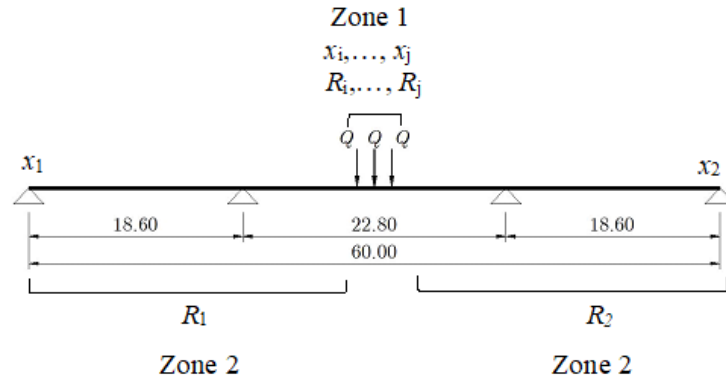

Fig 5.11 Zone 1 and 2 along the continuous beam.

Table 5.13 Comparison of correlation choices

Correlation length	Correlated to closest element	Correlated to farthest element
125 mm	$5.20 \cdot 10^{-2}$	$5.10 \cdot 10^{-2}$
2000 mm	$1.79 \cdot 10^{-2}$	$1.51 \cdot 10^{-2}$

6 Corrosion distribution on adjacent rebars

6.1 Overview

In the previous analysis in Chapter 5, the spatial variability of corrosion is assumed to exist along the length of the beam. The level of pitting corrosion is represented by pitting factors. Accordingly, the spatial variability is represented by a random field distributed in axial direction of the beam. The random field contains a set of variables that are set to the location of midpoint of each element. The variable stands for the pitting factor within the element. The values in the set of variables are different and thus the corrosion level varies along the axial of the beam (Fig 6.1).
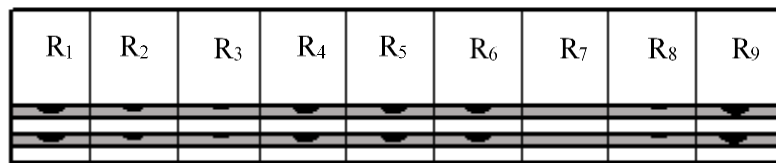

Fig 6.1 Assumed pitting corrosion distribution (side view)

Within the cross section, it was assumed that all bottom reinforcements in one element have the same pitting corrosion. However, such an assumption conflicts with the reality. The spatial variability not only exist along a single reinforcing bar, but also exist between adjacent reinforcing bars (Fig 6.2). Because the pits can occur at any location along reinforcing bars, the adjacent bars are likely to have pits at different locations. Also, the corrosion level could be different at adjacent bars. In order to reflect the spatial variability between adjacent bars, the pitting factor of adjacent bars should be represented by separate variables.
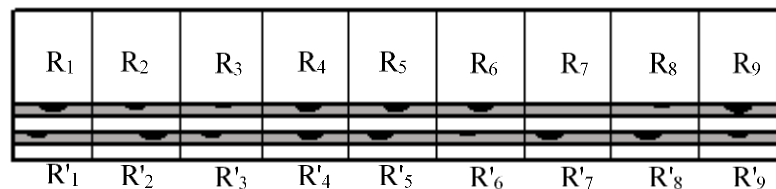
Fig 6.2 Independent pitting corrosion distributed at adjacent bars (side view)

6.2 Interference of pits

The pitting corrosion not only varies along the reinforcing bars, but also differs between them. The disparities of localized pitting corrosion between the reinforcing bars may result in interference of the cracks due to mechanical loading. Kioumarsi et al. (2016) studied an idealized case to quantify the interference of localized pitting corrosion on adjacent rebars in an reinforced concrete beam subjected to bending. There were two adjacent rebars in the beam, each with one corrosion pit within the maximum bending zone (Fig 6.3). The two corrosion pits were equal in size. The influence of two variables on the ultimate bending moment resistance was quantified through nonlinear finite element analyses: the ratio of the distance between pits in two adjacent rebars to the distance between the rebars, l_p/l_r, and the ratio of the cross-section reduction of the rebar due to localized corrosion to the initial cross-section of rebar A_{pit}/A_0.

Fig 6.3 Bottom view of interference of pits (Kioumarsi et al., 2017)

From the numerical simulations it was found that pits interference occurs within a critical distance between pits. Interference of localized corrosions reduces gradually for increasing distance between pits in two adjacent rebars. The interference of pits can b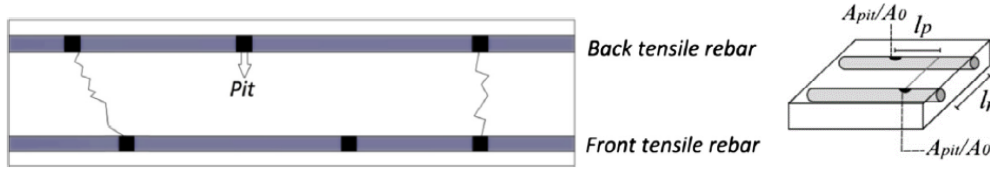e physical interpreted with the orientation and number of bending cracks. Coalescence of cracks can be observed with the occurrence of interference of pits. Kioumarsi et al. (2017) proposed to use a modified total residual cross-section of corroded tensile rebars in an analytical analysis of the strength of the cross-section:

$$A_{res(mod)} = 2A_0 - (2A_{uni} + A_{pit} + \beta_{int} A_{pit}) \tag{6-1}$$

$$\beta_{int} = -0.76(l_p / l_r)^2 + 0.16(l_p / l_r) + 1 \tag{6-2}$$

Where $A_{res(mod)}$ is the modified total residual cross section of two rebars, A_0 is the initial cross section of a rebar, A_{uni} is the cross section reduction of a rebar due to uniform corrosion, A_{pit} is the cross section reduction of a rebar due to pitting corrosion, and β_{int} reflects interference of the pits.
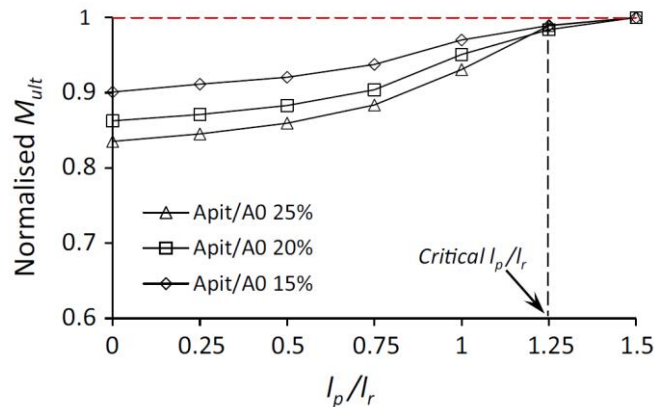
Fig 6.4 Influence of interference of pits on bending capacity (Kioumarsi et al., 2017)

6.3   Independent adjacent rebars

Although the spatial variability of corrosion between adjacent bars are widely recognized, the correlation of corrosion between adjacent bars is never quantified. In order to estimate the influence of such spatial variability, the analysis is targeted on two bounds of the problem: fully dependency and total independency. Chapter 5 shows the results of a reliability analysis assuming fully dependency of corrosion between adjacent bars. In this section, the same reliability analysis is performed with the assumption of total independency between the adjacent bars. In reality, the pits could occur at different locations at adjacent bars (Fig 6.5(a)) and results in a certain degree of interference. In the following analyses, the pits at adjacent bars within an discretized element are modelled as totally 'interferent' ($\beta_{int} = 1$), and the

capacity of one bar in an element is modeled based on the deepest pit on the bar (Fig 6.5 (b)).

(a)   (b)

Fig 6.5 Modeling approach (example of a beam element containing two bars)

In the previous section, there is one variable representing pitting factor applied to one element. All reinforcements within one element is assumed to have same pitting factor. In this section, there is one variable representing pitting factor applied to each reinforcement in the element. The reinforcements are assumed to have independent pitting factors. There are 11 random fields set to the 11 bottom reinforcements in the midspan 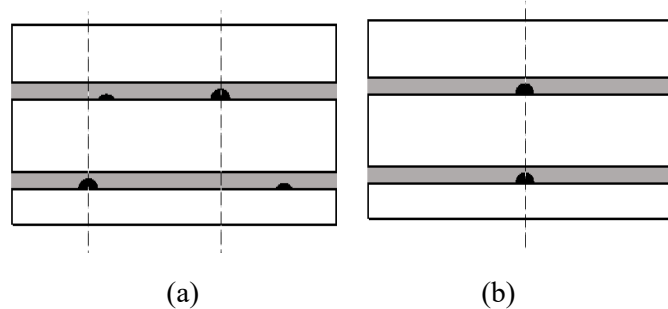region. Fig 6.6 shows a cross section view where the 11 bottom reinforcements have independent pitting corrosion. The finite element and random field discretization has element sizes of 300 mm. The random field covers the range of 3000 mm length in axial direction at the midspan. In total, there are 110 variables used to represent the pitting factor in the random fields. Subset Simulation is performed with the same settings as in Chapter 5. The convergence criteria of Subset Simulation is COV (P_f) < 0.1. Each subset contains 1000 samples. The predefined intermediate failure probability is 0.1s.
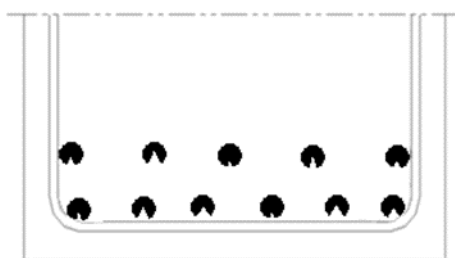
Fig 6.6 Cross section view of the independent pitting corrosion at adjacent bars

Table 6.1 Input parameters for reliability analysis

Random variable	Distribution	Mean	COV
Pitting factor (R_i)	Gumbel	8.05 for 300 mm element	0.149
Steel yield strength (f_{sy})	Lognormal	440 MPa	0.065
Steel tensile strength (f_{su})	Lognormal	550 MPa	0.07
Steel ultimate strain (ε_{su})	Lognormal	0.08	0.09
Live load for each point (Q)	Gumbel	150 kN	0.1
Deterministic term	Value		
Concrete compressive strength (f_{cc})	-51.2 MPa		
Top rebar area (total) (A_{st})	7856 mm^2		
Bottom rebar area (total) in midspan(A_{sm})	5400 mm^2		
Bottom rebar area (total) in sidespan(A_{ss})	7364 mm^2		
Self-weight (P)	30 kN/m		

Four spatial correlation situations in the axial direction are considered. Subset Simulation is performed for a fully correlated pitting corrosion along the axial direction of the reinforcing bars and with correlation length of 500 mm, 1000 mm and 2000 mm. Table 6.2 presents the failure probabilities of the four reliability analyses.

Table 6.2 Results of reliability analysis

Correlation length	Independent adjacent bars	Fully correlated adjacent bars
500 mm	$7.73 \cdot 10^{-5}$	$2.86 \cdot 10^{-2}$
1000 mm	$3.39 \cdot 10^{-5}$	$2.22 \cdot 10^{-2}$
2000 mm	$2.58 \cdot 10^{-5}$	$1.72 \cdot 10^{-2}$
Fully correlated	$2.27 \cdot 10^{-6}$	$2.40 \cdot 10^{-3}$
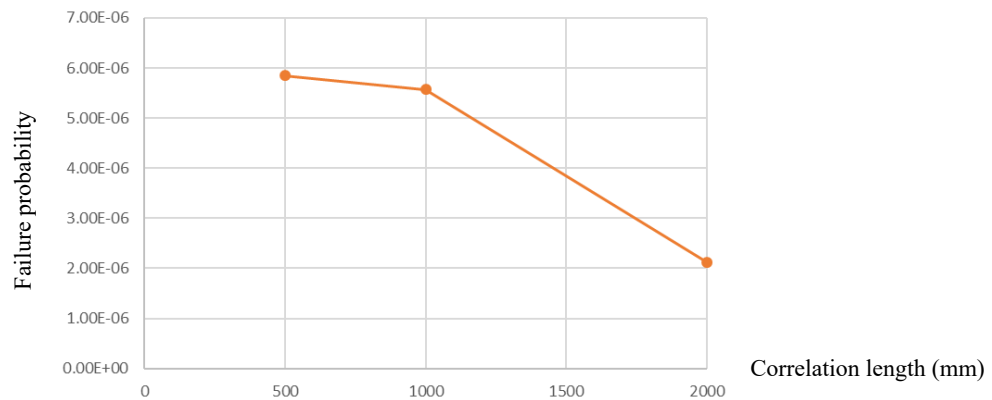
Fig 6.7 Failure probability with correlation length

Compared to fully correlated pitting corrosion at adjacent bars, the independency causes a difference of failure probability near three order of magnitude. In order to estimate the reasonability of such large difference, a Sanity check is performed based on probabilistic theory. The reinforcing bars within one elements can be regarded as a parallel system. On the contrary of series system, the failure of parallel system does not depend on the weakest element. The parallel system can be further classified into ductile parallel system and brittle parallel system. For ductile parallel system, the element can remain the strength in the plastic stage and the capacity of the system is the 'sum' of the capacity of elements. For brittle system, the element lose strength after failure and the strength of the system depends on $\max\{nS_1, (n-1)S_2, ..., S_n\}$, where S_i is the strength of element i and $S_1 \leq S_2 \leq ... \leq S_n$.

(a)   (b)
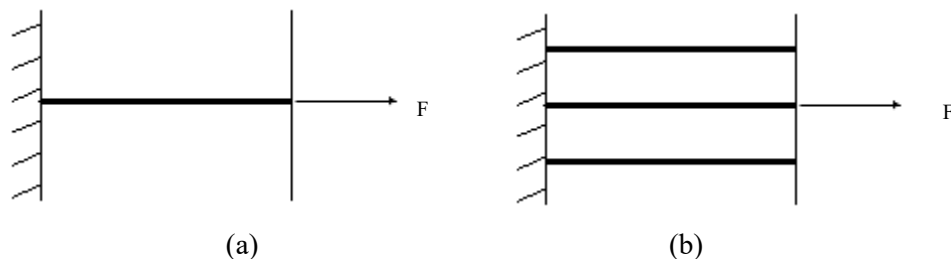
Fig 6.8 System of (a) the fully correlated rebars and (b) the fully independent rebars

The reinforcing bar system is neither totally brittle or ductile. Before yielding stage, the system can be regarded as ductile, while after yielding, the system is brittle for reaching ultimate strain. In addition, the reinforcing bars do not reach to same strength simultaneously. For bars at same layer, they have same strain simultaneously but could develop different force. The yielding strength, ultimate strength, ultimate strain and area of the bars are all varied. In the Sanity check, the reinforcing bar system is simplified as a ductile parallel system. However, such simplification could introduce unjustified effects and are not advised for reliability assessment. For fully correlated reinforcing bars, one variable represent the pitting factor for all bars in one element. The resistance of one element is a function of the pitting factor of this element. The failure of the element under a certain load can be regarded as the value of pitting factor exceed a threshold x_{th}. For fully independent reinforcing bar, each bar has a variable to represent pitting factor of this bar in the element. If the reinforcing bar system is simplified as a ductile parallel system, the resistance of the element can be approximated by a function of the averaged pitting factor of all bars in the element. The failure can be regarded as the average value of pitting factor of all bars exceed a threshold x_{th}'.

In both cases, the pitting factor of one reinforcing bar in an element is represented by variable R and is modeled with Gumbel distribution.

For dependent reinforcing bars: $P(R > x_{th}) = 1 - \exp(-\exp(-\alpha(x_{th} - \mu)))$ (6-3)

For independent reinforcing bars: $P(\bar{R} > x_{th}') = 1 - \exp(-\exp(-\alpha'(x_{th}' - \mu')))$, (6-4)

where $\bar{R}$ is the average value of pitting factor of all bars $\bar{R} = \dfrac{1}{11}\sum_1^{11} R_i$, and α', μ' are

Gumbel parameter of the distribution of $\bar{R}$. The distribution of $\bar{R}$ is also Gumbel, however

$$\sigma(\bar{R}) = \sigma(\frac{1}{11}\sum_1^{11} R_i) = \frac{1}{11} \cdot \sqrt{11} \cdot \sigma(R) = \frac{\sigma(R)}{\sqrt{11}}$$ (6-5)

Because $\alpha = \dfrac{\pi}{\sqrt{6}\sigma}$, $\dfrac{\alpha}{\alpha'} = \dfrac{\sigma(\bar{R})}{\sigma(R)} = \dfrac{1}{\sqrt{11}}$ (6-6)

First, a guess of the value of threshold x_{th} and x_{th}':
If $x_{th} - \mu = x_{th}' - \mu' = 2\sigma$

$$-\alpha(x_{th} - \mu) = -\frac{\pi}{\sqrt{6}\sigma} \cdot 2\sigma = -\frac{2\pi}{\sqrt{6}}$$ (6-7)

$$-\alpha'(x_{th}' - \mu') = -\sqrt{11}\frac{\pi}{\sqrt{6}\sigma} \cdot 2\sigma = -\frac{2\sqrt{11}\pi}{\sqrt{6}}$$ (6-8)

$$\frac{P(R < x_{th})}{P(\bar{R} < x_{th}')} = \frac{1 - \exp(-\exp(-\frac{2\pi}{\sqrt{6}}))}{1 - \exp(-\exp(-\frac{2\sqrt{11}\pi}{\sqrt{6}}))} = 366.6$$ (6-9)

If $x_{th} - \mu = x_{th}' - \mu' = 2.5\sigma$

$$-\alpha(x_{th} - \mu) = -\frac{\pi}{\sqrt{6}\sigma} \cdot 2.5\sigma = -\frac{2.5\pi}{\sqrt{6}}$$ (6-10)

$$-\alpha'(x_{th}'-\mu')=-\sqrt{11}\frac{\pi}{\sqrt{6}\sigma}\cdot 2.5\sigma=-\frac{2.5\sqrt{11}\pi}{\sqrt{6}} \tag{6-11}$$

$$\frac{P(R<x_{th})}{P(\bar{R}<x_{th}')}=\frac{1-\exp(-\exp(-\frac{2.5\pi}{\sqrt{6}}))}{1-\exp(-\exp(-\frac{2.5\sqrt{11}\pi}{\sqrt{6}}))}=1648.8 \tag{6-12}$$

The simulation result is: $\frac{P_f}{P_f'}=\frac{2.40\times10^{-3}}{2.27\times10^{-6}}=1057.3$. $x_{th}-\mu=x_{th}'-\mu'=2.5\sigma$ is a more close guess.

Assume $x_{th}-\mu=x_{th}'-\mu'=2.5\sigma$ and the design value of other four variables are near the mean value, for the dependent reinforcing bars:

$$0.5^4\cdot P(R>x_{th})=0.5^4\times(1-\exp(-\exp(-\frac{2.5\pi}{\sqrt{6}})))=2.48\times10^{-3}\approx P_f \tag{6-13}$$

The Sanity check suggests the order of magnitude of the difference between reliability analysis of fully correlated rebars and total independent rebars is reasonable. The methods and assumptions used in the sanity check is not advised to be used in a reliability assessment of independent rebars.

Although the failure probability of independent rebars are much lower, the trend of the change of failure probability with correlation length remains. As the correlation length increase, the failure probability decrease. The spatial variability of corrosion in adjacent bars do not change the influence of the spatial variability of corrosion in axial direction in the reinforcements. In conclusion:

(1) Correlation of adjacent bars decrease the spatial variability of pitting corrosion in the transverse direction.

(2) Large correlation length of random field increase the spatial correlation at different locations and decrease the spatial variability of pitting corrosion in the axial direction.

(3) High spatial variability of corrosion in axial direction increase the failure probability of the structure while high spatial variability of corrosion in transverse direction decrease the failure probability of the structure.

6.4   Corroded external layer with sound internal layer

All above analysis are based on assumption that all 11 bottom reinforcements suffer from pitting corrosion (Fig 6.9(a)). However, often the outer layers of the reinforcements are more severely corroded than the internal layers. Assuming all bottom reinforcements have same chance of getting corroded is a conservative assumption and results in an upper bound of the failure probability of the structure. On the contrary, assuming only external rebars are corroded results is a lower bound of the failure probability of the structure in the case study. The previous reliability analysis only target on the upper bound. In order to estimate the lower bound of the failure probability, the reliability analysis is performed with assumption that only the outer layer of reinforcements are corroded (Fig 6.9 (b)).

<div align="center">(a)   (b)</div>
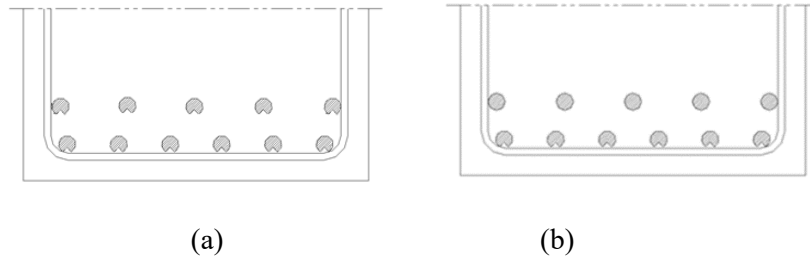
Fig 6.9 Corrosion only at external layer and corrosion at all bottom reinforcements

The probabilistic inputs and settings of reliability analysis are the same. Subset Simulation is performed with correlation length of 125 mm, 250 mm, 500 mm, 1000 mm and 2000 mm, assuming fully correlation between adjacent bars. The discretization is for area outside the random field the element length is 300 mm and for area inside the random field the element length is 125 mm. The random field covers 3000 mm length at the midspan. The results are listed in Table 6.3 and are plotted in Fig 6.10. As expected, the failure probability is smaller for approximately one order of magnitude.

Table 6.3 Comparison of failure probability for fully correlated bars

Correlation length	All corroded	External layer corroded
125 mm	$5.20 \cdot 10^{-2}$	$4.86 \cdot 10^{-3}$
250 mm	$4.37 \cdot 10^{-2}$	$2.68 \cdot 10^{-3}$
500 mm	$2.89 \cdot 10^{-2}$	$2.53 \cdot 10^{-3}$
1000 mm	$2.43 \cdot 10^{-2}$	$1.23 \cdot 10^{-3}$
2000 mm	$1.79 \cdot 10^{-2}$	$9.02 \cdot 10^{-4}$
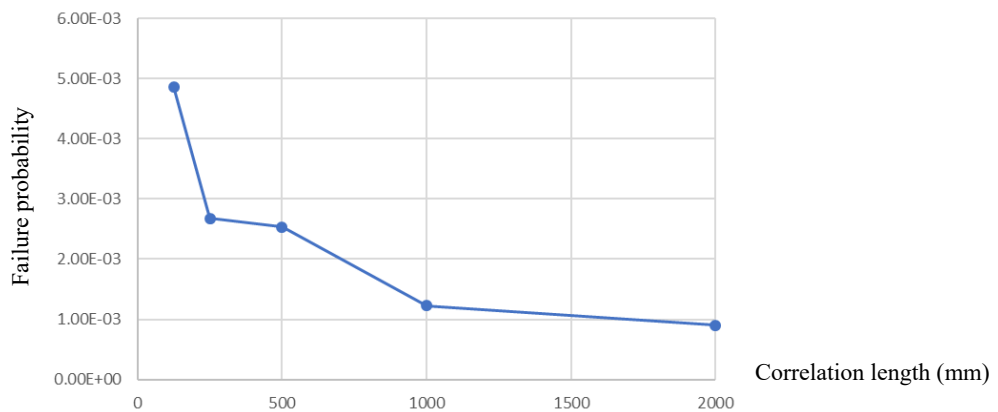
Fig 6.10 Failure probability with correlation length for fully correlated bars

Same reliability analysis is performed with correlation length of 500 mm, 1000 mm and 2000 mm, assuming fully independency between adjacent bars. The discretization is 300 mm element length for the entire beam. The results are listed in Table 6.4 and are plotted in Fig 6.11. The failure probability is also smaller for approximately one order of magnitude, which corresponds to the above analysis.

Table 6.4 Comparison of failure probability for independent bars

Correlation length	All corroded	External layer corroded
500 mm	$7.73 \cdot 10^{-5}$	$5.85 \cdot 10^{-6}$
1000 mm	$3.39 \cdot 10^{-5}$	$5.57 \cdot 10^{-6}$
2000 mm	$2.58 \cdot 10^{-5}$	$2.12 \cdot 10^{-6}$
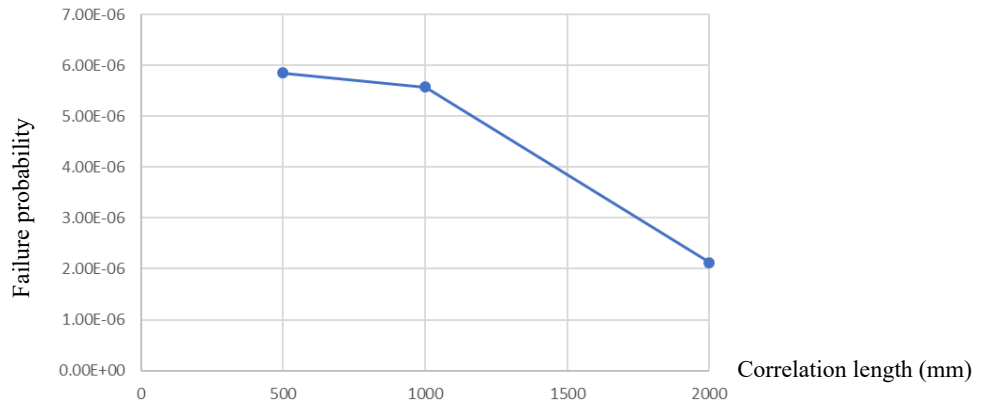
Fig 6.11 Failure probability with correlation length for independent bars

For both the case of fully correlated adjacent bars and fully independent adjacent bars, the situation with only external bars corroded shows lower failure probability. Also, in all the situations, the trend of larger correlation length resulting in lower failure probability remains.

7 Uncertainty of the bond model

As mentioned in Chapter 2 and 3, the probabilistic models for corroded RC structures such as quantified model uncertainties are not well founded. The analyses in Chapter 4, Chapter 5 and Chapter 6 do not take account the model uncertainties. This chapter is aimed at giving suggestions of the quantifications of model uncertainties for corroded RC structures and explore the influences on a simple case.

One of the corrosion damages is degradation of bond. Degradation of bond is not practicable to measure on site and affects anchorage capacity and composite interactions which leads to loss of ultimate strength or ductility of the concrete structures. Many researchers have studied the bond behaviour of corroded reinforcement and empirical models have also been proposed for predicting the bond strength of corroded reinforcement (Al-Sulaimani et al. (1990); Rodriguez et al. (1994); Cabrera (1996); Stanish et al. (1999); Coronelli (2002); Chung et al. (2004)). All the models are not expressed in probabilistic term, in spite that the reviews of test data (Bhargava et al. (2008); Mancini and Tondolo (2014)) reveal considerable uncertainty. Thus the quantification of uncertainty in empirical models is necessary.

In this chapter, the uncertainty of bond model is quantified, which can be also used to quantify uncertainties for other models of corrosion damage. Meanwhile, the coupled probabilistic finite element analysis scheme is used to propagation the uncertainty of bond model into reliability analysis of a simply supported RC beam.

7.1 Empirical bond model for corroded reinforcement

Bhargava et al. (2008) reviewed experimental data from a wide range of bending tests and pull-out specimen tests and proposed an empirical model to describe the progressive bond degradation for concrete specimens without stirrups. The model has three advantages:
a) The model is presented in the normalized form to take care of the varied primitive bond strength due to differences in strength of concrete, type of reinforcements and confinement conditions.
b) The model is in exponential format, which is capable to capture the nonlinearity when corrosion level changes from low to high.
c) The model separately takes account for flexural testing and pull-out testing, which prevents obstructions caused by large variety between test methods.

The uncertainty quantification and propagation is target on the model derived from flexural testing. For the model derived from pull-out testing, similar procedure can be applied. Based on the experimental data obtained from bending tests, the bond strength reduction is described by:

$$R_{fb}(X) = \begin{cases} 1.0 & \text{if } X < 1.5\% \\ 1.346 \cdot e^{0.198 \cdot X} & \text{otherwise} \end{cases} \tag{7-1}$$

In these equations, X is the corrosion level defined as the loss of weight of reinforcing bar due

to corrosion expressed as a percentage of the original bar weight, and R_{fb} is defined as the ratio of bond strength at X to the original bond strength for the uncorroded specimen.

7.2   Uncertainty quantification for the bond model

The bond model uncertainty is quantified using experimental data – collected in Bhargava et al. (2008) – on corroded, reinforcing bars embedded in concrete flexural members. The probabilistic model proposed satisfies the following requirements:

a) Its functional form follows that of the Bhargava model.
b) Respects the physically possible range of R (non-negative).
c) Has a relatively constant standard deviation along x (homoscedasticity).
This is a typical assumption in statistics and allows for a reasonable extrapolation outside of the data range that is often needed in structural reliability. This assumption is not driven by data but for the sake of convenience.

The mathematical structure of the model proposed by Bhargava et al. (2008) is used as the basis of the uncertainty quantification. In a parametric form:

$$R_{fb}(X) = \begin{cases} 1 & 0 \le X \le X_{th} \\ a \cdot e^{b \cdot X} & X > X_{th} \end{cases} \tag{7-2}$$

Where a, b, and X_{th} are the model parameters.

The continuity requirement at X_{th} makes these parameters dependent, hence only two of them are free. Compared to the model proposed by Bhargava et al., the enforcement of $R(X)=1$ before corrosion reaching the critical level X_{th} is kept to follow the widely accepted suggestion that bond strength of corroded structures should not be higher of the sound ones in structural assessment (fib, 2000). However, the value of crtical level X_{th} needs to be determined by a new fitting. It is because the value of X_{th} in Bhargava et al. is determined by pre-knowledge from experience rather than from analysis of the data. The bond model uncertainty is introduced as an explicit model uncertainty term in the form of a random variable. To ensure the non-negativity of R, the model uncertainty term is added in the log space:

$$R'_{fb}(X) = \exp\left[\log(R(X)) + E\right] \tag{7-3}$$

Where the accent is indicating that model uncertainty is included and E is a random variable that is distributed as:

$$E \sim \begin{cases} \mathcal{N}(0, \sigma_{E,0}) & 0 \le X \le X_{th} \\ \mathcal{N}\left(0, c \cdot (x-d)^2\right) & X > X_{th} \end{cases} \tag{7-4}$$

E is normally distributed in the log space, centered at zero and its standard deviation varies quadratically in log space, in the $X > X_{th}$ range. $\sigma_{E,0}$ is the standard deviation in the $0 \le X \le X_{th}$ range. Equations (2)-(4) constitute the proposed probabilistic model, apparently it has six parameters $[a, b, X_{th}, c, d, \sigma_{E,0}]$ out of which only four are independent (free) if we want to ensure the continuity (C^0) of R and the standard deviation of the model uncertainty as well. So the original, two-parameter, deterministic model is enriched by additional two to account for model uncertainty.

Before fitting the probabilistic model, a simplified analysis is made by the least square fitting without considering model uncertainty. The two-parameter model is fitted (in the least square sense) to different subsets of the available experimental data. The fitted models along with the Bhargava model are compared in Fig 7.1. It is salient that the fit which uses data only from Chung et al. (2004) agrees the best with the Bhargava model. The data form Al-Sulaimani et al, (1990) mainly lay in the range of where bond strength could be increased by low level of corrosion and contribute little to the fitting of bond degradation stage. The data from Al-Sulaimani et al. (1990) is far off from the bulk of other experimental results and only contains four measurements, which is not a proper data resource from the statistic view. As a result. The data from Chuang el al. (2004) is selected to be the data source in further fitting and analyses. This decision is expected to have a small influence in the descending part and can be easily revised in the future if needed. Moreover, using a different subset of data is not expected to change the results qualitatively or their order of magnitude.
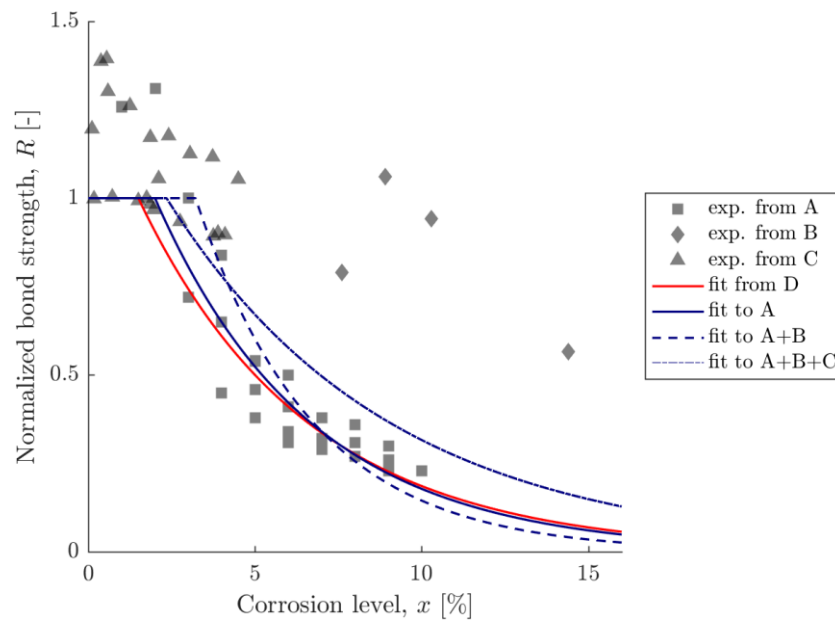
Fig 7.1 Experimental data of normalized bond strength and fitted models. A: Chung et al. (2004); B: Stanish et al. (1999); C: Al-Sulaimani et al. (1990); D: Bhargava et al. (2008).

The probabilistic bond model is fitted to Chung et al. (2004). To ensure requirement c), parameter c is fixed to meet the relatively constant standard deviation along the x axis. This is deemed to an acceptable approximation in the current context and considering the degree of accuracy the nature of the problem allows. The remaining three parameters are estimated using the maximum likelihood method. Maximum likelihood method is to determine the unknown parameters in the probability distribution of the events by maximizing the probability of getting a certain realization of the events (the measurements). The least square fit is equivalent to a maximum likelihood fit with an additive, normally distributed model error in the original (physical) space. The estimated parameters are summarized in Table 7.1. The models should not be used outside of the [0, 16%] interval. The fitted model is visualized in Fig 7.2 with a 70% confidence band.

Table 7.1 Summary of the considered bond strength reduction models.

Bond model	a	b	$X_{th}[\%]$	$\sigma_{E,0}$	c	d
Bhargava model, (1).	1.35	-0.198	1.50	NA	NA	NA
Deterministic, (2). least square fit	1.54	-0.216	2.00[†]	NA	NA	NA
Probabilistic, (2) - (4) maximum likelihood fit	1.55	-0.219	2.00[†]	0.143	0.004[§]	-3.99[‡]

[†] uniquely determined by a and b.

[‡] uniquely determined by a, b, c, and $\sigma_{E,0}$.

[§] Fixed (not the outcome of the maximum likelihood fit) to impose the prior knowledge we have on the mechanical problem and to ensure a relatively constant uncertainty band in the original space.
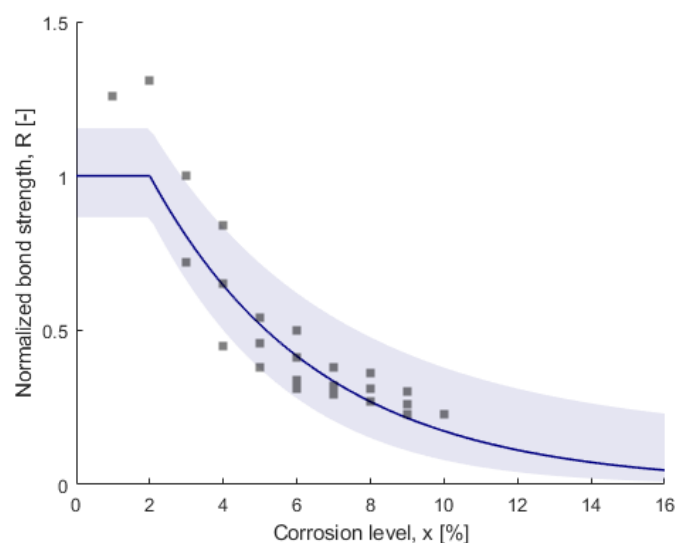
Fig 7.2 Data of normalized bond strength and fitted model with a 70% confidence band.

7.3   Case study : Uncertainty propagation

7.3.1   Simply supported beam with lap splices

To estimate the importance of the uncertainty of the bond model, a reliability assessment of an illustrative example is completed with a fully probabilistic approach. The reliability calculations concern ultimate limit state verifications, using non-linear finite element analysis.

The illustrative example is adopted from an experiment of beams with tension lap splices in the central region. Details of the experiment are described by Pantazopoulou et al. (2017). Fifteen beams were first subjected to different chloride contents in the lap region and different levels of bar section loss and cover cracking were obtained. Subsequently, the corroded beams and nine uncorroded control specimens were tested under four-point loading (see Fig 7.3), such that the corroded lap splice zones were placed in tension. To prevent corrosion outside the overlap region and premature shear failure, the beams were wrapped with fiber outside the constant moment region.

In the experiment, the mean value of cylinder compressive strength of concrete is determined as 42 MPa (A-series) and 45 MPa (B-series) at the time of testing. Four different spliced lengths, as 70 mm, 210 mm, 420 mm and 630 mm are considered. The reliability assessment in this

article only concerns the specimen with a spliced length of 630 mm and a mean cylinder concrete compressive strength of 42 MPa. With the exception of a few bar ruptures at pitted locations (B-series with 630 spliced length), the other specimens failed in the lap splice zone after extensive cracking and spalling of cover. The control specimen with lap length of 630 mm was sufficient to develop the reinforcement ultimate strength beyond yielding. Corroded specimens underwent slip along the lap early on and bond strength was seriously reduced by corrosion, converting the mechanism of failure from ductile to brittle.
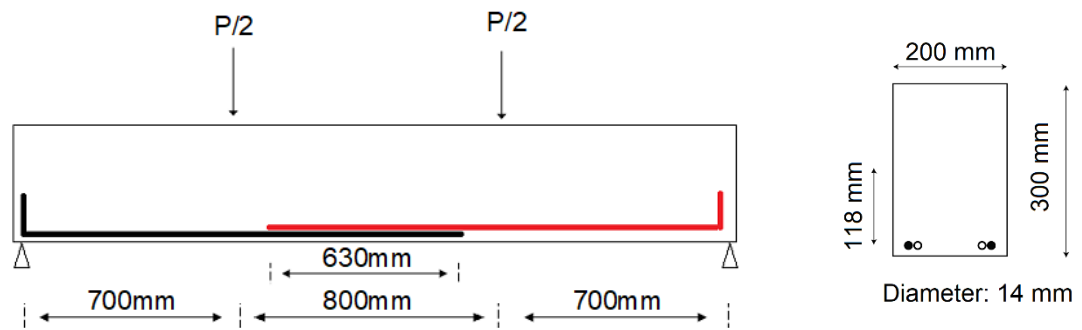
Fig 7.3 Layout overview of the beam.

7.3.2   Finite element model

The nonlinear finite element analysis (NLFEA) is performed with OpenSees (2016). The concrete is modelled with 88 beam elements, using a multilinear diagram that approximates an ideal plastic stress-strain diagram in compression and an exponential softening diagram in tension. The beam element is defined as displacement beam element with fiber section.

(a) Displacement beam element with fiber section   (b) Two-node link
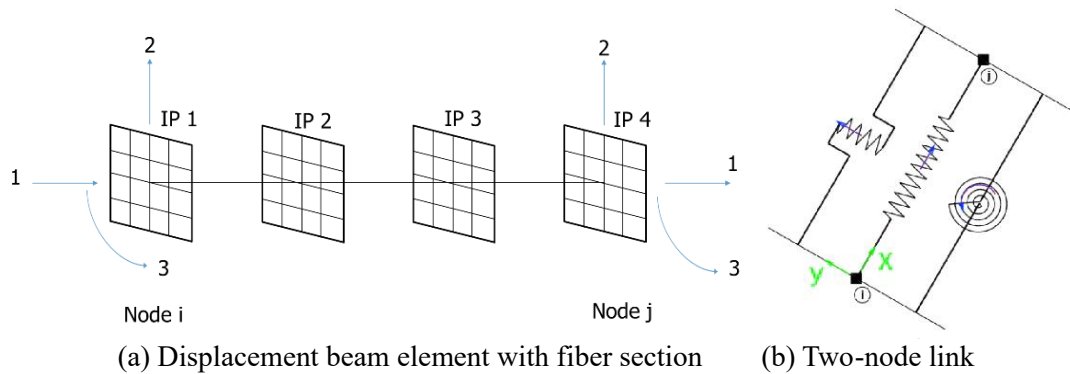
(c) Assemble of the elements

Fig 7.4 Elements used in numerical simulations.

| (a) beam element (concrete) | (b) truss element (reinforcement) | (c) zero length spring (bond). |
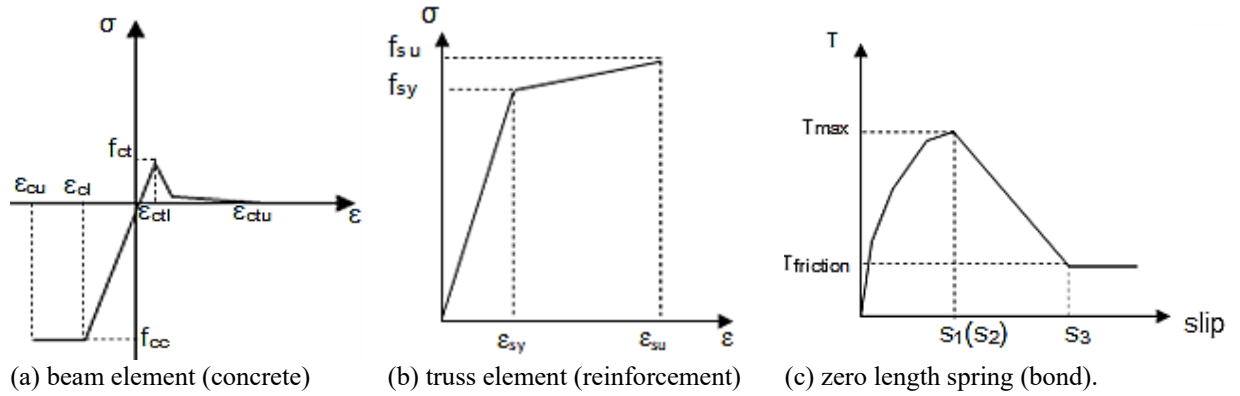
Fig 7.5 Material properties used in the numerical simulation.

Reinforcements are modeled with truss elements, adopting a bilinear stress-strain curve with hardening. The nodes in concrete at the location of reinforcement are connected with the nodes at the location of beam center with two-node link elements, of which stiffness is set to form a rigid connection. The bond behavior is modelled by two-node link elements, which connect the nodes in concrete and nodes in reinforcement at the very same location. The stiffness and strength of the bond interface is modeled with multilinear diagram suggested in the Model Code 2010 (fib, 2012). Fig 7.4 and Fig 7.5 demonstrate the finite element model and adopted material properties.

The loads are applied with two phases: for self-weight, the distributed load is applied with 10 equal steps with load control; for point load, displacement control is used with 0.005 mm per step. Krylov-Newton algorithm (Scott, 2010) is used with displacement convergence criteria of 0.001. Krylov-Newton algorithm is an accelerated Newton algorithm based on Krylov subspaces. The algorithm uses a low-rank least-squares analysis to advance the search for equilibrium at the degrees of freedom where the largest changes in structural state occur; then it corrects for smaller changes at the remaining degrees of freedom using a modified Newton computation.

The nonlinear finite element model is tested with given bond strength of 3.9 MPa (0 % section loss), 3.2 MPa (6.45 % section loss) and 3.0 MPa (9.77 % section loss) to compare with the experimental results. Fig 7.6 shows the comparison between numerical simulations and experimental tests. The ultimate load capacity shows a good consistency. The finite element analysis also shows the structure lose ductility with insufficient bond, which was observed by the experiment. Although no loss of stiffness before failure was shown by the corroded specimens in experiment, the simulation is sufficient to capture the decrease of ultimate strength and lose of ductility due to corrosion.

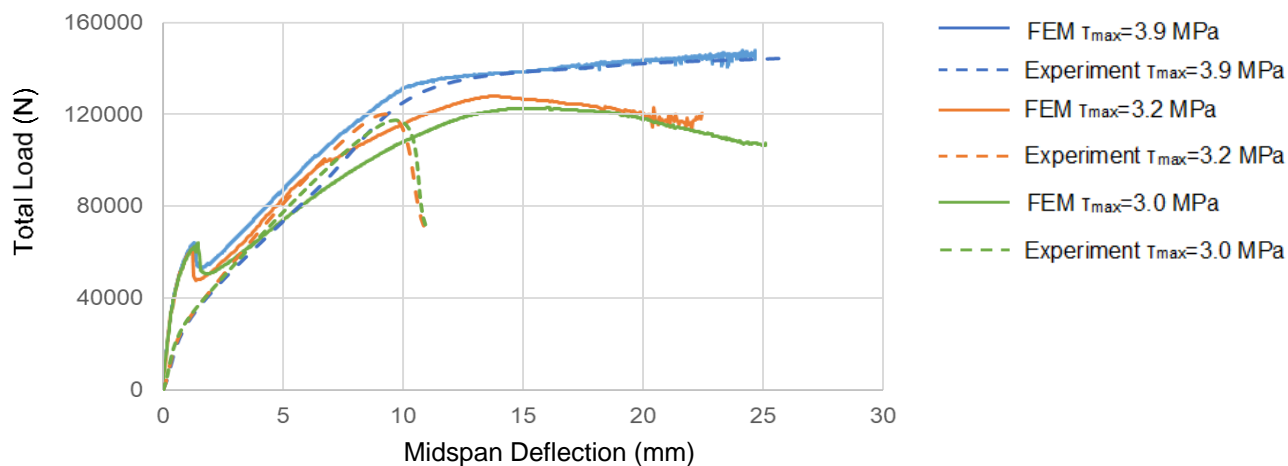Fig 7.6 Load-deflection curves from numerical simulations and experimental tests.

7.3.3 Reliability analysis

The reliability analysis targets on ultimate limit state, where external load – the point load Q – reaches the resistance capacity $R(X_{-Q})$ of the structure. When the limit state function $G(X) = R(X_{-Q}) - Q < 0$, the structure is defined as failed. The probabilistic models are based on the recommendations in the Probabilistic Model Code (JCSS, 2000) and fib bulletin 80 (fib, 2010). Table 7.2 summarizes the probabilistic models for inputs. In case of mean value of the concrete compressive strength, steel yield strength and steel tensile strength, direct measurements are available from the experimental report and so the measured value are used in reliability analysis. Corrosion is represented with the average cross section loss of bar. Severe corrosion (mean value 7 % for average section loss) is assumed, where the failure caused by insufficient bond strength (bond fails before yielding of reinforcements). Standard deviation of average section loss is assumed to be 0.1, which is a reasonable value in reality. Standard deviation of the model uncertainty term is 0.483, which corresponds to the 7 % section loss according to equation (4). Because the specimen does not have realistic/practical structural dimensions, the value of live load is chosen such that with the reliability index will be close to the target reliability index 3.1 (for low failure consequence in ULS).

Table 7.2   Probabilistic models for inputs.

Random variable	Distribution	Mean	COV
Concrete compressive strength (f_{cc})	Lognormal	42 MPa	0.15
Steel yield strength (f_{sy})	Lognormal	560 MPa	0.05
Steel tensile strength (f_{su})	Lognormal	660 MPa	0.06
Steel ultimate strain (ε_{su})	Lognormal	0.05	0.09
Cross section loss (X)	Normal	7 %	0.1
Model uncertainty for bond reduction (E)	Normal	0	see (4)
Self-weight (P)	Normal	1500 N/m	0.04
Live load (Q)	Normal	45000 N	0.1

The yield strength, ultimate tensile strength and ultimate strain of the reinforcing bars are all treated as random variables, which are independent from each other. For the concrete material, the compressive strength is the only random variable. The tensile strength, bond strength of

uncorroded structures, fracture energy and Young's modulus are derived from the value of compressive strength according to the relations in Model Code 2010 (fib, 2012):

Two reliability assessments are compared here: (i) including the model uncertainty E of the bond model for corroded reinforcement; and (ii) without this model uncertainty E. Both reliability calculations are performed with an adaptive response surface reliability method, Adaptive Directional Importance Sampling (ADIS) (Grooteman, 2011). The ADIS algorithm is based on a directional simulation scheme. In a directional simulation scheme, only the important directions are sampled exactly and the other directions are sampled with a response surface approach. These most important directions are determined by a β-sphere enclosing the most important part(s) of the limit state. The β-sphere and response surface are constantly updated during sampling. From the exact evaluations information becomes available to make the scheme adaptive. The ADIS method has been demonstrated as highly efficient, accurate and robust with a low probability of failure and medium number (up to about 40) of variables.

The approximate design point from the result of ADIS is subsequently verified by importance sampling, using exact evaluation of limit state. Table 7.3 presents the main results of the two reliability calculations in terms of probability of failure P_f, reliability index β, and the number of NLFEA calls. These results reveal that the neglect of uncertainties in the bond models for corroded reinforcement considerably influences the failure probability, changing an order of magnitude from $3.17 \cdot 10^{-3}$ to $2.69 \cdot 10^{-4}$. If the target reliability index is chosen as 5.3 (low failure consequence in ULS), then including the bond model uncertainty results in a unsafe conclusion, while neglecting the bond model uncertainty results in a safe conclusion.

Table 7.3   ADIS, importance sampling and FORM results.

	With model uncertainty		Without model uncertainty	
ADIS Results				
Number of NLFEA calls	175		199	
Probability of failure P_f	$3.17 \cdot 10^{-3}$		$2.69 \cdot 10^{-4}$	
Reliability index β	2.73		3.46	
Convergence criteria for P_f	0.1		0.1	
IS Results				
Number of NLFEA calls	1780		6200	
Probability of failure P_f	$4.60 \cdot 10^{-3}$		$3.38 \cdot 10^{-4}$	
Reliability index β	2.60		3.37	
Convergence criteria for P_f	0.1		0.1	
FORM Results	α	Design point	α	Design point
Concrete compressive strength (f_{cc})	-0.53	34.03 MPa	-0.49	32.38 MPa
Steel yield strength (f_{sy})	0.02	560.5 MPa	0.001	559.4 MPa
Steel tensile strength (f_{su})	-0.01	657.8 MPa	-0.03	654.7 MPa
Steel ultimate strain (ε_{su})	0.03	0.0502	0.015	0.0500
Cross section loss (X)	0.40	8.24 %	0.76	10.86 %
Model uncertainty for bond reduction (E)	-0.60	-0.7223	--	--
Self-weight (P)	0.02	1503 N/m	0.006	1485 N/m
Live load (Q)	0.44	49962 N	0.42	51018 N

Table 7.3 also includes a first order reliability method (FORM) analysis using the response surface generated by ADIS, where approximate sensitivity factors are obtained. The sensitivity factors suggest that the relative importance of variables changes when uncertainty of bond

degradation model is taken into account. The major change is the importance of the corrosion level X (expressed by average section loss) reduced while additional importance of the model uncertainty term raised. The sensitivity factors correspond to the expectation of the physical problem, which also confirms the reasonability of the generated response surface.

7.4 Discussion

This chapter studies the effect of the prevalently neglected bond strength model uncertainty on corroded reinforced concrete structures. First, the uncertainty is quantified: a probabilistic bond strength reduction model is fitted to experimental data on corroded, reinforcing bars embedded in concrete members under flexure. Then, the uncertainty is propagated to structural reliability using an illustrative example – a simply supported beam with lap splices – with and without bond model uncertainty.

It is shown that the inclusion of bond model uncertainty increases the calculated failure probability by an order of magnitude. This indicates the importance of bond model uncertainty in the assessment of concrete structures affected by reinforcement corrosion. The large change in calculated failure probability is validated for the illustrative example in the present chapter. In reality, the influence of bond strength on global reliability of a structure may varies, depending on whether bond is the dominant component of the structure and whether its model uncertainty can be well controlled. However, the force transferred between concrete and steel should be verified in any cases before the assessment of other potential failures. In the verification of bond strength of corroded reinforcement, its uncertainty is advised to be taken into account.

8 Conclusion and recommendation

8.1 Conclusion

The thesis fills the knowledge gap of probabilistic nonlinear finite element analysis of reinforced concrete structures with spatial varied corrosion and shows the effects of spatial variability of corrosion. A computational scheme to couple reliability analysis with finite element analysis is designed. With this scheme, nonlinear structural behavior and response of static indeterminate structures can be captured in the limit state function for reliability analysis. Model uncertainty of the bond property of corroded reinforcement is quantified, which can facilitate the reliability analysis of corroded reinforced concrete structures.

The research question of this research is:

What are the effects of the spatial variability of corrosion on the reliability of reinforced concrete structures?

A series analyses is conducted for the case study to answer the research question. First, finite element analysis is performed to study the mechanics characteristic. Then, reliability analysis without spatial variability is performed to determine the important variables. Third, reliability analyses with random field are performed to study the effect of spatial variability of corrosion. Finally, extra reliability analysis with random field is performed to check the influence of some assumptions. The following conclusions are drawn based on the analyses:

(1) When corrosion develops, pitting corrosion can severely reduce resistance of the structure and very localized damages can lead to a brittle structural response of the statically indeterminate structure. For the case study when corrosion has initiated for 50 years, the localized damage at the most sensitive location could reduce the structural capacity of approximately 20 % compared to the same level uniform damage.

(2) In the case study, high spatial variability of corrosion in axial direction of the beam increase the failure probability of the beam. Compared to fully spatial correlated corrosion (infinite long correlation length), the spatial varied corrosion with 125 mm correlation length increase the failure probability for approximately 20 times. This result is the collective effect of the probabilistic characteristic of a series system and the physical characteristic of static indeterminate structure.

(3) In the case study, high spatial variability of corrosion in transverse direction of the beam decrease the failure probability of the beam. Compared to fully correlated adjacent bars, the totally independent adjacent bars decrease the failure probability for approximately 1000 times. This result is caused by the probabilistic characteristic of a parallel system.

(4) If only external layer of reinforcements are corroded, the failure probability would be

decreased, but the above conclusions are still valid. The value of failure probability and the quantified effect of spatial variability of corrosion would change in terms of different level of corrosion. The qualitative effect of spatial variability of corrosion is not determined by the corrosion level.

In addition to answer the research question, there are two other findings in the thesis:
(1) The model of bond property of corroded reinforcement contains considerable model uncertainty which may have significant influence on the global reliability of corroded reinforced concrete structure. The quantified influence may varies according to the specific structures, but can be as large as one order of magnitude.

(2) Reliability method with evaluation of approximated limit state (surrogate modelling of the exact results) is effective in computation compared to reliability method with evaluation of exact limit state (exact results of nonlinear finite element analysis). However, the surrogate modelling methods are not robust to capture nonlinear performance function. The surrogate models used in for the case study are either unable to capture irregular nonlinear functions or too sensitive to small fluctuation of the performance function.

8.2 Recommendations

The analysis of the case study reveals the considerable effect of spatial variability of corrosion on structural reliability. However, the study of spatial variability of corrosion is far from thorough. For example, there are rare measurements of the spatial distribution of corrosion and little existing data of the correlation of corrosion along reinforcement or between adjacent bars. In the current guideline of assessment of existing structures, whether with full probabilistic method or semi probabilistic method, the spatial variability of corrosion is not carefully involved. In addition, the probabilistic models for corroded reinforced concrete structures are not yet well founded and the probabilistic approaches to solve high dimensional reliability problem are not well developed. Therefore, the following research topics are recommended for further study.

To provide reliable input data for study of spatial variability of corrosion:
(1) Measurements of the spatial variability of corrosion in reinforced concrete structures.
(2) Quantification the spatial correlation of corrosion in probabilistic format.

To further study the influence of spatial variability of corrosion on different types of structures and with different level/type of corrosion:
(3) Reliability analysis of corroded reinforced concrete structures involving the spatial variability of corrosion
(4) Quantification of the uncertainties in structural verifications of corroded reinforced concrete structures in probabilistic format.

To facilitate reliability assessment of corroded reinforced concrete in practice and improve the efficiency of computation:
(5) Development of semi-probabilistic methods to equivalent the influence of spatial variability of corrosion in reliability analysis.

(6) Improvement of the performance of surrogate modelling approaches to robustly capture nonlinear performance function.

Reference

Akgül, F., & Frangopol, D. M. (2004). Time-dependent interaction between load rating and reliability of deteriorating bridges. *Engineering Structures, 26*(12), 1751-1765. doi:10.1016/j.engstruct.2004.06.012

Al-Sulaimani, Kaleemullah, G. J., Basunbul, M. I. A., & Rasheeduzzafar. (1990). Influence of corrosion and cracking on bond behaviour and strength of reinforced concrete members. *ACI Struct, 87*(2), 220–231.

Allaix, D. L., Carbone, V. I., & Mancini, G. (2011). *Random fields for the modeling of deteriorated structures*. Paper presented at the Applications of Statistics and Probability in Civil Engineering, London.

Almusallam, A. A. (2001). Effect of Degree of Corrosion on the Properties of Reinforcing Steel Bars. *Construction and Building Materials, 15*(8), 361–368.

Bhargava, K., Ghosh, A. K., Mori, Y., & Ramanujam, S. (2008). Suggested Empirical Models for Corrosion-Induced Bond Degradation in Reinforced Concrete. *Journal of Structural Engineering, 134*(2), 221-230. doi:10.1061//ASCE/0733-9445/2008/134:2/221

Biondini, F. (2004). *A Three-dimensional Finite Beam Element for Multiscale Damage Measure and Seismic Analysis of Concrete Structures*. Paper presented at the 13th World Conference on Earthquake Engineering, Canada.

Biondini, F., & Vergani, M. (2012). *<Damage modeling and nonlinear analysis of concrete bridges under corrosion.pdf>*. Paper presented at the Bridge Maintenance, Safety, Management, Resilience and Sustainability, London.

Cabrera, J. G. (1996). Deterioration of concrete due to reinforcement steel corrosion. *Cem. Concr. Compos., 18*(1), 47–59.

CEB/fib. (2000). Bond ofreinforcement in concrete. In *fib Bulletin No. 10*.

CEB/fib. (2016). Partial factor methods for existing concrete structures: Recommendation. In *fib Bulletin No. 80*.

Cheng, J. (2014). Random field-based reliability analysis of prestressed concrete bridges. *KSCE Journal of Civil Engineering, 18*(5), 1436-1445. doi:10.1007/s12205-014-0253-4

Chiu, C.-K., Tu, F.-C., & Fan, C.-Y. (2014). Risk assessment of environmental corrosion for reinforcing steel bars embedded in concrete in Taiwan. *Natural Hazards, 75*(1), 581-611. doi:10.1007/s11069-014-1349-3

Chung, L., Cho, S.-H., Jay Kim, J.-H., & Yi, S.-T. (2004). Correction factor suggestion for ACI development length provisions based on flexural testing of RC slabs with various levels of corroded reinforcing bars. *Engineering Structures, 26*(8), 1013-1026. doi:10.1016/j.engstruct.2004.01.008

Coronelli, D. (2002). Corrosion cracking and bond strength modeling for corroded bars in reinforced concrete *ACI Struct. J, 99*(3), 267– 276.

Coronelli, D., & Gambarova, P. (2004). Structural assessment of corroded RC beams modeling guidelines. *Journal of Structural Engineering, 130*(8), 1214-1224. doi:10.1061//ASCE/0733-9445/2004/130:8/1214

Der Kiureghian, A., & Ke, J.-B. (1988). The stochastic finite element method in structural

reliability. *Probabilistic Engineering Mechanics, 3*(2), 83-91.

Du, Y. G., Clark, L. A., & Chan, A. H. C. (2005). Residual capacity of corroded reinforcin. *Magazine of Concrete Research, 57*(3), 135–147.

Engelund, S., & Sorensen, J. D. (1998). *Struct. Safety, 20*(1), 69.

Engen, M., Hendriks, M. A. N., Köhler, J., Øverli, J. A., & Åldstedt, E. (2017). A quantification of the modelling uncertainty of non-linear finite element analyses of large concrete structures. *Structural Safety, 64*, 1-8. doi:https://doi.org/10.1016/j.strusafe.2016.08.003

Frangopol, D. M., Messervey, T.B. (2009). Maintenance Principles for Civil Engineering (chapter 89). In M. Abe, et al. (Ed.), *Encyclopedia of structural health monitoring*: Wiley Online Library.

Frier, C., & Sørensen, J. D. (2007). Stochastic analysis of the multi-dimensional effect of chloride ingress into reinforced concrete. *Structure and Infrastructure Engineering, 3*, 355–366.

Grooteman, F. (2011). An adaptive directional importance sampling method for structural reliability. *Probabilistic Engineering Mechanics, 26*(2), 134-141. doi:10.1016/j.probengmech.2010.11.002

Hajializadeh, D., Stewart, M. G., Enright, B., & Obrien, E. (2015). Spatial time-dependent reliability analysis of reinforced concrete slab bridges subject to realistic traffic loading. *Structure and Infrastructure Engineering, 12*(9), 1137-1152. doi:10.1080/15732479.2015.1086385

Han S., P. W. Y. E. (2013). Evaluation of concrete durability due to carbonation in harbor concrete structures. (48), 1045−1049.

Jacinto, L., Neves, L. C., & Santos, L. O. (2015). Bayesian assessment of an existing bridge: a case study. *Structure and Infrastructure Engineering, 12*(1), 61-77. doi:10.1080/15732479.2014.995105

JCSS. (2000). JCSS Probabilistic Model Code. In.

Kenshel, O., & O'Connor, A. (2009). Assessing chloride induced deterioration in condition and safety of concrete structures in marine environments. *European Journal of Environmental and Civil Engineering, 13*(5), 593-613. doi:10.1080/19648189.2009.9693136

Kioumarsi, Mahdi; Hendriks, Max; Kohler, Jochen; Geiker, Mette Rica. (2016) The effect of interference of corrosion pits on the failure probability of a reinforced concrete beam. Engineering structures. vol. 114

Koch, G. H., Brongers, M. P. H., Thompson, N. G., Virmani, Y. P., & Payer, J. H. (2001). *Corrosion Costs and Preventive Strategies in the United States* (FHWA-RD-01-156). Retrieved from Springfield:

Lay, S., & Schießl, P. (2003). *Service life models*. Retrieved from

Li, Y. (2004). *Effect of Spatial Variability on Maintenance and Repair Decisions for Concrete Structures.*

Lim, S., Akiyama, M., & Frangopol, D. M. (2016). Assessment of the structural performance of corrosion-affected RC members based on experimental study and probabilistic modeling. *Engineering Structures, 127*, 189-205. doi:10.1016/j.engstruct.2016.08.040

Liu, T., Weyers, R.W. (1998). Modeling the dynamic corrosion process in chloride contaminated concrete structures. *Cement and Concrete Research, 28*(3), 365–379.
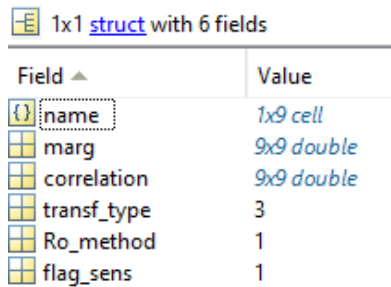
Mancini, G., & Tondolo, F. (2014). Effect of bond degradation due to corrosion – a literature survey. *Structural Concrete, 15*, 408-418.

Marsh, P. S., & Frangopol, D. M. (2008). Reinforced concrete bridge deck reliability model incorporating temporal and spatial variations of probabilistic corrosion rate sensor data. *Reliability Engineering & System Safety, 93*(3), 394-409. doi:10.1016/j.ress.2006.12.011

Matthies, H. G., Brenner, C. E., Bucher, C. G., & Soares, C. G. (1997). Uncertainties in probabilistic numerical analysis of structures and solids - Stochastic finite elements. *Structural Safety, 19*(3), 283-366.

Melchers, R. E. (2005). Representation of uncertainty in maximum depth of marine corrosion pits. *Structural Safety, 27*, 322–334.

Nogueira, C. G., & Leonel, E. D. (2013). Probabilistic models applied to safety assessment of reinforced concrete structures subjected to chloride ingress. *Engineering Failure Analysis, 31*, 76-89. doi:10.1016/j.engfailanal.2013.01.023

Pantazopoulou, S. J., Petrou, M. F., Spastri, V., Archontas, N., & Christofides, C. (2017). The performance of corroded lap splices in reinforced concrete beams. *Corrosion Reviews, 0*(0). doi:10.1515/corrrev-2017-0086

Papakonstantinou, K. G., & Shinozuka, M. (2013). Probabilistic model for steel corrosion in reinforced concrete structures of large dimensions considering crack effects. *Engineering Structures, 57*, 306-326. doi:10.1016/j.engstruct.2013.06.038

Rodriguez, J., Ortega, L. M., & Garcia, A. (1994). *Corrosion of reinforcing bars and service life of R/C structures: Corrosion and bond deterioration.* Paper presented at the Concrete across Borders, Odense,   Denmark,.

Ryan, P. C., & O'Connor, A. J. (2013). Probabilistic analysis of the time to chloride induced corrosion for different self-compacting concretes. *Construction and Building Materials, 47*, 1106−1116.

Sajedi, S., & Huang, Q. (2015). Probabilistic prediction model for average bond strength at steel–concrete interface considering corrosion effect. *Engineering Structures, 99*, 120-131. doi:https://doi.org/10.1016/j.engstruct.2015.04.036

Sarja, A. (2005). *Integrated Life Cycle Design of Structures*: e-Library: Taylor & Francis.

Scott, M. H. a. F., G. L. (2010). A Krylov Subspace Accelerated Newton Algorithm: Application to Dynamic Progressive Collapse Simulation of Frames. *Journal of Structural Engineering, 136*(5), 473-480.

Shayanfar, M.-A., Barkhordari, M.-A., & Ghanooni-Bagha, M. (2015). Probability calculation of rebars corrosion in reinforced concrete using css algorithms. *J. Cent. South Univ., 22*, 3141−3150.

Sheikh, A. K., Boah, J. K., & Hanen, D. A. (1990). Statistical modeling of pitting corrosion and pipeline reliability. *Corrosion,, 46*(3), 190–197.

Stanish, K., Hooton, R. D., & Pantazopoulou, S. J. (1999). Corrosion effects on bond strength in reinforced concrete. *ACI Struct. J., 96*(6), 915–921.

Stewart, M. G. (2004). Spatial variability of pitting corrosion and its influence on structural fragility and reliability of RC beams in flexure. *Structural Safety, 26*(4), 453-470. doi:10.1016/j.strusafe.2004.03.002

Stewart, M. G. (2009). Mechanical behaviour of pitting corrosion of flexural and shear

reinforcement and its effect on structural reliability of corroding RC beams. *Structural Safety, 31*(1), 19-30. doi:10.1016/j.strusafe.2007.12.001

Stewart, M. G., & Al-Harthy, A. (2008). Pitting corrosion and structural reliability of corroding RC structures: Experimental data and probabilistic analysis. *Reliability Engineering & System Safety, 93*(3), 373-382. doi:10.1016/j.ress.2006.12.013

Stewart, M. G., & Suo, Q. (2009). Extent of spatially variable corrosion damage as an indicator of strength and time-dependent reliability of RC beams. *Engineering Structures, 31*(1), 198-207. doi:10.1016/j.engstruct.2008.08.011

Sudret, B. (2008). Probabilistic models for the extent of damage in degrading reinforced concrete structures. *Reliability Engineering & System Safety, 93*(3), 410-422. doi:10.1016/j.ress.2006.12.019

Sudret, B., & Der Kiureghian, A. (2000). *Stochastic Finite Element Methods and Reliability*.

Unanwa, C., & Mahan, M. (2014). Statistical Analysis of Concrete Compressive Strengths for California Highway Bridges. *Journal of Performance of Constructed Facilities, 28*(1), 157-167. doi:doi:10.1061/(ASCE)CF.1943-5509.0000404

Val, D. V. (2007). Deterioration of Strength of RC Beams due to Corrosion and Its Influence on Beam Reliability. *Journal of Structural Engineering, 133*(9), 1297-1306. doi:10.1061//ASCE/0733-9445/2007/133:9/1297

Val, D. V., & Melchersz, R. E. (1997). RELIABILITY OF DETERIORATING RC SLAB BRIDGES. *J. Struct. Eng, 123*(12), 1638-1644.

Val, D. V., Stewart, M. G., & Melchers, R. E. (1998). Effect of reinforcement corrosion on reliability of highway bridges. *Engineering Structures, 20*(11), 1010–1019.

Vergani, M. (2010). *Modellazione del degrado di strutture in calcestruzzo armato soggette a corrosione.* (PhD), Politecnico di Milano, Italy.

Zandi, K. (2015). Corrosion-induced cover spalling and anchorage capacity. *Structure and Infrastructure Engineering, 11*(12), 1547-1564. doi:10.1080/15732479.2014.979836

Zhang, X., Wang, J., Zhao, Y., Tang, L., & Xing, F. (2015). Time-dependent probability assessment for chloride induced corrosion of RC structures using the third-moment method. *Construction and Building Materials, 76*, 232-244. doi:10.1016/j.conbuildmat.2014.10.039

Annex

Usage of the computational framework

The framework starts with the definition of the inputs. These inputs include: name of variables, probabilistic distribution of variables (i.e. distribution type, mean value and standard deviation), information of finite element mesh, and correlation length. Furthermore, the input contains settings, such as the chosen reliability method, convergence criteria, etc. Fig (i) shows how the inputs are defined in MATLAB.

1x1 struct with 6 fields

Field ▲	Value
{} name	1x9 cell
marg	9x9 double
correlation	9x9 double
transf_type	3
Ro_method	1
flag_sens	1

(a) Structure of the inputs

probdata.name

	1	2	3	4	5	6	7	8	9
1	fc	fsy	fsu	esu	As1	As2	As3	R	Q

(b) Name of the variables

probdata.marg

	1	2	3	4	5	6	7	8	9
1	2	51.2000	3.5840	51.2000	3.9333	0.0699	0	0	0
2	2	440	28.6000	440	6.0847	0.0649	0	0	0
3	2	550	38.5000	550	6.3075	0.0699	0	0	0
4	2	0.0800	0.0072	0.0800	-2.5298	0.0898	0	0	0
5	2	7859	157	7859	8.9692	0.0200	0	0	0
6	2	5400	108	5400	8.5940	0.0200	0	0	0
7	2	7364	147	7364	8.9042	0.0200	0	0	0
8	15	9.2400	1.2000	9.2400	8.6999	1.0688	0	0	0
9	15	150000	15000	150000	1.4325e+05	8.5503e-05	0	0	0

(c) Probabilistic distribution of the variables

probdata.correlation

	1	2	3	4	5	6	7	8	9
1	1	0	0	0	0	0	0	0	0
2	0	1	0	0	0	0	0	0	0
3	0	0	1	0	0	0	0	0	0
4	0	0	0	1	0	0	0	0	0
5	0	0	0	0	1	0	0	0	0
6	0	0	0	0	0	1	0	0	0
7	0	0	0	0	0	0	1	0	0
8	0	0	0	0	0	0	0	1	0
9	0	0	0	0	0	0	0	0	1

(d) Correlation matrix of the variables

Fig (i) Inputs of the program

Before the analysis, the finite element model and analysis settings should be specified. The MATLAB code for finite element model generation should be modified accordingly if necessary. All the inputs, including name of the variables, probabilistic distribution of variables, field discretization (default setting is the same as finite element discretization) and correlation length, should be specified in the main code as required by the template. The toolboxes used for reliability analyses in this thesis are FERUM and UQLAB. For each toolbox, there are templates for reliability method settings. The methods and settings should be specified before all analysis. Fig (ii) shows examples of settings of the methods.

```
% FORM analysis options
analysisopt.i_max              = 500;
analysisopt.e1                 = 0.05;
analysisopt.e2                 = 0.05;
analysisopt.step_code          = 0;
analysisopt.Recorded_u         = 1;
analysisopt.Recorded_x         = 1;

% FORM, SORM analysis options
analysisopt.grad_flag          = 'ffd';
analysisopt.ffdpara            = 10;

analysisopt.ffdpara_thetag     = 100;
```

(a) Settings for the FORM (FERUM toolbox)

```
SSimOptions.Type          = 'Reliability';
SSimOptions.Method        = 'Subset';
SSimOptions.Simulation.TargetCoV = 0.1;
SSimOptions.Subset.p0 = 0.1;
SSimOptions.Simulation.MaxSampleSize = 1e4;
SSimOptions.Simulation.BatchSize = 1000;
```

(b) Settings for the Subset Simulation (UQLAB toolbox)
Fig (ii) Settings for reliability methods

With the application of methods available in the toolboxes, the outputs should be interpreted in terms of convergence, physical meanings and calculation efficiency. First, information of convergence is available in the outputs of all methods and can be compared with an acceptable criterion. For FORM and SORM, the convergence criteria are based on the closeness to the limit state and the vector point from origin to the design point in the standard Gaussian space. For simulation approaches, the convergence criteria are based on the coefficient variation of the failure probability. For analysis with response surface, additional convergence criteria for the formation of response surface is also necessary.

In addition to the convergence criteria, the reliability analysis results should correspond to the physical domain of the problem. For example, the sensitivity factor and design point obtained from the FORM analysis can be used to interpret a physical problem and the values should have valid physical meanings. The third important criterion is to judge the efficiency of the calculation: the number of the exact evaluation of performance function. With same accuracy of the failure probability, the calculation is more efficient if fewer exact performance function evaluations are performed.

Algorithm of reliability methods

The FORM approach contains three steps:

(1) An isoprobabilistic transformation of the input random vector $X \sim f_X(x)$ into a space spanned by independent standard normal variables $U \sim N(0, I_M)$. Nataf transformation is used in this work.

(2) A search for the most likely failure point in the standard normal space, known as the design point u^*. Finding the coordinates of the U^* consists solving the following constrained optimization problem: $U^* = \arg\min\left\{\|U\| \,\middle|\, g(x(U), \theta_g) = G(U, \theta_g) = 0\right\}$

(3) A linearization of the limit-state surface at the design point u^* and the analytical computation of the resulting integral that is an approximation of P_f.

The subset simulation algorithm can be summarized in the following steps:

(1) Sample the original space with standard MC sampling.

(2) Calculate the empirical quantile t_k in the current subset such that $P_k \approx P_0$

(3) Use the samples below the identified quantile as the seeds of parallel MCMC chains, sample $D_{k+1} | D_k$ until a predetermined number of samples is available.

(4) Repeat Steps 2 and 3 until the identified quantile $t_m < 0$

(5) Calculate the failure probability of the last subset P_m by setting $t_m = 0$

(6) Combine the intermediate calculated failure probabilities into the final estimate of P_f.

The adaptive experimental design algorithm for Kriging based Monte-Carlo simulation is summarized as follows:

(1) Generate a small initial experimental design $X = \left\{x^{(1)}, ..., x^{(N_0)}\right\}$ and evaluate the corresponding limit-state function responses $Y = \left\{y^{(1)}, ..., y^{(N_0)}\right\} = \left\{g(x^{(1)}), ..., g(x^{(N_0)})\right\}$

(2) Train a Kriging metamodel $\hat{g}$ based on the experimental design $\{X, Y\}$

(3) Generate a large set of NMC candidate samples $S = \left\{s^{(1)}, ..., s^{(N_{MC})}\right\}$ and predict the corresponding metamodel responses $\left\{\hat{g}(s^{(1)}), ..., \hat{g}(s^{(N_0)})\right\}$

The algorithm of polynomial response surface based adaptive importance sampling follows the steps:

(1) An isoprobabilistic transform of the input random vector $X \sim f_X(x)$ into a standard normal vector $U \sim N(0, I_M)$

(2) A number of directional simulations are pre-sampled.

(3) The obtained performance function information is used to construct a response surface (RS) and is used to determine a threshold β-sphere βth.

(4) If an important direction is sampled having an (approximated) distance to the limit-state lying within the threshold β-sphere, then this direction is re-evaluated using exact g-function evaluations.

(5) After each directional simulation the convergence is checked. At convergence, it is checked whether new exact g-function evaluations have performed resulting in an update of the response surface and threshold β-sphere.